A STUDY OF THE CRITICAL WEISSENBERG NUMBER IN MECHANICALLY DEGRADING POLYMER SOLUTIONS

By

CLAUDE CLIFFORD EBERLE

Bachelor of Science in Mechanical Engineering

Oklahoma State University

Stillwater, Oklahoma

1983

Submitted to the Faculty of the Graduate College
of the Oklahoma State University
in partial fulfillment of the requirements
for the Degree of
MASTER OF SCIENCE
December, 1984

A STUDY OF THE CRITICAL WEISSENBERG NUMBER IN MECHANICALLY DEGRADING POLYMER SOLUTIONS

Thesis Approved:

A. J. Ghajar
Thesis Adviser

Jerald D. Parker

P. W. Woods

Norman N. Durham
Dean of the Graduate College

ACKNOWLEDGMENTS

I wish to thank my adviser, Dr. A. J. Ghajar, for his advice, encouragement, and assistance during this project. Thanks also to Dr. P. M. Moretti and Dr. J. D. Parker for their helpful comments.

A number of people from the School of Mechanical Engineering, Oklahoma State University, assisted me in various ways. Special thanks to George Cooper, Judith Waldron, Janet Torrance, Dr. R. L. Lowery, Dr. J. K. Good, Gary Ferrell, and Dr. K. N. Reid. Also, thanks to H. K. Yoon for his helpfulness in the technical and experimental phases of this work.

This study was partially financed by a Fellowship granted by Dow Chemical, U.S.A., Texas Division, and through Graduate Teaching and Research Assistantships provided by School of Mechanical Engineering at Oklahoma State University.

Thanks to Ms. Charlene Fries for typing the manuscript, and to Mr. Eldon Hardy for his excellent artwork.

Finally, much love and thanks to Mr. and Mrs. Gayle Ward, Mr. and Mrs. Claude Eberle, and to my wife Linda. This work is dedicated to them.

TABLE OF CONTENTS

LIST OF TABLES

LIST OF FIGURES

NOMENCLATURE

% CH	Change in time constant, percent
D	Inside diameter of the pipe
De	Deborah number
% DEV	Deviation of f_A from f, percent
F	Turbine meter frequency, Hz
f	Fanning friction factor, $f = \tau_w / \frac{1}{2} \rho V^2$
$\hat{f}$	Predicted Fanning friction factor
f_A	Asymptotic Fanning friction factor
g	Gravitational acceleration
h	Manometer height difference
K'	10^b, where b is the y-intercept of a log-log plot of shear stress versus shear rate
L	Distance between pressure taps
n	Slope of the log-log plot of shear stress versus shear rate
Q	Flow rate, gpm
Re'	Generalized Reynolds number, $Re' = \rho V^{2-n} D^n / K' 8^{n-1}$
Re_a	Reynolds number based on the apparent viscosity at the wall, $Re_a = \rho VD/\mu_a$
s	Standard deviation
$\bar{T}$	Characteristic flow time
t_R	Residence time
V	Fluid mean velocity
Ws	Weissenberg number, $Ws = \lambda V/D$

Ws_{cf}	Critical Weissenberg number of momentum transfer
X	Axial position along the test section

Greek Letters

$\dot{\gamma}$	Shear rate
$\dot{\gamma}_{max}$	Maximum experimental shear rate
$\dot{\gamma}_w$	Shear rate at the pipe wall
λ	Characteristic fluid time (time constant)
λ^*	The ratio $\lambda/2\lambda_L$
λ_3	Time constant calculated using rheological data with three significant digits
λ_5	Time constant calculated using rheological data with five significant digits
λ_B	Best value of the time constant for a data set
λ_E	Eyring time constant
λ_L	Ellis time constant
λ_P	Powell-Eyring time constant with infinite shear viscosity defined as the experimental viscosity at the maximum experimental shear rate
λ_{PW}	Powell-Eyring time constant with infinite shear viscosity defined as the viscosity of water
μ	Viscosity
μ_∞	Infinite shear viscosity
μ_o	Zero shear viscosity
μ_a	Apparent viscosity at the wall
ρ	Fluid density
ρ_m	Density of the manometer fluid

ρ_s	Density of the system fluid
$\tau_{1/2}$	Shear stress when experimental shear viscosity is one-half the zero shear viscosity
τ_w	Shear stress at the pipe wall

CHAPTER I

INTRODUCTION

It has been found that adding small amounts of certain high molecular weight polymers to water flowing turbulently in a circular pipe reduces the friction factor significantly when compared to that of water alone. This phenomenon is known as drag reduction. The resulting fluids are called viscoelastic fluids because their physical properties are intermediate to those of viscous Newtonian fluids and elastic Hookean solids [1].

The potential effects of drag reduction on industry are staggering. Drag reduction may be used for faster ships, submarines, and other marine vehicles; increased capacity in pipelines, firehoses, and other fluid transport systems; improved efficiency in low viscosity hydraulic fracturing processes; and noise suppression in pipes and heat exchangers. In addition, most industrial chemicals as well as many fluids in the food processing and biochemical industries exhibit viscoelastic characteristics. An understanding of heat transfer in viscoelastic fluids is therefore necessary to design more efficient heat exchangers for those industries [1, 2, 3], and knowledge of fluid mechanics necessarily precedes knowledge of heat transfer.

Currently, numerous problems are associated with drag reduction by polymer addition. As a result, few of the potential applications

mentioned have realized any practical use. This work is intended to be one step in the solution of one problem--mechanical degradation.

An increase in polymer concentration increases the amount of drag reduction, thus further reducing the friction factor. Eventually a saturation concentration is reached beyond which further polymer addition has no effect on the friction factor [1]. The minimum friction factor lies on the dotted line of Figure 1 (Appendix A), which presents the friction factor as a function of the Reynolds number for different concentrations of Separan AP-273 [1]. This is called the asymptotic condition, and the saturation concentration is the minimum concentration required to reach the asymptote [4, 5].

Mechanical degradation is a phenomenon which reverses the effect of increasing the polymer concentration, so that the friction factor may increase [2, 6-10]. The proposed mechanicsm by which friction is reduced is the suppression of turbulence by the highly elastic, long-chain polymer molecules. The shear stresses present in the moving fluid tend to rupture the polymer's molecular bonds, thus reducing the elasticity and energy-storage capability of the long-chain molecules [7, 11, 12]. This is called mechanical degradation. The degraded polymer molecules are unable to suppress turbulence due to the loss of energy-storage capability; therefore, they become ineffective in drag reduction. The polymer molecules which have <u>not</u> been degraded, since they are still effectively storing energy, constitute an "effective concentration," which is measured by the dimensionless Deborah number.

The Deborah number is defined as

$$De = \frac{\lambda}{\bar{T}} \tag{1.1}$$

where λ is the characteristic fluid time, and $\bar{T}$ is the characteristic flow time [1, 2]. There are several particular forms of the Deborah number. The difference among the forms lies in the mathematical definition of $\bar{T}$. The particular form used in this work is the Weissenberg number, which shall be discussed in further detail later. The Deborah (or Weissenberg) number actually measures the ratio of the elastic forces to the viscous forces in the fluid [2]. Since increasing the polymer concentration increases the fluid's elasticity and mechanical degradation decreases the elasticity, the Deborah number is ultimately a measure of the "effective concentration."

If the pressure gradient is fixed, the maximum flow rate is achieved when the fluid is just sufficiently elastic to achieve the asymptotic condition. The asymptotic friction factor therefore suggests the optimum point compromising economics and performance of polymer solutions [3]. As a result, accurate prediction of the asymptotic friction factor becomes a very important problem. The asymptotic value can be predicted; however, presently [1, p. 132] "there exist no firm criteria for determining whether asymptotic conditions exist." Tung et al. [6] proposed that there is a critical Deborah number above which the pressure drop is constant and independent of mechanical degradation. The critical Deborah number defines the minimum elasticity required for asymptotic conditions. At Deborah numbers below the critical value, the friction factor lies between the asymptotic and Newtonian values (see Figure 1), a region described as the intermediate region. At Deborah numbers greater or equal to the critical value, the asymptotic condition exists. The relation between the friction factor and Deborah number for fixed Reynolds numbers is illustrated in Figure 2.

The reported works have generally used the Weissenberg numbers as the particular form of the Deborah number, and henceforth this thesis shall refer primarily to the Weissenberg number. It is appropriate to note that trends and functions involving the Weissenberg number should be similar for all forms of the Deborah number, although the specific numbers may change.

Some previous works have reported the critical Weissenberg number. Ng and Hartnett [2] reported the critical Weissenberg number in solutions containing Separan AP-273. Kwack et al. [13] reported a similar work. Kwack and Hartnett [14, 15] have reported the critical Weissenberg numbers for various pipe diameters, solutes, and solvent chemistry.

Although these reports contain some very important results and conclusions, most lack either or both precision and sufficient amounts of experimental data to provide clearly conclusive evidence. In those works which have reported critical Weissenberg numbers, Ws_{cf} has usually been reported as an interval estimate rather than a point estimate. However, the interval is not presented as a statistical confidence interval. In addition, the conclusions presented were based on only a few experimental tests, a situation which translates into small statistical sample sizes and thus a significant probability of erroneous conclusions. Finally, the author is unaware of any works reporting the critical Weissenberg number except those discussed heretofore, and all of them were produced by a single team of researchers. Therefore, at this time there exists a definite need for

1. verification by one more independent research teams of the reported critical Weissenberg numbers; and

2. increased precision in the estimates of the critical Weissenberg number.

The primary objective of this work was to investigate and report precise estimates of the critical Weissenberg number for polyacrylamide (Separan AP-273), an industrial polymer additive manufactured by Dow Chemical U.S.A. The work was accomplished in the following succession of steps:

1. Design, construction, and instrumentation of the experimental facilities. Part of this work was done by senior students enrolled in project courses. This phase required the largest amount of work and time.

2. Calibration runs in the experimental apparatus. The friction factor of water was measured and compared to accepted values. Agreement indicated that the system was in good working order.

3. Experimental tests to find Ws_{cf} using Separan AP-273 as the solute.

4. The data from step 3 were analyzed with the results and conclusions presented later in this thesis.

CHAPTER II

IMPORTANT PARAMETERS

This chapter contains the major portion of background work which establishes a theoretical basis for the problem. Included are considerations of physical properties, entrance length, important dimensionless numbers, and a brief review of relevant published literature. Much of the theory is a simple adaptation of Newtonian fluids theory such that it reasonably well predicts the behavior of viscoelastic fluids.

2.1 Physical Properties

The study of momentum transfer in non-Newtonian fluids requires knowledge of the fluid's density, viscosity, and elasticity.

Yoo [16] studied the physical properties of solutions using Carbopol-934, Separan AP-30, and Polyox WSR-301. He found that the density of each solution agreed within 0.4 percent of the value for water over the range of normal concentrations. Based on Yoo's results, Cho and Hartnett [1] recommended using the density of water in studies of aqueous polymer solutions.

The viscosity of polymer solutions is not so easily determined. For non-Newtonian fluids, the viscosity is a function of not only temperature and pressure, but also of molecular weight, solvent chemistry, concentration, shear rate, and the length of time at a given shear rate (i.e., mechanical degradation) [17]. Therefore, the viscosity must be

experimentally determined under the existing conditions for every situation in which it is needed. The specific methods by which viscosity was measured are discussed in Chapter III.

The elasticity of polymer solutions was not measured directly. The fluid characteristic time is considered to be a measure of the fluid's elasticity, and it can be related to the fluid's shear viscosity by procedures discussed in section 2.5.

2.2 Hydrodynamic Entrance Length

In order to obtain the fully developed friction factor, it is necessary to take the measurements in the fully developed velocity profile region. In Newtonian flow, the hydrodynamic entrance length is about 10 to 15 diameters [18]. The entrance length for viscoelastic fluids is much larger. Most early investigators were unaware of this fact, and thus measured data in the entrance region. These values were then reported as the fully developed friction factor. This mistake is suspected to be a major contributor to the discrepancies found among early works [3].

Yoo [16] found the hydrodynamic entrance length for concentrated viscoelastic fluids to be about 80 diameters. Tung et al. [19] confirmed Yoo's results and concluded that the entrance length for 2000 wppm Separan solution is approximately 100 diameters. Cho and Hartnett [1] found that for all concentrations of aqueous Polyox and Separan solutions studies, no changes were observed by changing tap locations for $x/D > 110$. These works all support the conclusion that the hydrodynamic entrance length is about 100 diameters or less for viscoelastic fluids, and data collected at $x/D > 100$ should reasonably well represent the fully developed value of the friction factor.

2.3 Reynolds Numbers

At least five different definitions of the Reynolds number have been used in the study of non-Newtonian fluids [1]. The most useful forms for circular tube flows with wide concentration ranges are a generalized Reynolds number and a Reynolds number based on the apparent viscosity at the wall.

The generalized Reynolds number Re' is useful for non-Newtonian, laminar pipe flow. For such flows, the wall shear stress is

$$\tau_w = K' \, (8V/D)^n \tag{2.1}$$

where K' and n vary with 8V/D for most polymer solutions [1, 20]. Metzner and Reed [21] derived Re' from the definition of the Fanning friction factor,

$$f = \tau_w / (\tfrac{1}{2} \rho V^2) \tag{2.2}$$

Combining Equations (2.1) and (2.2) yields

$$f = 16/(\rho V^{2-n} \, D^n / K' \, 8^{n-1}) \tag{2.3}$$

Thus all laminar friction data lie on the line f = 16/Re' if the denominator of Equation (2.3) is defined as Re' [1]. The constants K' and n can be evaluated using a log-log plot of Newtonian wall shear stress and Newtonian shear rate from viscosity measurements. A log-log plot of f versus Re' can then be used as a calibration tool by checking laminar flow results prior to a turbulent flow experiment [1]. Re' also correlates turbulent flow data for Separan and some other solutions, and is therefore sometimes used in turbulent flow experiments. The onset of

transition to turbulent flow occurs at approximately Re' = 5500 in Separan solutions [22].

The Reynolds number based on the apparent viscosity at the wall [23] is defined as

$$Re_a = \frac{\rho V D}{\mu_a} \tag{2.4}$$

and is obviously a slightly modified version of the Newtonian Reynolds number. The apparent viscosity at the wall is evaluated from an approximate relation for the wall shear stress,

$$\tau_w = \mu_a \dot{\gamma}_w \tag{2.5}$$

where for capillary tube flow,

$$\dot{\gamma}_w = [(3n+1)/4n](8V/D) \tag{2.6}$$

By substituting into Equation (2.2), it can be shown that the Fanning friction factor is a function of both Re_a and n. As a result, a log-log plot of f versus Re_a for laminar flow is not a unique line. According to Cho and Hartnett [1],

> However, the presentation of heat transfer results based on Re_a is believed to be more practical since it allows more direct comparisons of experimental results in turbulent flows with those predicted from the analytical studies. This results from the fact that most analytical studies of friction and heat transfer for non-Newtonian fluids in turbulent pipe flow have been carried out under the assumption of constant viscosity in the radial direction at a fixed flow rate to avoid mathematical complexity. Additionally, the non-Newtonian viscosity is found experimentally to be almost constant for most aqueous polymer solutions in the shear rate range corresponding to the turbulent flow conditions (p. 69).

Since momentum transfer forms the basis for heat transfer studies, a Reynolds number should be chosen which adequately correlates momentum and heat transfer results. Also, the elasticity of viscoelastic fluids does

not affect laminar flow [24, 25], so laminar friction results are unaffected by mechanical degradation [1, 26]. Thus mechanical degradation and hence the Weissenberg number are important only in turbulent flows. Therefore, because of its superiority in the turbulent flow region, Re_a shall be used to present turbulent flow data in this thesis.

2.4 The Weissenberg Number

Polymer solutions lose their drag-reduction ability in the presence of high shear stresses, a phenomenon called mechanical degradation [2, 7-10]. Mechanical degradation of polymer solutions has been investigated previously [2, 6-10, 13-15, 27, 28] but many characterizations consider only the specific apparatus used [6-8, 10, 27, 28], which is not particularly useful to most cases. It is preferable to relate the physical properties of the polymer solution and the experimental apparatus through nondimensionalization or some other approach which lends itself to general application. The more recent studies [2, 13-15] have employed such an approach. This work is an extension of those studies.

The most common general approach now used to describe mechanical degradation is the Deborah number concept introduced by Reiner [29]. Mechanical degradation reduces the fluid's elasticity; however, the turbulent shear viscosity is relatively unaffected [6]. Therefore, a degrading fluid experiences a continuously decreasing ratio of elastic forces to viscous forces. This ratio is represented by the Deborah number, which is determined by finding the ratio of the characteristic fluid time to the characteristic flow time [1, 2].

The Deborah number is defined by

$$De = \lambda/\bar{T} \tag{1.1}$$

Ng and Hartnett [2] recommend using the relation

$$\bar{T} = D/V \tag{2.7}$$

to find the characteristic flow time (V/D is a characteristic shear rate), so the Deborah number becomes

$$De = \lambda V/D \tag{2.8}$$

where V and D represent the mean velocity and the diameter, respectively. The particular form of the Deborah number defined by Equation (2.8) is the Weissenberg number.

2.5 Determination of Fluid Characteristic Time

The fluid characteristic time λ is used to measure the fluid's elasticity. It is a material property and should therefore be obtainable from a constitutive equation. Molecular theories and phenomenological nonlinear constitutive equations are available. However, most molecular theories predict neither the shear rate dependence of viscosity nor the normal force difference. Also, the best phenomenological nonlinear equations require the experimental determination of the first normal force difference and other dynamic properties, which are difficult to determine for all but high polymer concentrations [1].

Since concentrations of a few hundred wppm are effective in drag reduction, a good model should accurately predict the fluid characteristic time for dilute polymer solutions. Phenomenological nonlinear equations are therefore considered to be poor models.

Changes in the fluid's elasticity are reflected by changes in the zero shear rate viscosity (see Figures 3-5, Appendix A) and the primary normal force difference [2]. Thus it seems that good models might be

based on one or both of these parameters. There exist some simple models of the generalized Newtonian fluids which Bird [30] suggested could be effectively used to find the characteristic time using only steady shear viscosity data. These are the preferred models because of the difficulty encountered in primary normal force difference measurement in dilute solutions. Elbirli and Shaw [31] thoroughly investigated several of the simple models. They suggested that the Ellis and Eyring models [32-34] yield the best results, with the Eyring model being slightly better.

The Ellis time constant is given by

$$\lambda_L = \mu_o/\tau_{1/2} \tag{2.9}$$

where μ_o is the fluid's zero shear rate viscosity, $\tau_{1/2}$ $(= \mu\dot{\gamma})$ is the shear stress at which $\mu = 1/2\ \mu_o$, and $\dot{\gamma}$ is the shear rate which produces μ $(= 1/2\ \mu_o)$. The solution viscosity should be measured over a wide range of shear rates and the results evaluated from Equation (2.9) to find λ_L. Making a plot similar to Figures 3, 4, and 5 may be helpful. As an example, consider data set 3.0500 (see Appendix D for explanation of data set number system). The zero shear rate viscosity μ_o is 16.64 centipoise. Therefore, μ is 8.32 centipoise and the corresponding shear rate $\dot{\gamma}$ is 23.7 sec^{-1}. From Equation (2.9), $\lambda_L = 0.0843$ sec.

The Ellis model was one of the most accurate models tested by Elbirli and Shaw, with an average error of about 11 percent. They did not mention specifically why the Eyring model was judged superior to the Ellis model, nor are the polymer concentrations tabulated in their report. The author notes that the Ellis time constant cannot be calculated for very dilute or degraded fluids, for example, data sets 3.0010, 3.0050,

3.0100, 4.29, and 4.56 (see Appendix D). In addition, Kwack [35] compared five different models and found that the Ellis model yields results inconsistent with other models at very high concentrations.

The Eyring time constant is evaluated from

$$\mu = \frac{\mu_o \sinh^{-1} (\lambda_E \dot{\gamma})}{\lambda_E \dot{\gamma}} \tag{2.10}$$

Again μ_o is the zero shear rate viscosity. However, for the Eyring model μ can be any measured viscosity and $\dot{\gamma}$ is the associated shear rate. The solution viscosity must be experimentally determined over a large range of shear rates and a nonlinear regression fit of Equation (2.10) to the experimentally determined shear viscosity and shear rates must be performed to find the Eyring time constant [2]. The author has written a simple interactive computer program which utilizes a numerical search technique and the least squares method to find the Eyring time constant which yields the best fit of Equation (2.10) to the experimental data. The program, a user's manual, and theory of the numerical search technique are included as Appendix E. Using this program, the Eyring time constant for the previous example was found to be $\lambda_E = 0.194$ seconds. This yields $\lambda_E/\lambda_L = 2.3$, a not unexpected result since the Eyring time constant is generally about twice as large as the Ellis time constant [2].

Elbirli and Shaw found the Eyring model to be the best of the two-parameter models. It yielded an average error of 13 percent and a maximum error of 23 percent. In addition, they found it to perform better than most other models on data which has a broad transition from zero shear to power law behavior. Kwack [35] found that the Eyring model

yielded results inconsistent with other models for highly degraded solutions, however, an obvious area of concern.

The Powell-Eyring model [30] is a simple modification of the Eyring model which improves the curve-fit significantly. It is defined by the equation

$$\mu = \mu_\infty + (\mu_o - \mu_\infty) \frac{\sinh^{-1}(\lambda\dot{\gamma})}{\lambda\dot{\gamma}} \tag{2.11}$$

where all variables except μ_∞ are defined exactly as in the Eyring model. The definition of infinite shear viscosity μ_∞ is somewhat ambiguous; a judicious method of choosing μ_∞ shall be discussed shortly. The computer program is actually written for the Powell-Eyring form, and is converted to the Eyring model by proper definition of μ_∞.

Note that if μ_∞ is defined as zero, the Powell-Eyring model is reduced to the Eyring model. Elbirli and Shaw considered the two models as one, and their conclusions concerning the Eyring model should generally be true of the Powell-Eyring model, though the error should be different. Kwack [35] found that the Powell-Eyring time constant compares favorably with other models; thus in recent works the University of Illinois at Chicago Circle team [13-15, 35] has used the Powell-Eyring model.

Kwack [35] chose to define the infinite shear viscosity as the viscosity at very high shear rates, about 10^5 sec^{-1}. Unfortunately, many laboratories do not have equipment capable of accurate viscosity measurements at such high shear rates. A different definition of infinite shear viscosity may therefore be preferable.

The author has compared three definitions of infinite shear viscosity, noting particularly the effects of fluid elasticity and experimental shear rate range on the resulting Powell-Eyring time constant. The

data analyzed may be found in Figures 3 through 5. The rheological data were originally tabulated by Kwack [35].

The influence of fluid elasticity was found by comparing calculated time constants at different concentrations and at various degrees of mechanical degradation. The influence of experimental shear rate range was determined by choosing a maximum shear rate, $\dot{\gamma}_{max}$, and ignoring all rheological data for which $\dot{\gamma} > \dot{\gamma}_{max}$. For example, the time constant of data set 3.0500 (see Figure 3) was initially calculated using all the data points in the data set, or $\dot{\gamma}_{max} = 98{,}800\ sec^{-1}$. The time constants were then recalculated, ignoring all data points with $\dot{\gamma} > 43{,}100\ sec^{-1}$, i.e., $\dot{\gamma}_{max} = 43{,}100\ sec^{-1}$. Calculations were repeated with maximum shear rates of $26{,}500\ sec^{-1}$, $8410\ sec^{-1}$, $4460\ sec^{-1}$, $2630\ sec^{-1}$, $869\ sec^{-1}$, and $28.1\ sec^{-1}$.

The infinite shear viscosity was defined three different ways. In the first case, $\mu_\infty = 0$, which results in the Eyring model. Second, infinite shear viscosity is experimentally determined at the maximum shear rate, $\mu_\infty = \mu\ (\dot{\gamma}_{max})$. Finally, infinite shear viscosity is that of water at the experimental temperature, $\mu_\infty = \mu\ (H_2O)$. The calculated time constants are represented by λ_E, λ_P, and λ_{PW}, respectively. Also, let λ_B represent the <u>best</u> value of the time constant for a data set; it was assumed to equal the value calculated using <u>all</u> data points. Finally, let λ be the time constant calculated in any general situation. Two new variables may then be defined:

$$\lambda^* = \frac{\lambda}{2\lambda_L} \tag{2.12}$$

and

$$\% \text{ CH} = 100 \times \frac{\lambda - \lambda_B}{\lambda_B} \tag{2.13}$$

Ideally, λ^* should be near one because the Ellis time constant is roughly one-half the Eyring time constant. For dilute solutions, the Ellis time constant is fairly accurate and thus a good tool for comparison [31]. In addition, % CH should ideally equal zero in all cases. This does not occur, of course, because a wide shear rate range and many data points yield better statistical reliability and a better curve fit than a restricted shear rate range and sample size. Tabulation of λ^* and % CH should, however, aid in choosing a definition of infinite shear viscosity which results in the best practical model. Relevant data may be found in Figures 6 through 17 of Appendix A and Tables I through III of Appendix B.

The time constant is directly proportional to fluid elasticity, and should therefore decrease with decreasing concentration and increasing hours of shear. Figures 6, 7, and 8 demonstrate that λ_E and λ_{PW} behave as expected; however, λ_P fails even this test. The observed behavior apparently results from the fact that many of the data sets have a small $\dot{\gamma}_{max}$; λ_P is usually about equal to λ_E and λ_{PW} when $\dot{\gamma}_{max}$ is large.

At very low concentrations or high residence times (Figures 9, 10, 11, and 18) % CH is alarmingly high for the Eyring model. Inconsistent behavior characterizes λ_P; λ_{PW} performs well, although % CH is somewhat larger than is desirable. Note also from Figure 6 that λ_E has an unusually low value at such low elasticities, confirming Kwack's observation.

At normal concentrations and residence times, λ_P again performs inconsistently and very poorly. λ_E and λ_{PW} both perform excellently. The Eyring model outperforms the "water model" because λ^* is generally closer to one. As λ decreases, however, % CH becomes larger for λ_E than for λ_{PW}.

The Eyring model is judged to be superior for highly elastic fluids; however, its performance is poor at low Weissenberg numbers. The "water model" performs adequately for all data studied. The only comparison possible between the "water model" and Kwack's [35] version of the Powell-Eyring model is the value of λ^*, and the actual values of λ. At very low elasticities, the "water model" exhibits more drastic changes, and the time constants may differ by a factor of three or four. There is little difference in λ^* where it can be calculated. Kwack's version is probably the most accurate Powell-Eyring model. However, the "water model" appears to be quite accurate and consistent. Its advantage lies in the wide availability of viscosity data for water, as compared to the limited accessibility to viscometers which can operate to shear rates of 10^5 sec^{-1}. For this reason, the author recommends use of the Powell-Eyring model with the infinite shear viscosity defined as that of water.

From Figures 9 through 18, it is evident that in every case except one, % CH < 10 at $\dot{\gamma}_{max} = 2500$ sec^{-1}. Therefore, λ should be reasonably accurate if $\dot{\gamma}_{max} \geq 2500$ sec^{-1}. It should also be noted that three-digit accuracy is quite sufficient. The author compared λ_{PW} calculated from seven data sets. Rheological data were considered at both three- and five-digit accuracy. The maximum difference in percent was 2 percent (Table III), which is insignificant when compared to the average error of 13 percent found by Elbirli and Shaw.

2.6 Important Results From Published Works

Tung et al. [6] suggested that there is a critical Deborah (Weissenberg) number above which the pressure drop is constant and independent of mechanical degradation. The critical Weissenberg number is the

smallest Weissenberg number for which the asymptotic condition of Figure 1 exists. If $Ws \geq Ws_{cf}$, the friction data should lie on the minimum drag asymptote; if $Ws < Ws_{cf}$, the friction data should lie in the intermediate region. Recent works [2, 13-15] have confirmed this hypothesis.

Kwack et al. [13] proposed that for $Ws < Ws_{cf}$, the friction factor is a function of both Reynolds and Weissenberg numbers, while for $Ws \geq Ws_{cf}$, the friction factor is a function of Reynolds number only. Their experimental results support their hypothesis, as well as showing that the Weissenberg number is a function of both concentration and mechanical degradation. They found that for a 1000 wppm solution of Separan AP-273, $Ws_{cf} = 5 \sim 10$ when $20{,}000 \leq Re_a \leq 30{,}000$. Their results also indicate that Ws_{cf} is a weak function of Re_a, with Ws_{cf} increasing slightly as Re_a was increased. Ng and Hartnett [2] tested a 1500 wppm solution of Separan AP-273 solution using the Ellis and Eyring models. They found that $Ws_{cf} \approx 4$ based upon the Ellis model, while $Ws_{cf} \approx 8$ based upon the Eyring model. Their results agreed very closely with those reported by Tung et al. [6] for a 2500 wppm solution of Separan AP-273. Comparison of these reports indicates that the critical Weissenberg number is independent of concentration. Results from these studies are shown in Figures 19 and 20.

Early studies [1, 36-38] indicated that the friction factor is a function of solvent chemistry and solute as well as Reynolds number, concentration, and mechanical degradation. The solute effect may result from changing polymer additives or from changing batches (which may have different mean molecular size and weight) of one particular polymer. In addition, the percentage of drag reduction is dependent on pipe diameter

[39, 40]. The rate of mechanical degradation has been found to depend on pipe diameter [7, 40] and solute [28].

Cho and Hartnett [1] compared data from two different reports by Kwack et al. [19, 26] and concluded that the critical concentration is dependent on pipe diameter, which implies that the critical Weissenberg number is dependent on pipe diameter. However, the data compared were for different polymers as well as different pipe diameters, leaving a question as to which variable caused the difference in critical concentration. More recently, Kwack and Hartnett [14] found the critical Weissenberg number to be independent of pipe diameter, thus contradicting the conclusion of Cho and Hartnett. A separate study indicates that neither solvent chemistry nor solute affects the critical Weissenberg number [15]. The recent studies also confirmed the earlier reported values of the critical Weissenberg number.

Kwack and Hartnett's [14, 15] conclusions are based on a limited number of observations (small sample sizes). This results in a significant probability of error. Their conclusions seem logical and sensible in light of most previous works, so the author believes they are correct, and the conclusions of this study are based on that premise. However, until their results and conclusions are confirmed by other studies, they should be regarded with some skepticism. The author has therefore included such pertinent data as solvent pH and pipe diameter in Chapters III and IV.

A review of previous studies reveals the following important points:

1. The Weissenberg number is dependent on concentration, the state of mechanical degradation, solute, and solvent chemistry. In addition,

by the definition of Weissenberg number ($Ws = \lambda V/D$), it must change with pipe diameter if the mean fluid velocity is fixed.

2. For Weissenberg numbers below the critical value, the friction factor is a function of both Reynolds and Weissenberg numbers. For Weissenberg numbers above the critical value, it is dependent only on Reynolds number. Functionally stated,

$$f = f\ (Re_a, Ws) \qquad Ws < Ws_{cf}$$

$$f = f\ (Re_a) \qquad Ws \geq Ws_{cf}\ .$$

3. The critical Weissenberg number is independent of concentration. It apparently is independent of solute, solvent chemistry, and pipe diameter, but more studies are required to confirm these conclusions. It is weakly dependent on the Reynolds number and was found to be

$$Ws_{cf} = 5 \sim 10 \qquad \text{if } 20{,}000 \leq Re_a \leq 30{,}000$$

when evaluated using the Eyring and Powell-Eyring models.

Table IV is a brief summary of published studies of mechanical degradation. It is convenient for reference and comparison.

CHAPTER III

EXPERIMENTAL FACILITIES AND PROCEDURE

This chapter is devoted to documentation of the experimental facilities and the procedures used to obtain experimental data.

3.1 Experimental Facilities

The experiments were performed in the Fluid Mechanics Laboratory at Oklahoma State University. A schematic of the experimental apparatus is shown in Figure 21. At the time of the reported experiments, only the 3/8 inch nominal diameter test section had been completed. Special features of the experimental facilities are described in the following pages.

3.1.1 Test Section

The test section is a 38 foot length of type 304, seamless, stainless steel pipe. Stainless steel resists corrosion, an important feature for use with polymer solutions. In addition, it performs well in resistance heating applications, a desirable feature in heat transfer experiments scheduled for the future. The pipe is 3/8 inch nominal diameter, schedule 80. The standard ID is 0.423 inch; the actual ID was measured as 0.436 inch ±0.002 inch. The L/D ratio is 1046, which is much larger than that required to achieve the hydrodynamically fully developed condition for polymer solutions at normal concentrations. To

determine the hydrodynamic entrance lengths for different polymers at different concentrations, numerous pressure taps were affixed to the test section, with locations shown in Figure 22. It was necessary that the ratio of wall thickness to tap hole diameter be greater than 1.5 and less than 15 to insure best results from the pressure taps [16]. The tap hole diameter is 5/64 inch, yielding a thickness to diameter ratio of 1.62.

The pressure drop may be measured using one of three differential pressure gages or a U-tube mercury manometer. The gage ranges are 0-30 inches of water, 0-5 psid, and 0-20 psid. The manometer range is 50 inches. All gages have a maximum error of ±2 percent of full scale; manometer accuracy is ±0.1 inch. The pressure taps are fitted with brass needle valves which are installed so as to avoid flow disturbances (see Figure 23). From the needle valves, 1/4 inch plastic tubes lead to a gage panel, where they are connected to the female ends of hydraulic "quick-couplers." Similarly, the differential pressure gages are connected to the male ends of the hydraulic "quick-couplers." The "quick-couplers" allow the operator to easily connect the gages to any pressure line, thus allowing pressure drop measurement between any two pressure taps. The different ranges of pressure gages provide maximum flexibility and accuracy. The U-tube manometer is permanently attached to the last two pressure taps. Since the manometer yields better accuracy, it was used to determine the fully developed friction factor, with the gages used for comparison and for entrance length measurement.

The flow rate was measured by a one-inch turbine meter located upstream from the test section. Turbine meter frequency was monitored by

a Hewlett Packard frequency counter. Turbine meter calibration is discussed in section 3.3.2.

3.1.2 Operation Modes

The overall flow system can be operated in the continuously pumped, 600 gallon (2270 liter) blowdown, or 3600 gallon (13,600 liter) blowdown modes. The pumped flow mode is capable of producing a 200 gpm (757 liters/min) flow rate by isolating the circulation system and using the catch tank as an inlet reservoir for the pump. The blowdown flow modes are utilized when the working fluid is a polymer solution, thereby minimizing polymer degradation and flow disturbances. A constant flow rate can be maintained by monitoring the tank pressure and the Vernier flow control valve position. Flow rates as high as 200 gpm may be achieved in the blowdown modes. The flow rates which can be obtained by these operation modes, though severely diminished due to considerable friction drag in the test section, may easily achieve Reynolds numbers based on the apparent viscosity of 5×10^4 and higher.

3.1.3 Viscometers

The viscosity of the polymer solutions used in this work was measured as a function of shear rate. Solution samples were taken from the downstream head tank during or shortly after each run, with the exception that samples of the initial mixture were collected before the fluid was circulated through the test section. Two Couette viscometers (Brookfield Synchro-Electric Model LVF with UL adaptor and a Fann model 35) were used to obtain the shear rate dependence of viscosity. The Brookfield viscometer measured Newtonian shear rates of 6.88 sec^{-1} to 68.8

sec^{-1}; the Fann viscometer from 340 sec^{-1} to 3254 sec^{-1}. Wider shear rate ranges may be measured in fluids considerably more viscous than those used in this experiment. The maximum possible system flow rate yielded a shear rate of about 7500 sec^{-1} using Equation (2.6). The flow rate was therefore restricted to values low enough that the system shear rate was reasonably near the viscometer shear rate range.

3.2 Safety and Reliability

This or any similar system demands good design and a well-researched, rigorously executed operating procedure to increase safety and reduce unexpected delays and costly repairs. Researchers must remember at all times that carelessness around the equipment involved in this work may easily result in injury and possibly death.

Reasonable care and judgment would prevent most accidents. Polymer solutions are very slick, so all actions inviting a fall should be avoided. The most dangerous part of the experiment, however, is pressurization and depressurization of the blowdown tanks. If a blowdown tank were exploded by excessive pressure, almost certainly everyone nearby would be hurt or killed. For example, if the 600 gallon tank exploded at 300 psia and 72°F, about 18,000 Btu, or 10 TNT lb-equivalents, would be released instantaneously. The following safety measures were implemented to prevent a major accident.

The 600 gallon blowdown tank critical pressure was estimated by conventional methods to be about 500 psi. The tank was then hydrostatically tested and found safe to at least 200 psi. A pneumatically controlled relief valve was installed, allowing the operator to release air from the tank; in addition, it automatically opens at a tank pressure of

40 to 50 psig, the exact value depending on supply pressure. A 0 to 160 psig pressure gage on the control panel allows the operator to visually monitor tank pressure. The air compressor controls were adjusted such that the maximum supply pressure is 100 psi. All of these safety systems were checked and found to be in good working order shortly before the experiments herein reported were performed. A rupture disc rated at 90 psi has since been installed. Since a rupture disc cannot "stick" or rust closed, it provides a failsafe reserve system in case all other safety systems fail.

Because several of the above-mentioned safety steps had not been implemented on the 3600 gallon tank at the time of these experiments, it was not used.

Even when safety is not a concern, reliability is demanded to prevent unnecessary expenses and delays. Good system reliability requires strict maintenance and operating procedures. A poor operating procedure resulted in "water hammer" and thus pipe failure during this work, requiring expensive and time-consuming repairs. A more carefully prepared operating procedure probably would have prevented the accident.

3.3 Experimental Procedure

3.3.1 Mixing Procedure

The polymers are shipped in powder form. The powder does not readily dissolve in water; therefore, proper mixing procedure is important.

Prior to mixing, the amount of polymer required for the desired concentration was weighed on a balance scale. Approximately 300 to 400 gallons of water was pumped into the 600 gallon catch tank. The water

was agitated with a wooden paddle, and the polymer was added into the turbulent wake by gently sifting through a triple-screen flour sifter. The sifting effectively prevented clumping, which would have resulted in nearly insoluble "fish-eyes." After all the polymer was added, the mixture was diluted to the proper concentration by adding more water. The final mixture was not circulated for at least 10 hours after mixing, allowing time for complete dissolution into a homogeneous mixture.

The method of measuring water volume was inaccurate, resulting in an estimated maximum error of ±10 percent for concentration. Since the data are correlated by the Weissenberg number, however, accurate estimation of the polymer concentration was unimportant.

3.3.2 System Calibration

The turbine meter was calibrated using water, 200 wppm solution of Separan AP-273, and 800 wppm solution of Separan AP-273. The water calibration resulted in a simple straight-line equation, as expected:

$$Q = 0.3515 + 0.06542\ F \qquad (3.1)$$

where Q is in gpm and F is in Hz. Equation (3.1) correlates the measured flow rates of water within ±2 percent of the reading as long as $F \geq 50$ Hz. For $F < 50$ Hz, flow through the 1 inch turbine meter at room temperature is no longer turbulent; thus the calibration curve is different [41]. Equation (3.1) correlates the measured flow rates of 200 wppm Separan AP-273 solution within ±4 percent for $F \geq 50$ Hz. It also correlates the measured flow rates of 800 wppm Separan AP-273 solution within $^{+4\%}_{-0\%}$ for $50 \text{ Hz} \leq F \leq 100$ Hz, with the error increasing dramatically beyond 100 Hz. However, 100 Hz corresponds to about 7 gpm, which

yields approximately the maximum shear rate attainable with the available viscometers. The flow rates were necessarily restricted to the viscometer shear rate ranges, so the error at F > 100 Hz was unimportant.

The turbine meter calibration results show that flow rates were correlated by Equation (3.1) to within ±4 percent for the experimental data reported herein.

The test section was calibrated by measuring the friction factor of water, then comparing to accepted standards. The data were compared to Blasius and Prandtl as given in Reference [43], and to Colebrook and Moody as given in Reference [44]. Results may be found in Table V. Prandtl's results are widely considered the most accurate, with the accuracy of other equations often determined by comparing results with Prandtl [43]. The calibration results agree quite satisfactorily with Prandtl's equation, with most errors well below 10 percent. Four points do have errors greater than 10 percent, but none is significantly higher.

3.3.3 Friction Factor and Reynolds Number Measurement

In addition to the system parameters and constant fluid properties, required data included a shear viscosity-shear rate curve, flow rate, and pressure drop.

The shear rate-shear viscosity curves were obtained using the viscometers discussed previously. The fluid was usually tested immediately after collection; however, in some cases it was stored and tested later. The results were computer analyzed to determine the Powell-Erying time constant.

The flow rate was determined by monitoring a frequency counter wired to the turbine meter. Frequencies were recorded several times during the experiment and the mean value was used to calculate the flow rate.

The manometer pressure drop was recorded several times also, and the mean value used in analysis. The Fanning friction factor is

$$f = \frac{\pi^2 (\rho_M - \rho_S) g h D^5}{32 \rho_S L Q^2} \tag{3.2}$$

which reduces to

$$f = 8.278 \times 10^{-3} \frac{h}{Q^2} \tag{3.3}$$

for the specific apparatus, where h is the pressure drop in inches of mercury, and Q is the flow rate in gpm.

To avoid polymer deposits on the pipe walls which might have resulted in erroneous data, the system was periodically flushed with water. Flushing was performed every time a batch of mixture was degraded and discarded. In addition, flushing was systematically performed as polymer batches were being degraded.

Each batch of mixture required several passes through the test section before it was degraded enough that $Ws < Ws_{cf}$. Since $Ws_{cf} = Ws_{cf}(Re_a)$, it was necessary to hold Re_a approximately constant for all data runs with the same batch. Two batches of polymer were degraded. The experimental results are reported in Chapter IV.

CHAPTER IV

RESULTS AND DISCUSSION

Three batches of polymer were mixed and degraded, with concentrations of 200, 200, and 400 wppm, respectively. Batch No. 1 was allowed to sit idle far too long, and passively degraded so much that all friction factor measurements deviated significantly from the asumptotic value. Batch No. 2 was circulated six times, with about 50 minutes required for each pass. The data runs were labeled R2.01 through R2.06, respectively. The Reynolds number was approximately constant, with a mean value of Re_a = 34,700 and a standard deviation of s = 900. Batch No. 3 required 21 passes, each about 40 minutes in duration. Data runs were labeled R3.01 through R3.21, respectively. Again, Re_a was approximately constant with mean Re_a = 28,900 and s = 500. In each case, the solvent was Stillwater, Oklahoma, tap water. The pH is normally between 7.5 and 8.0.

In each case, the Fanning friction factor increased with residence time, as expected. The friction factor of the 200 wppm batch increased much more rapidly than that of the 400 wppm batch, possibly because the former was subjected to higher shear stresses [7, 10]. Figure 24 shows that the friction factor is not a monotonically increasing function of time, but the trend is obvious and consistent.

A trend is again obvious in Figure 25, which shows the friction factor as a function of Weissenberg number at constant Re_a. However,

there is a considerable amount of scatter in the data, a rather disturbing fact. The Reynolds number did vary slightly, in spite of attempts at fixing it. Variations in the Reynolds number cause variations in the measured friction factor. Similar changes are observed in the asymptotic friction factor [44],

$$f_A = 0.20\ Re_a^{-0.48} \tag{4.1}$$

The data of Figure 25 are replotted in Figure 26 as % DEV versus Ws. % DEV is the deviation of measured friction factor from the asymptotic friction factor. Unfortunately, this is not an improvement. Rather, the scatter is slightly worse, although the difference is negligible.

A close look at Figures 25 and 26 reveals several disturbing facts. First, the problem of scatter arises as has already been mentioned. Second, there is no clearly identifiable region where $f \neq f(Ws)$, or a flat portion of the curve. This fact suggests that $Ws \leq Ws_{cf}$, even at the initial state; however, the earliest measured friction factors were 12 percent less than the predicted asymptotic value. Finally, there is no sudden increase in f or even in the slope of the curve, $df/d(Ws)$, to suggest an obvious critical Weissenberg number.

4.1 Estimates of the Critical Weissenberg Number

The lack of any clearly identifiable sudden change in the curves of Figures 25 and 26 complicate the method of estimating Ws_{cf}. Since friction data are generally considered acceptable if within ±10 percent of the correct value, the author has chosen to define Ws_{cf} as the value of Ws which results in a measured friction factor 10 percent greater than the asymptotic value. From Figure 26, the estimated values are

$$Ws_{cf} = 0.60 \sim 0.75, \qquad Re_a = 34{,}700$$

and

$$Ws_{cf} = 1.7 \sim 2.2, \qquad Re_a = 28{,}900.$$

4.2 Data Reliability and Accuracy

Scatter in the data is a primary concern, as related earlier. The observed scatter causes all the data to be suspect. An error analysis was performed by the method of Kline and McClintock [45] (details are presented in Appendix C), and yields probable errors of 8.6 percent for measured friction factor, 9.0 percent for Reynolds number, and 4.3 percent for asymptotic friction factor.

Probable error in the estimated Weissenberg number is much greater. Elbirli and Shaw [31] found a mean error of 13 percent. The time constant ideally is inversely proportional to absolute temperature [46], so at room temperature changes of a few degrees should have negligible effects on the time constant. The author, however, noted changes in the time constant which were apparently attributable to temperature changes in the range $23° \pm 3°C$. Note particularly the rheological data from R3.21, for which $T = 21°C$ during viscosity measurements.

The major contributor to error in the time constant was the measurement of zero shear viscosity. Elbirli and Shaw [31] found that accurate measurement of the zero shear viscosity is extremely important to the accuracy of the time constant estimate. The rheological data plots of Figure 27 indicate problems in the zero shear region. For Run R2.06, the viscosity is dependent on shear rate even at the very lowest shear rates. For R3.20, the viscosity is roughly constant at the lower

shear rates. These results indicate that the lower Newtonian region of zero shear for R2.06 lies in the shear rate range below 6.88 sec^{-1}. The transition from the lower Newtonian to the non-Newtonian region appears to be above 13.8 sec^{-1} for R3.20; however, R3.20 yields a larger time constant than R2.06. This is unexpected, since Ng and Hartnett [2] found that the transition from the lower Newtonian to the non-Newtonian region shifts toward higher shear rates as the fluid elasticity decreases. One would therefore expect R2.06 to exhibit a higher shear rate transition than any other data run.

The time constant should monotonically decrease as residence time increases. If Re_a is constant, Ws should also decrease. Figure 28 shows that the measured value of Ws tended to decrease with increasing residence time; however, the decrease was inconsistent rather than monotonic.

The result of discussion in the previous paragraphs is a very large error in the measured time constant, and thus of Ws. The Kline and McClintock method cannot be used to estimate the uncertainty in the time constant because Equation (2.11) contains a complicated function, $\sinh^{-1}(\lambda \dot{\gamma})$, it is implicit in λ, and it is curve-fit to the experimental data. If the uncertainty in zero shear viscosity is estimated as suggested by Kline and McClintock, the uncertainty in the time constant can be estimated. The author estimated a 20 percent error in the zero shear viscosity at 10 to 1 odds. The measured zero shear viscosity was multiplied by 1.2, and the resulting value assumed to be the viscosity at a shear rate of one sec^{-1}. This data point was added to the measured data and the time constant recalculated. The uncertainty was defined to be the difference between the time constant calculated in this manner and that

reported in Table VII. At the fluid's critical condition, uncertainty estimates at 10 to 1 odds were 0.150 percent for batch No. 2 (Re_a = 34,700) and 100 percent for batch No. 3 (Re_a = 28,900). From Appendix C the corresponding uncertainty estimates in the critical Weissenberg number were 150 and 100 percent, respectively.

CHAPTER V

CONCLUSIONS AND RECOMMENDATIONS

5.1 Conclusions

The estimated values of Ws_{cf} are:

$$Ws_{cf} = 0.60 \sim 0.75, \qquad Re_a = 34{,}700$$

$$Ws_{cf} = 1.7 \sim 2.2, \qquad Re_a = 28{,}900.$$

The large error in Ws renders these estimates useless, however. In the author's opinion, two useful conclusions result from this work. They are:

1. The Powell-Eyring model with the infinite shear viscosity defined as that of the solvent is a good model for determination of the fluid characteristic time. It yields fairly accurate results and solvent viscosities are easily found. At very low elasticities it tends to yield too low values of the time constant; however, these values are consistently reproducible, with minimum sensitivity to the experimental shear rate range. Many users do not have the capability of measuring the fluid viscosity at shear rates of 0.10^5 sec^{-1}, which is the most accurate infinite shear viscosity. The author therefore recommends use of the Powell-Eyring model with infinite shear viscosity defined as that of water.

2. The estimates of Ws_{cf} differ from the previously reported values [2, 13-15] by factors of 2 to 17. Very large errors would be required

to cause such discrepancies. The uncertainty in zero shear viscosity and the differences between the Powell-Eyring models used certainly contribute to the discrepancies. However, they are not completely explained by allowance for the expected errors. Therefore, investigations should be performed by researchers not associated with the University of Illinois at Chicago Circle to verify their results.

5.2 Recommendations

There exists a definite need for further research of viscoelastic fluid flows. The zero shear viscosity must be measured more accurately than in these experiments. Currently, a falling sphere viscometer is being tested at Oklahoma State University. When these tests are complete, the falling sphere viscometer shall be used to measure the zero shear viscosity in future research efforts at that institution.

There have been several investigations of viscoelastic heat transfer, but much more work is required in that area. Estimates of the critical Weissenberg number for heat transfer are much higher than Ws_{cf} [2, 13-15], and are unaffected by the error at low elasticities in the proposed Powell-Eyring model. These, too, require verification by independent researchers. Many of the works referenced in Chapters I through IV also contain discussions of heat transfer phenomena. The author particularly recommends five works [1, 2, 13-15] as good background material for a study of heat transfer in viscoelastic fluids.

Currently, there is no satisfactory method to predict the friction factor and heat transfer coefficient of intermediate viscoelastic fluids (Weissenberg number below the critical value). Hopefully, this aspect of viscoelastic fluid flow will receive attention in the near future.

The experimental apparatus used by the author also was constructed for heat transfer studies. The test section shall be heated by resistance in the pipes, producing a constant heat flux. Much valuable research of viscoelastic fluid flow and heat transfer is expected from the Oklahoma State University team during the next few years.

REFERENCES

[1] Cho, Y. I., and J. P. Hartnett. "Non-Newtonian Fluids in Circular Pipe Flow." Advances in Heat Transfer, Vol. 15 (1982), pp. 59-141.

[2] Ng, K. S., and J. P. Hartnett. "Effects of Mechanical Degradation on Pressure Drop and Heat Transfer Performance of Polyacrylamide Solutions in Turbulent Pipe Flow." Studies in Heat Transfer. New York: McGraw-Hill Book Co., 1979.

[3] Ghajar, A. J. "Investigation of Heat Transfer in Flows With Drag Reduction." Research proposal, January, 1983.

[4] Virk, P. S., H. S. Mickley, and K. A. Smith. "The Ultimate Asymptote and Mean Flow Structure in Toms' Phenomenon." Trans. ASME, Vol. 37 (June, 1970), p. 488.

[5] Kwack, E. Y., Y. I. Cho, and J. P. Hartnett. "Heat Transfer to Polyacrylamide Solutions in Turbulent Pipe Flow: The Once-Through Mode." AIChE J., Vol. 27 (1981), p. 123.

[6] Tung, T. T., K. S. Ng, and J. P. Hartnett. "Influence of Rheological Property Changes on Friction and Convective Heat Transfer in a Viscoelastic Polyacrylamide Solution." Heat Transfer, 6th Int. Heat Transfer Conf., 1978, Vol. 5 (1978), p. 329.

[7] Patterson, R. W., and F. H. Abernathy. "Turbulent Flow Drag Reduction and Degradation With Dilute Polymer Solutions." J. Fluid Mech., Vol. 43, No. 4 (1970), p. 689.

[8] Fisher, D. H., and F. Rodriquez. "Degradation of Drag-Reducing Polymers." J. Appl. Polymer Sci., Vol. 15 (1971), p. 2975.

[9] Ting, R. Y., and R. C. Little. "Characterization of Drag Reduction and Degradation Effects in the Turbulent Pipe Flow of Dilute Polymer Solutions." J. Appl. Polymer Sci., Vol. 17 (1973), p. 3345.

[10] Ram, A., and A. Kadim. "Shear Degradation of Polymer Solutions." J. Appl. Polymer Sci., Vol. 14 (1970), p. 2145.

[11] Stratton, R. A. "The Dependence of Non-Newtonian Viscosity on Molecular Weight for 'Monodisperse' Polystyrene." J. Colloid Interface Sci., Vol. 22 (1966), p. 517.

[12] Ferry, J. D. Viscoelastic Properties of Polymers. New York: John Wiley & Sons, 1969.

[13] Kwack, E. Y., Y. I. Cho, and J. P. Hartnett. "Effect of Weissenberg Number on Turbulent Heat Transfer of Aqueous Polyacrylamide Solutions." Presented at the 7th International Heat Transfer Conference, Munich, West Germany, September, 1982.

[14] Kwack, E. Y., and J. P. Hartnett. "Effect of Diameter on Critical Weissenberg Numbers for Polyacrylamide Solutions in Turbulent Pipe Flow." Int. J. Heat Mass Transfer, Vol. 25, No. 6 (1982), p. 797.

[15] Kwack, E. Y., and J. P. Hartnett. "Effect of Solvent Chemistry on Critical Weissenberg Numbers." Int. J. Heat Mass Transfer, Vol. 25, No. 9 (1982), p. 1445.

[16] Yoo, S. S. "Heat Transfer and Friction Factors for Non-Newtonian Fluids in Turbulent Pipe Flow." (Unpub. Ph.D. thesis, University of Illinois at Chicago Circle, 1974.)

[17] Rodriquez, F. Principles of Polymer Systems. 2nd Ed. New York: McGraw-Hill Book Co., 1982.

[18] Kays, W. M., and M. E. Crawford. Convective Heat and Mass Transfer. 2nd Ed. New York: McGraw-Hill Book Co., 1980.

[19] Tung, T. T., K. S. Ng, and J. P. Hartnett. "Heat Transfer to Polyacrylamide Solutions in Turbulent Pipe Flow: The Once-Through Mode." 20th National Heat Transfer Conf., 1981.

[20] Skelland, A. H. P. Non-Newtonian Flow and Heat Transfer. New York: John Wiley & Sons, 1967.

[21] Metzner, A. B., and J. C. Reed. "Flow of Non-Newtonian Fluids--Correlation of the Laminar, Transition, and Turbulent-Flow Regions." AIChE J., Vol. 1 (1955), p. 434.

[22] Ng, K. S., Y. I. Cho, and J. P. Hartnett. "Heat Transfer Performance of Concentrated Polyethylene Oxide and Polyacrylamide Solutions." AIChE J., Vol. 26 (1980), p. 250.

[23] Edwards, M. F., and R. Smith. "The Turbulent Flow of Non-Newtonian Fluids in the Absence of Anomalous Wall Effects." J. Non-Newtonian Fluid Mech., Vol. 7 (1980), p. 77.

[24] Ng, K. S., J. P. Hartnett, and T. T. Tung. "Heat Transfer of Concentrated Drag Reducing Viscoelastic Polyacrylamide Solutions." AIChE Paper. 17th Heat Transfer Conf., 1977, p. 74.

[25] Sylvester, N. D., and S. L. Rosen. "Laminar Flow in the Entrance Region of a Cylindrical Tube. Part II. Non-Newtonian Fluids." AIChE J., Vol. 21 (1975), p. 699.

[26] Kwack, E. Y., Y. I. Cho, and J. P. Hartnett. "Pressure Drop Measurements of Aqueous Polyox Solutions in Square Duct and Capillary Tube Flows." 73rd AIChE Annual Meeting, 1980, 1980.

[27] Gold, P. I., P. K. Amar, and B. E. Swaidan. "Friction Reduction Degradation in Dilute Poly (Ethylene Oxide) Solutions." J. Appl. Polymer Sci., Vol. 17 (1973), p. 333.

[28] Kenis, P. R. "Turbulent Flow Friction Reduction Effectiveness and Hydrodynamic Degradation of Polysaccharides and Synthetic Polymers." J. Appl. Polymer Sci., Vol. 15 (1971), p. 607.

[29] Reiner, M. "The Deborah Number." Physics Today, Vol. 17 (1964), p. 62.

[30] Bird, R. B. "Experimental Tests of Generalized Newtonian Models Containing a Zero-Shear Viscosity and a Characteristic Time." Can. J. Chem. Eng., Vol. 43 (1965), p. 161.

[31] Elbirli, B., and M. T. Shaw. "Time Constant From Shear Viscosity Data." J. Rheology, Vol. 22 (1978), p. 561.

[32] Bird, R. B., R. C. Armstrong, and O. Hassager. "Dynamics of Polymeric Liquids." Fluid Mechanics. Vol. 1. New York: John Wiley & Sons, 1977.

[33] Middleman, S. The Flow of High Polymers. New York: Interscience, 1968.

[34] Ree, F. H., T. Ree, and H. Eyring. "Relaxation Theory of Transport Problems in Condensed Systems." Ind. Eng. Chem., Vol. 50 (1958), p. 1036.

[35] Kwack, E. Y. "Effect of Weissenberg Number on Turbulent Heat Transfer and Friction Factor of Viscoelastic Fluids." (Unpub. Ph.D. thesis, University of Illinois at Chicago Circle, 1983.)

[36] Kwack, E. Y., J. P. Hartnett, and Y. I. Cho. "Chemical Effects in the Flow of Dilute Polymer Solutions." Letters Heat Mass Transfer, Vol. 7 (1980), p.1.

[37] Banijamali, S. H., E. W. Merrill, K. A. Smith, and L. H. Peebles, Jr. "Turbulent Drag Reduction by Polyacrylic Acid." AIChE J., Vol. 20 (1974), p. 824.

[38] Sellin, R. H. J., and E. J. Loeffler. "Drag Reduction Measurements With Polyacrylic Acid Under Different Solvent pH and Salt Conditions." Proc. 2nd Int. Conf. Drag Reduction, 1977, C2-11, 1977.

[39] Elliott, J. H., and F. S. Stow, Jr. "Solutions of Drag-Reducing Polymers--Diameter Effect and Rheological Properties." J. Appl. Polymer Sci., Vol. 15 (1971), p. 2743.

[40] Ting, R. Y. "Diameter Dependence of the Cutoff Molecular Weights of Drag-Reducing Polymers." J. Appl. Polymer Sci., Vol. 20 (1976), p. 3017.

[41] Ellison, B. A. "Turbine Meters for Liquid Measurement." Mechanical Engineering, Vol. 105, No. 2 (1983), p. 52.

[42] White, F. M. Viscous Fluid Flow. New York: McGraw-Hill Book Co., 1974.

[43] Haaland, S. E. "Simple and Explicit Formulas for the Friction Factor in Turbulent Pipe Flow." J. Fluids Eng., Vol. 105 (March, 1983), p.89.

[44] Cho, Y. I., and J. P. Hartnett. "Analogy for Viscoelastic Fluids--Momentum, Heat, and Mass Transfer in Turbulent Pipe Flow." Letters Heat Mass Transfer, Vol. 7 (1980), p. 339.

[45] Kline, S. J., and S. A. McClintock. "Describing Uncertainties in Single-Sample Experiments." Trans. Mech. Engr. (January, 1953), p. 3.

[46] Rouse, P. E. "A Theory of the Linear Viscoelastic Properties of Dilute Solutions of Coiling Polymers." J. Chem. Phys., Vol. 21 (1953), p. 1272.

APPENDIX A

FIGURES

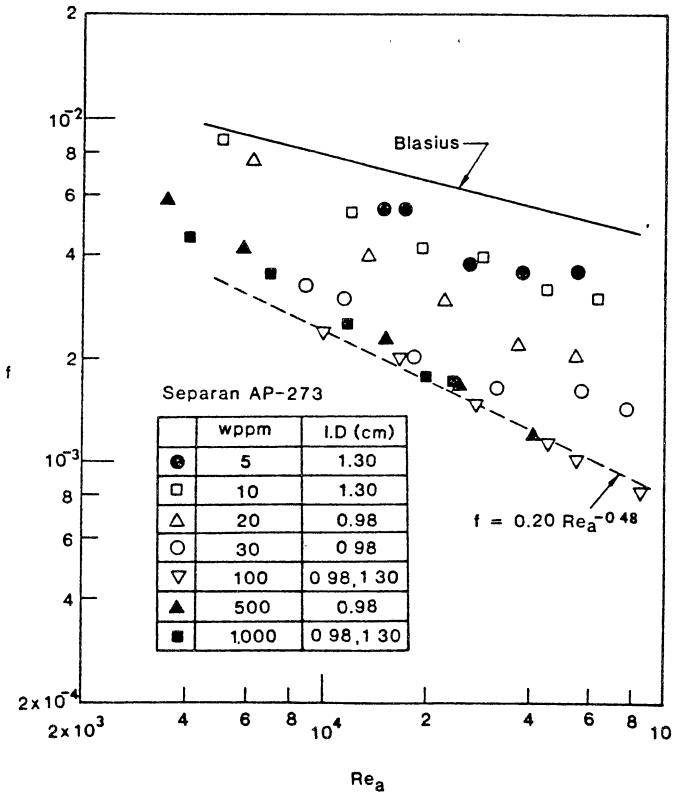

Figure 1. Fanning Friction Factor Versus Re_a for Separan Solutions in Once-Through Flow System, Taken From [1]

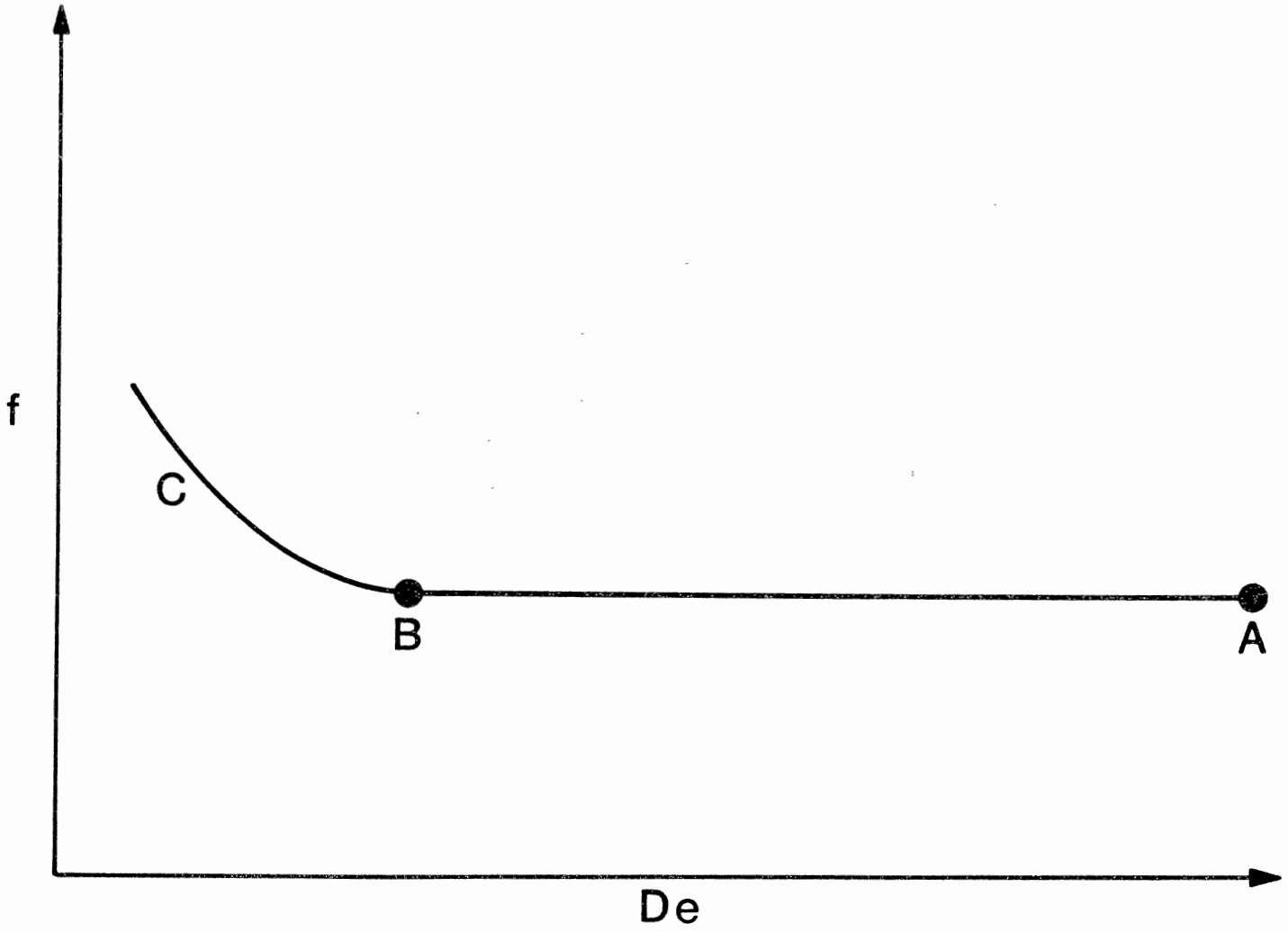

Figure 2. Mechanical Degradation at a Fixed Reynolds Number (A, Fresh Solution; B, Critical Deborah Number; C, Degraded Solution)

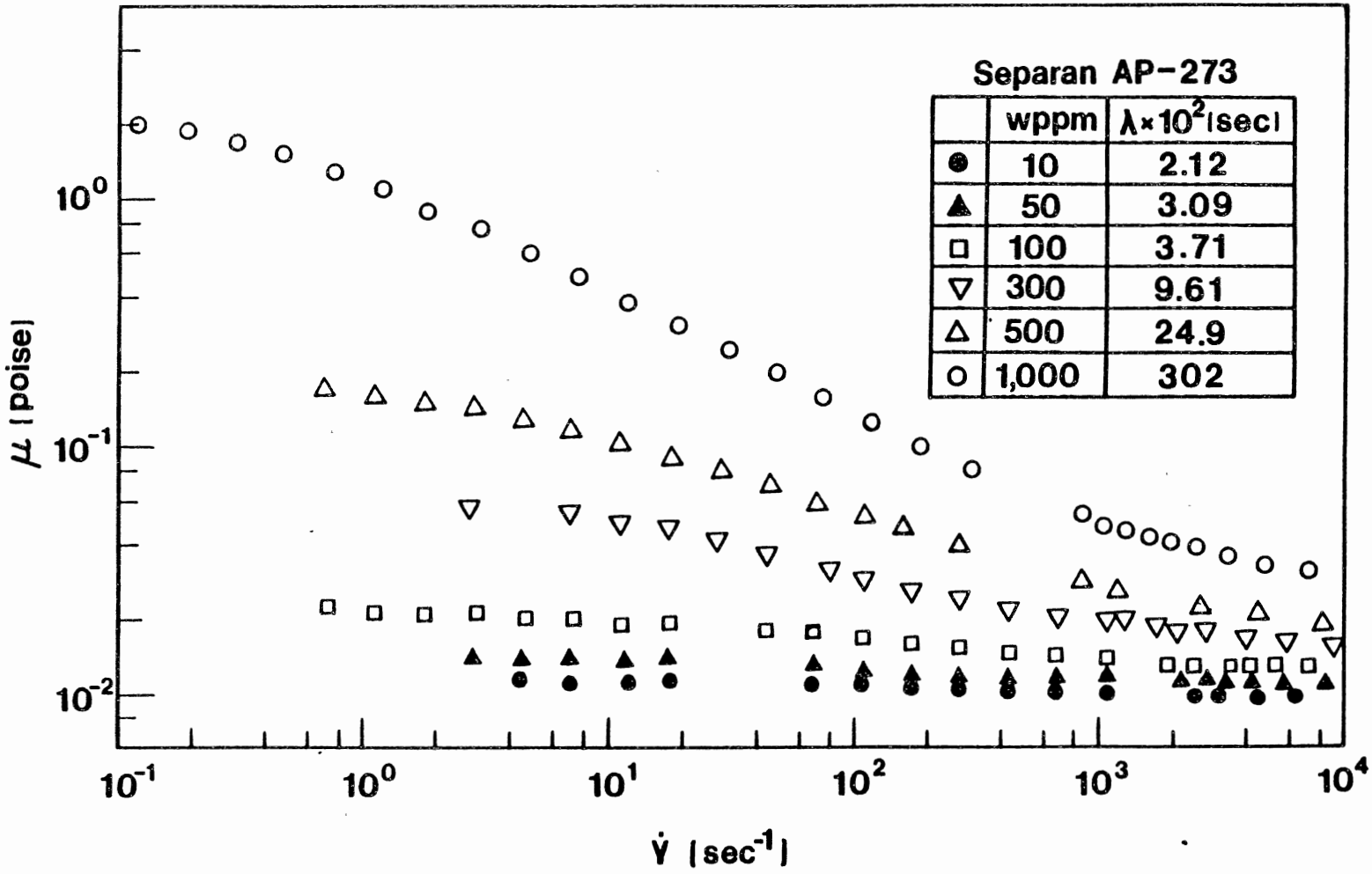

Figure 3. Concentration Effect on Apparent Viscosity of Separan Solutions, Taken From [35]

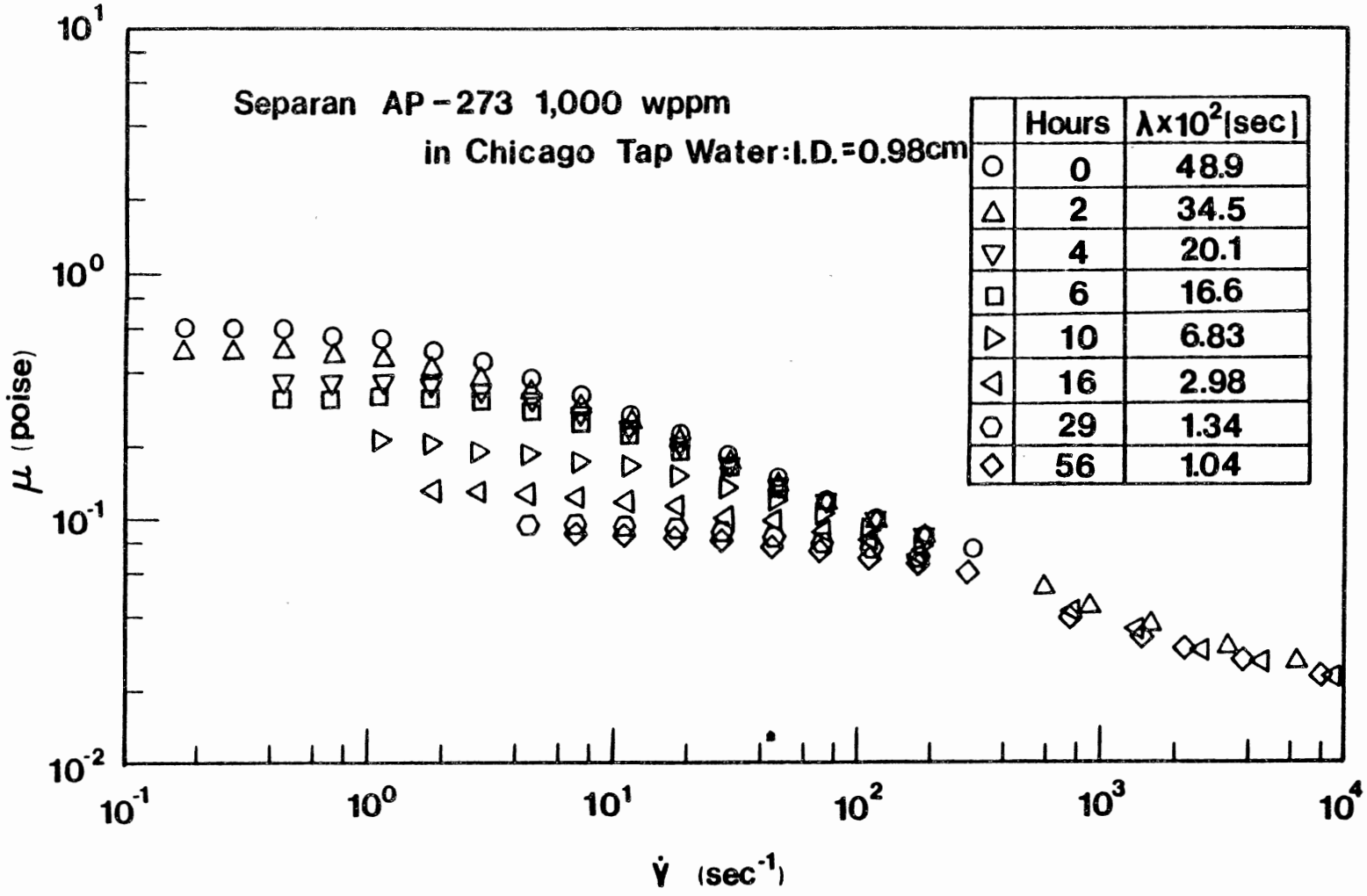

Figure 4. Degradation Effect on Apparent Viscosity of Separan 1,000 wppm Solution in a 0.98 cm I.D. Tube, Taken From [35]

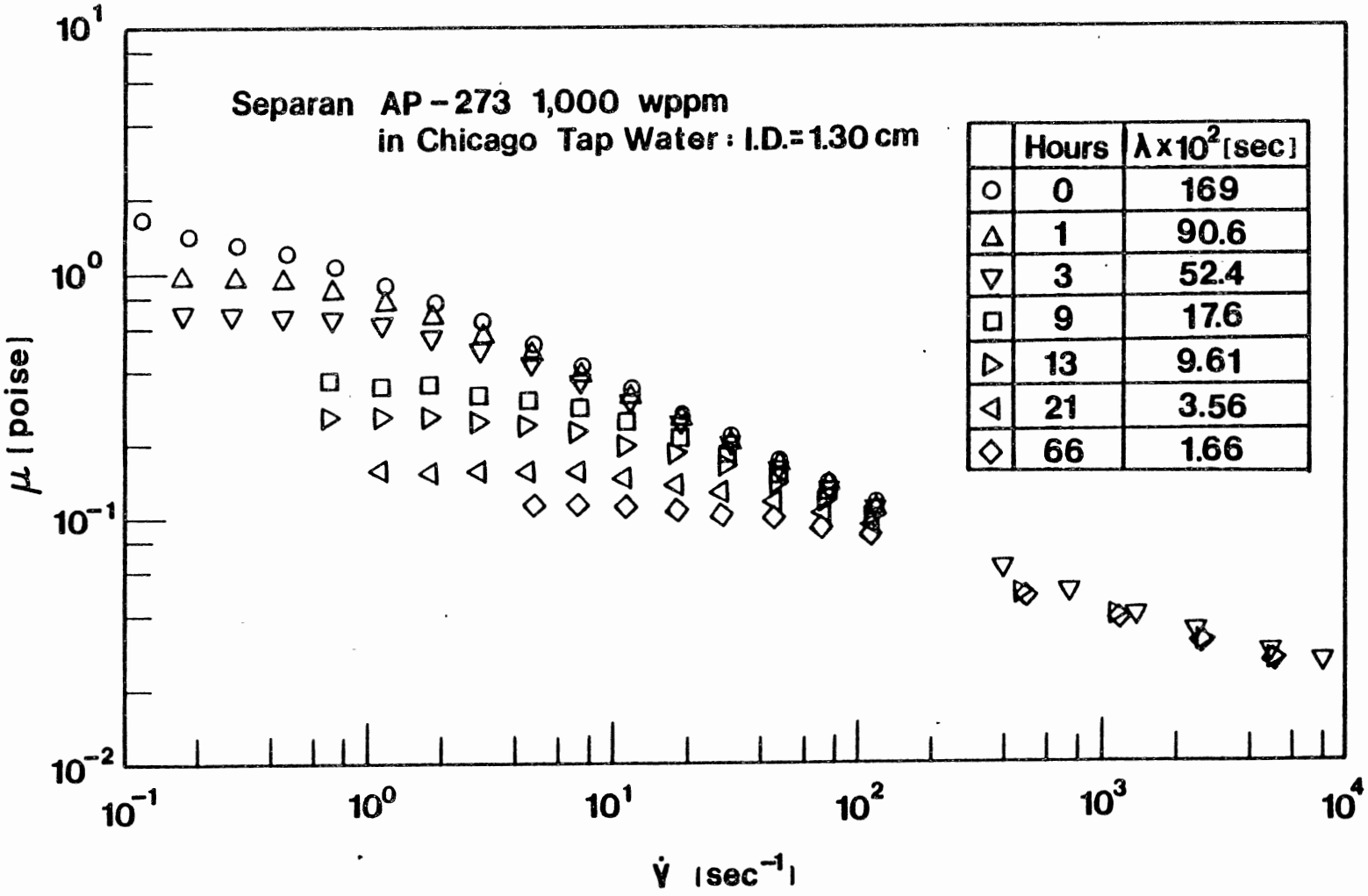

Figure 5. Degradation Effect on Apparent Viscosity of Separan 1,000 wppm Solution in a 1.30 cm I.D. Tube, Taken From [35]

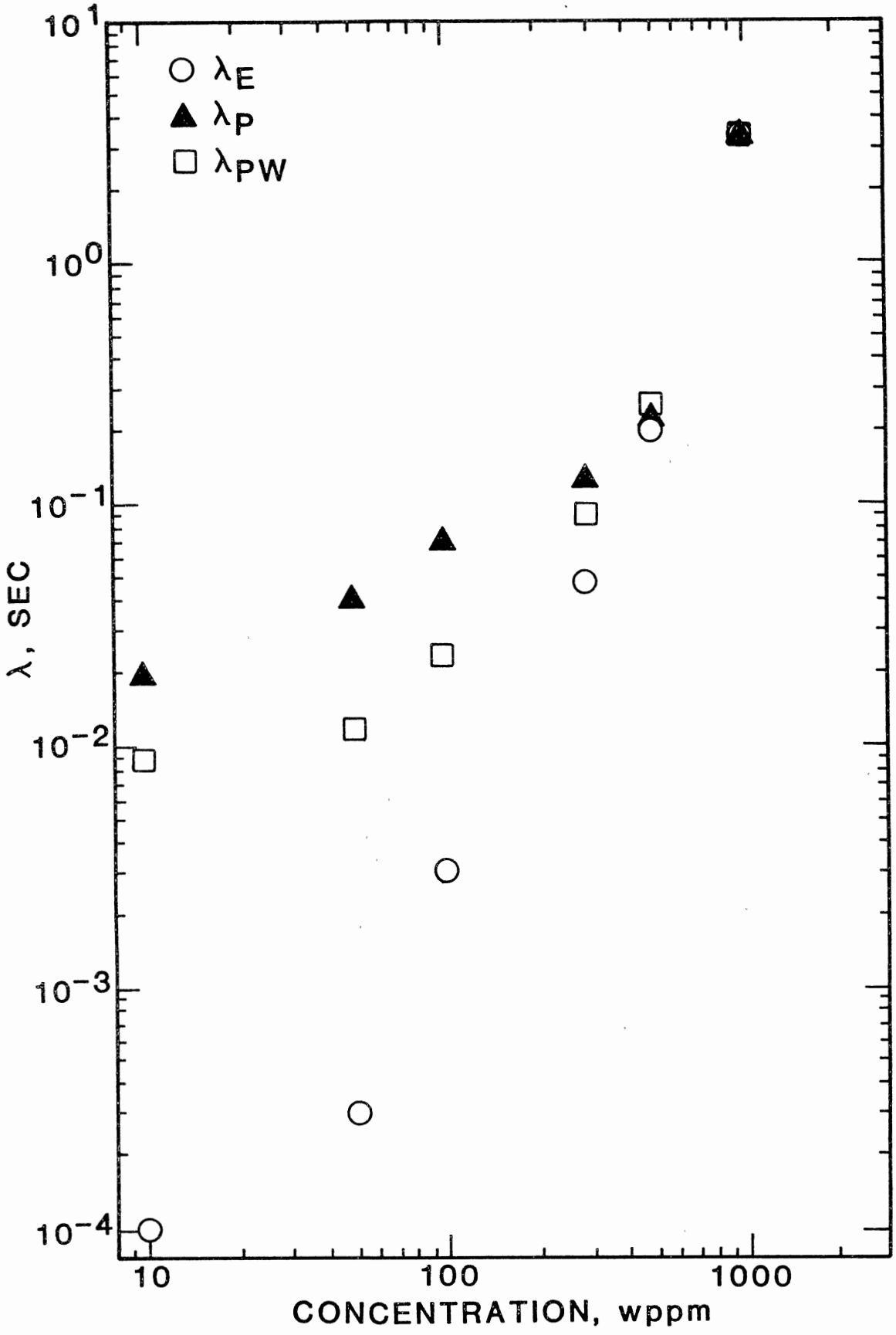

Figure 6. Concentration Dependence of Different Time Constants

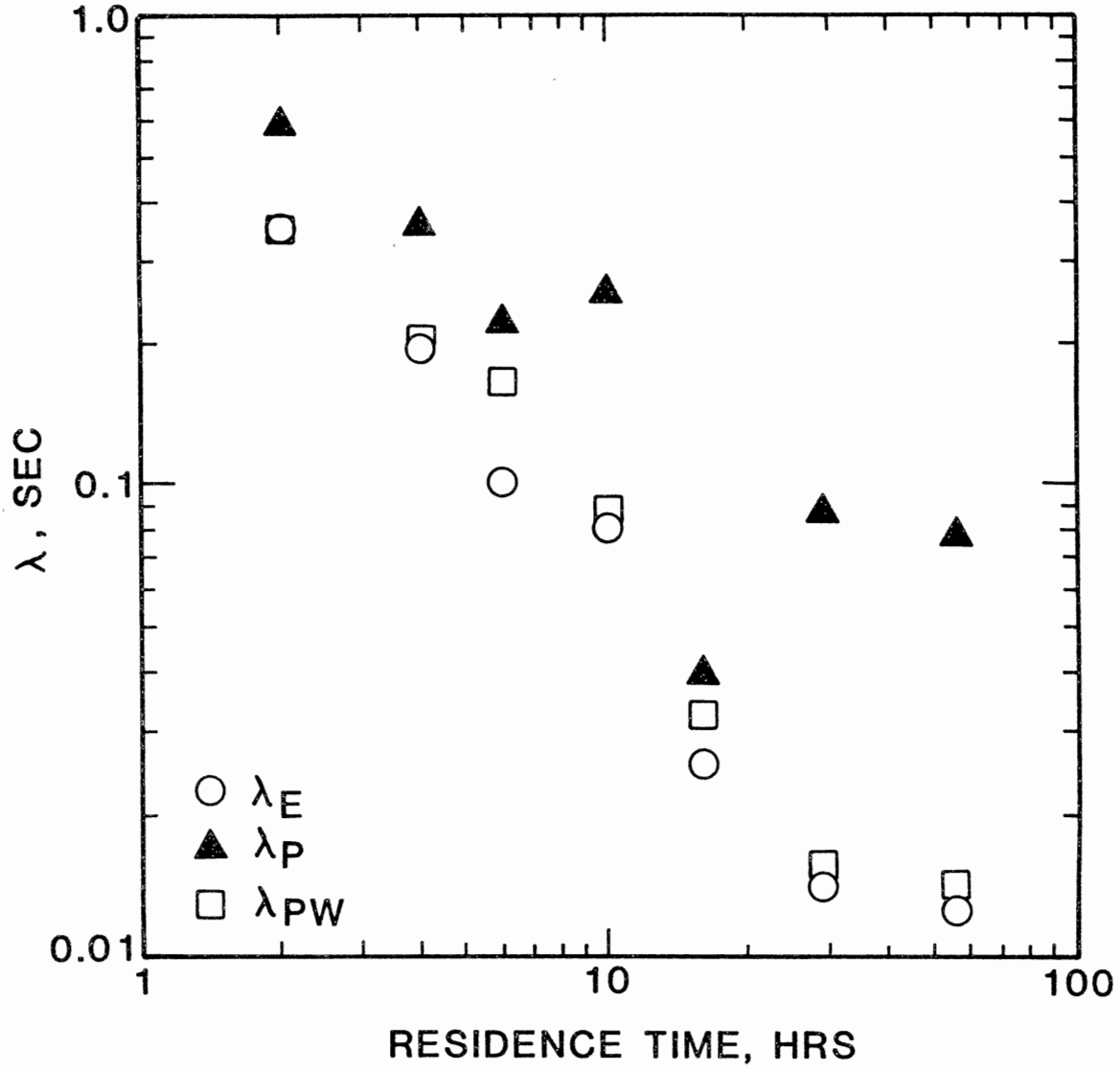

Figure 7. Residence Time Dependence of Different Time Constants

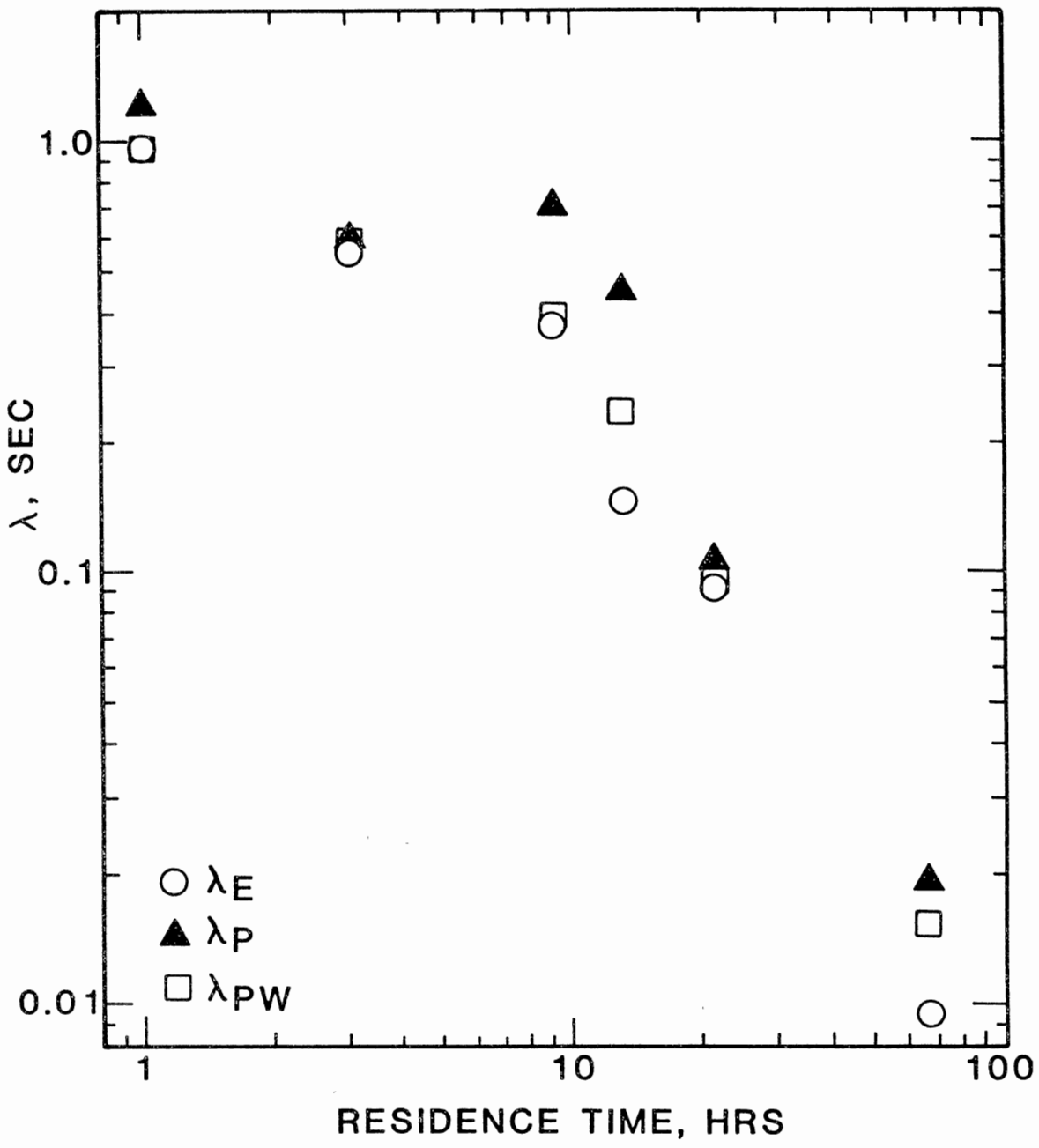

Figure 8. Residence Time Dependence of Different Time Constants

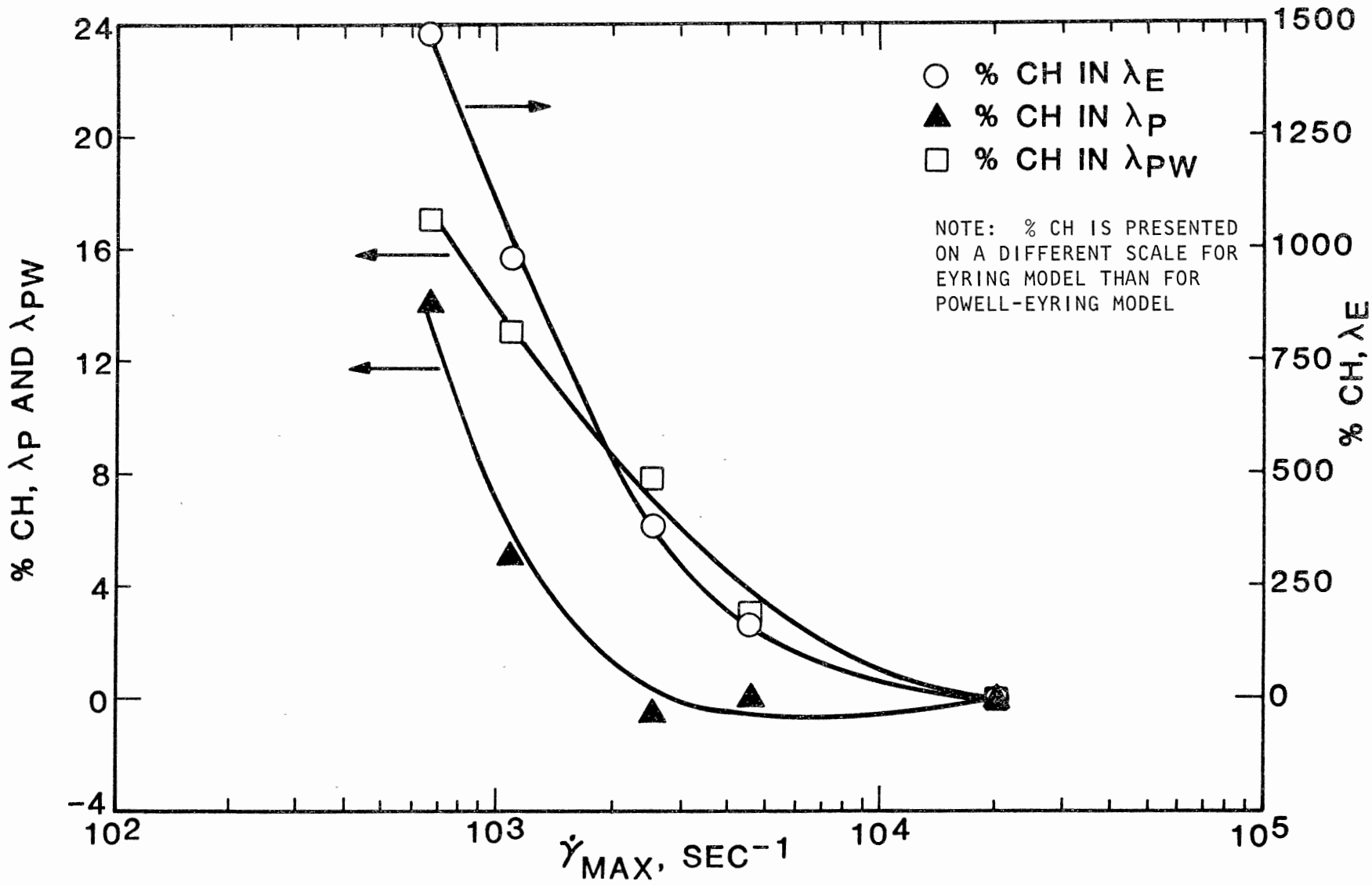

Figure 9. Effect of Shear Rate Range on Different Time Constants From Data Set 3.0010

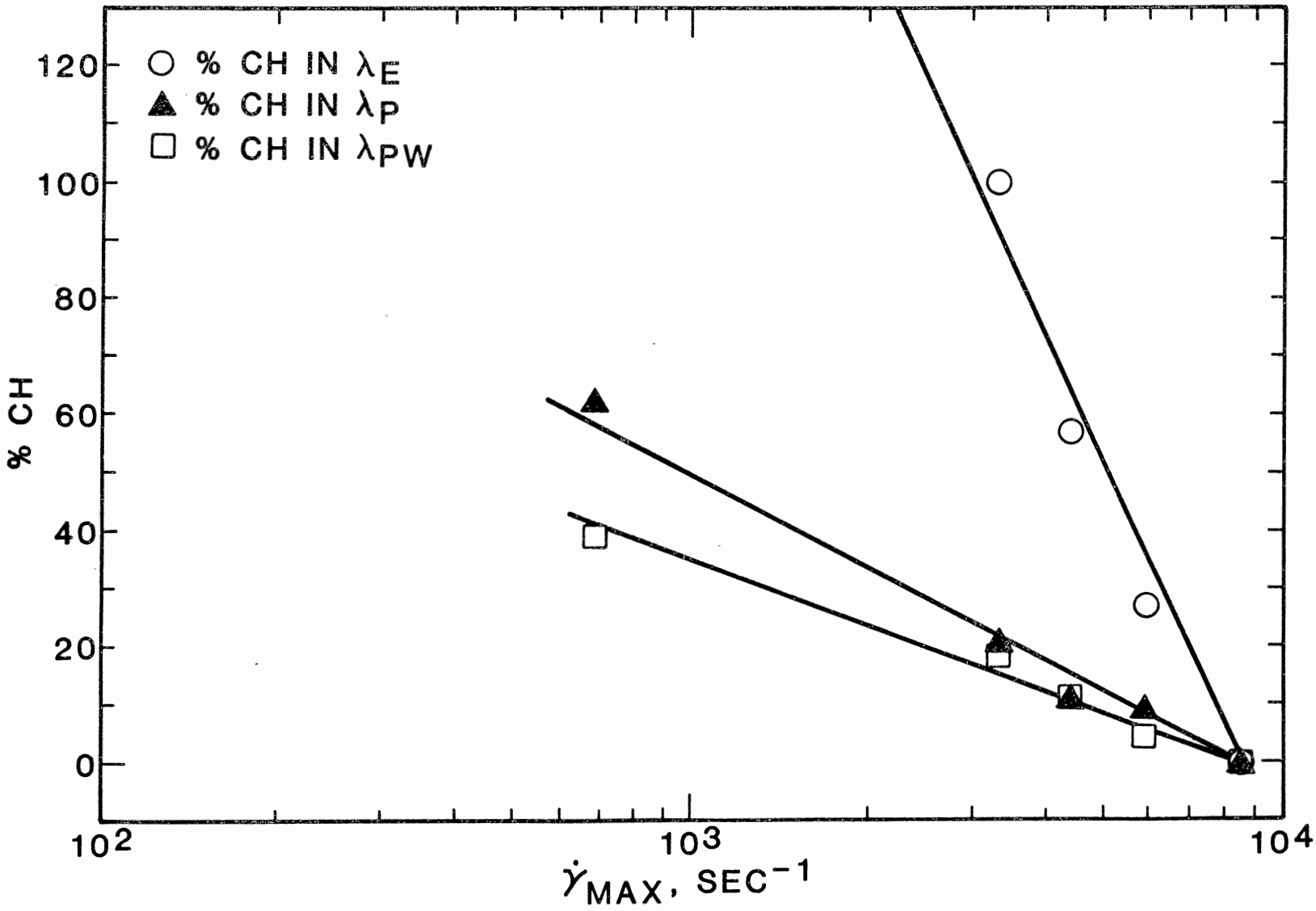

Figure 10. Effect of Shear Rate Range on Different Time Constants From Data Set 3.0050

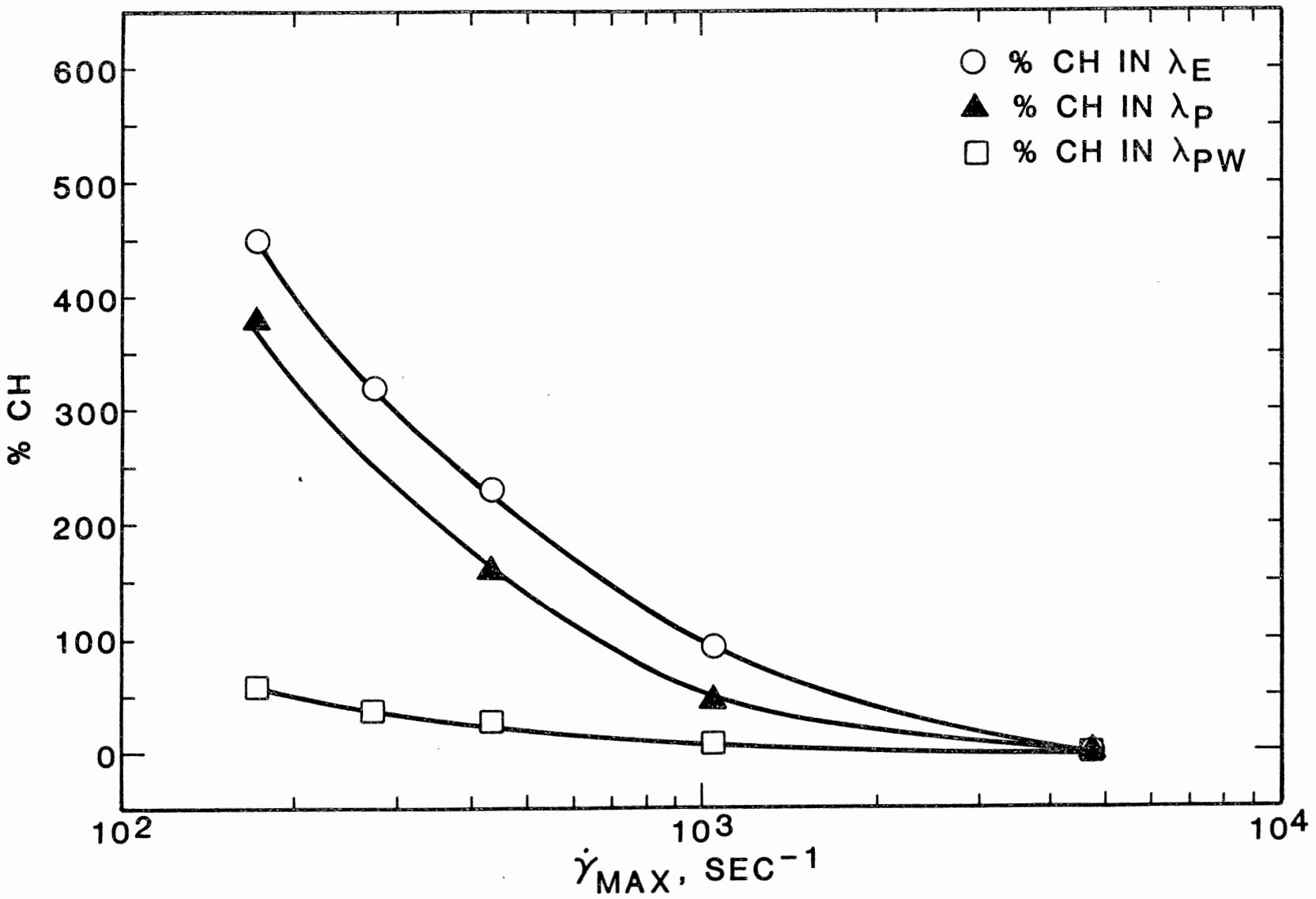

Figure 11. Effect of Shear Rate Range on Different Time Constants From Data Set 3.0100

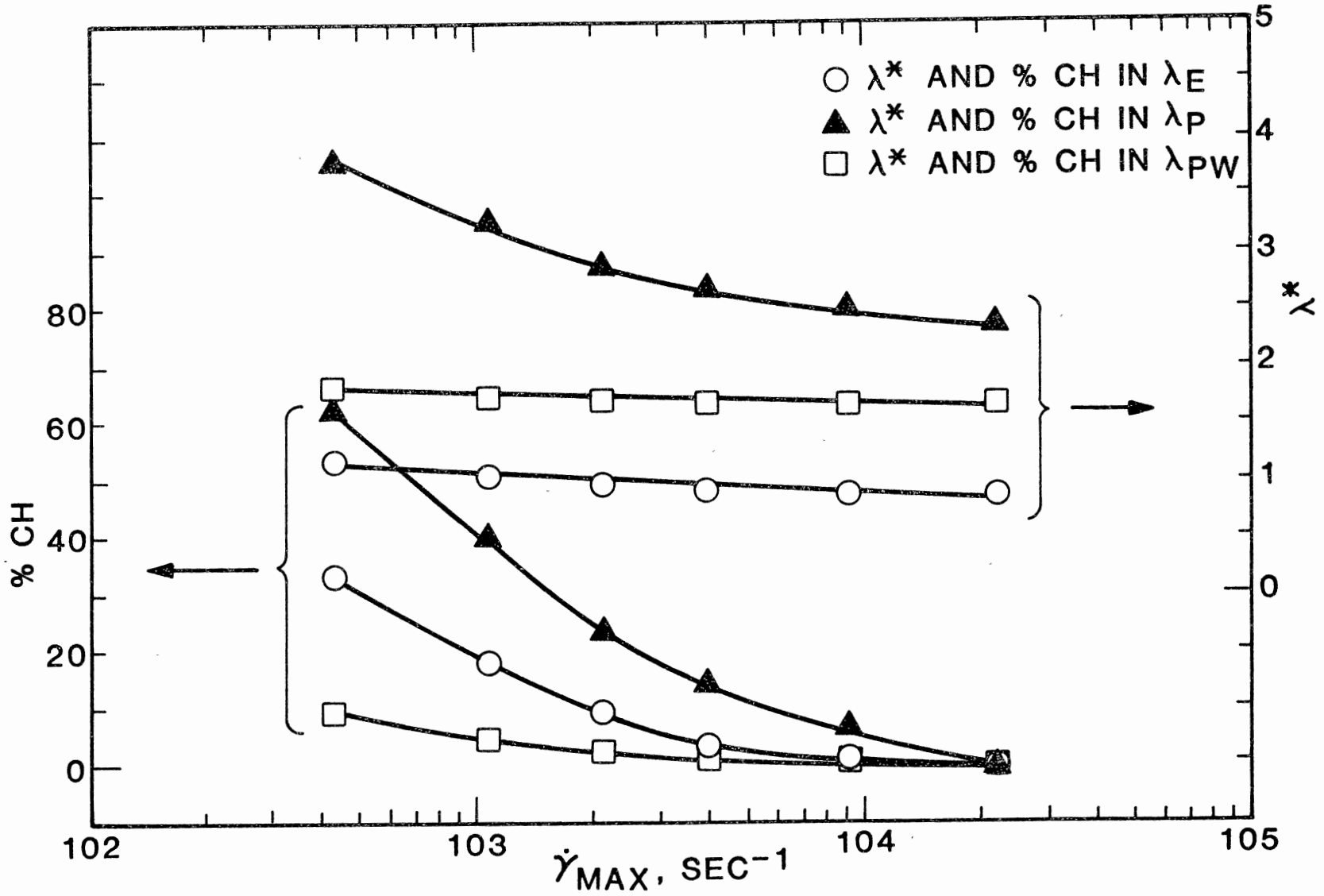

Figure 12. Effect of Shear Rate Range on Different Time Constants From Data Set 3.0300

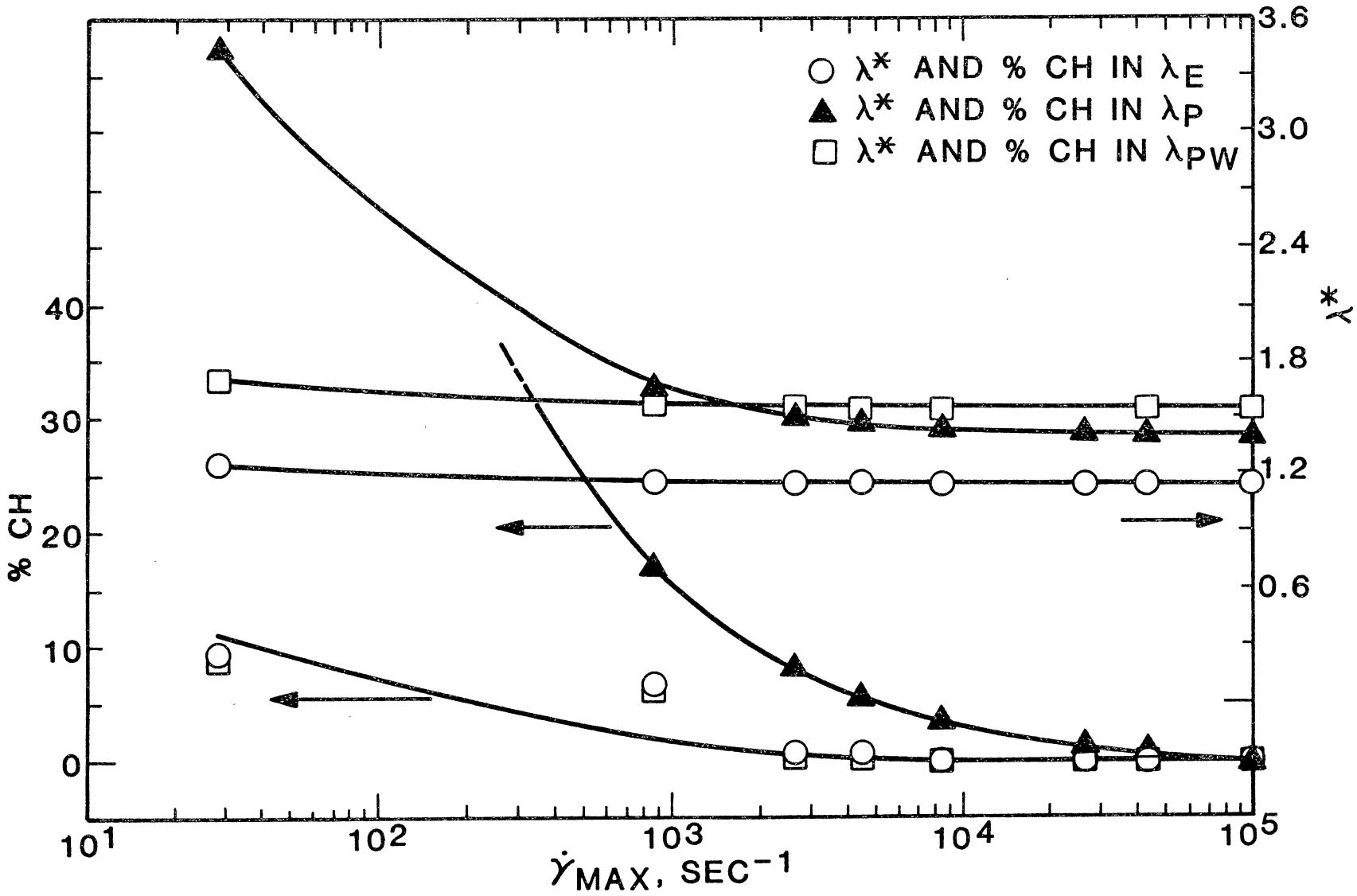

Figure 13. Effect of Shear Rate Range on Different Time Constants From Data Set 3.0500

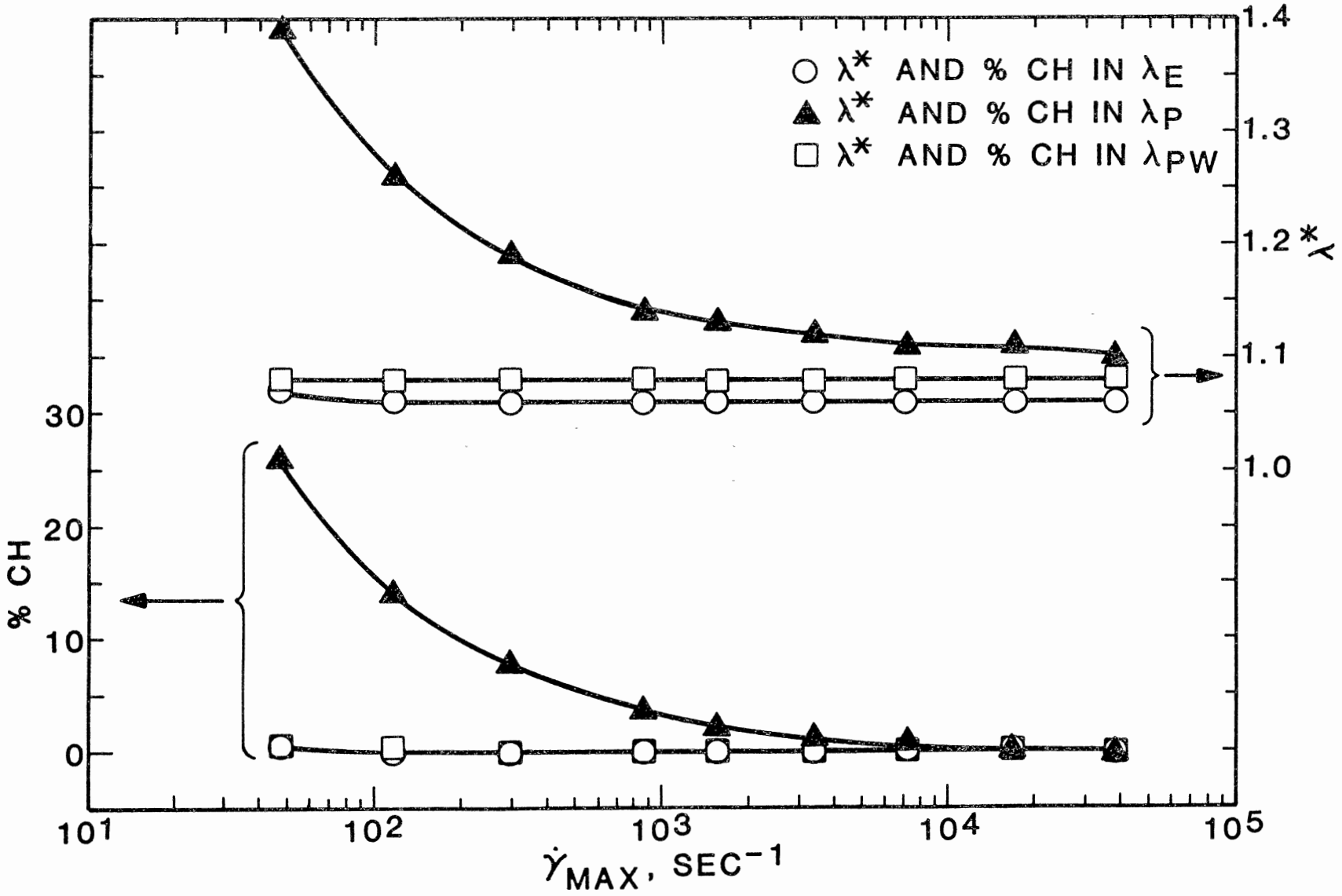

Figure 14. Effect of Shear Rate Range on Different Time Constants From Data Set 3.1000

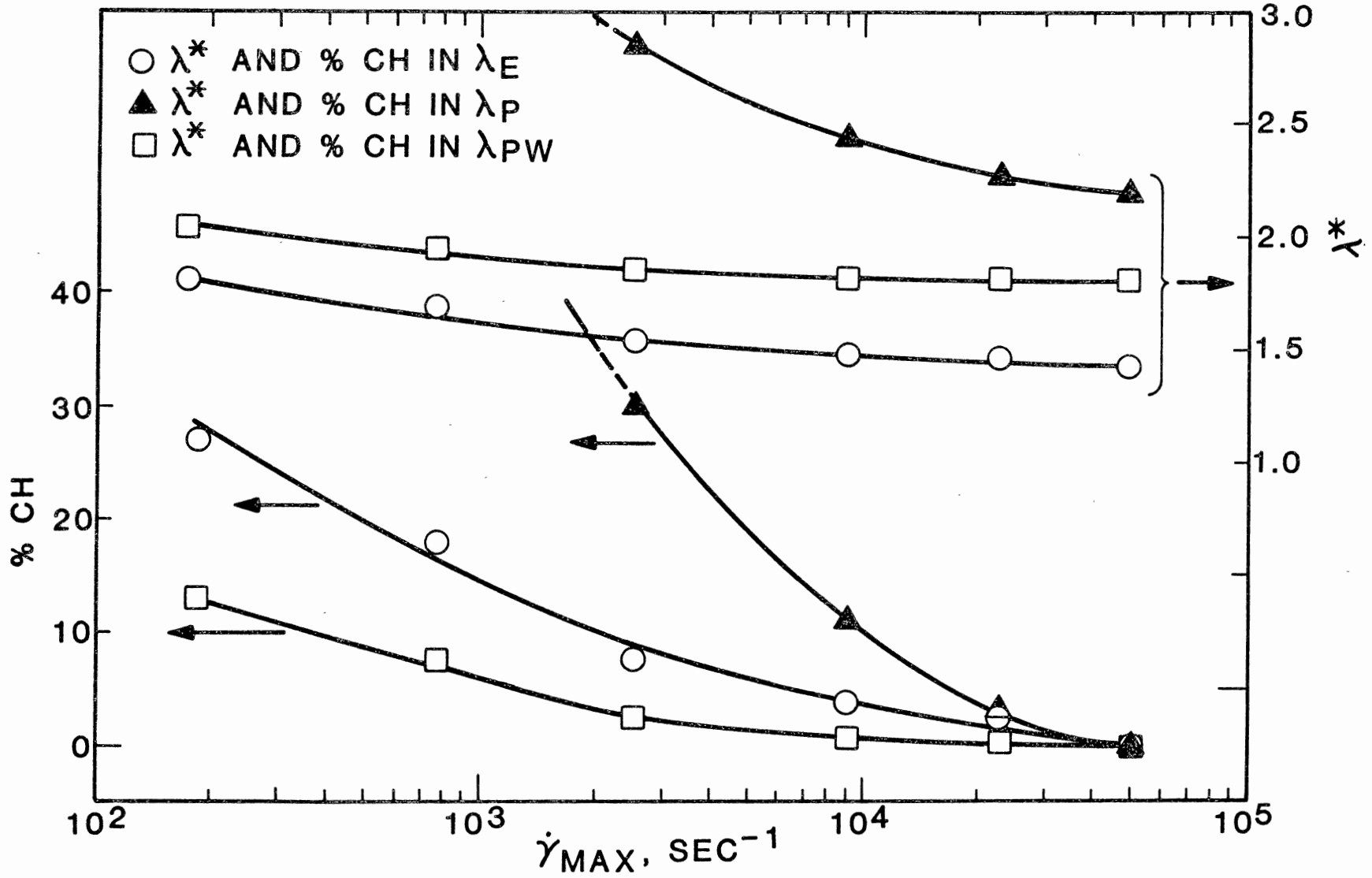

Figure 15. Effect of Shear Rate Range on Different Time Constants From Data Set 4.16

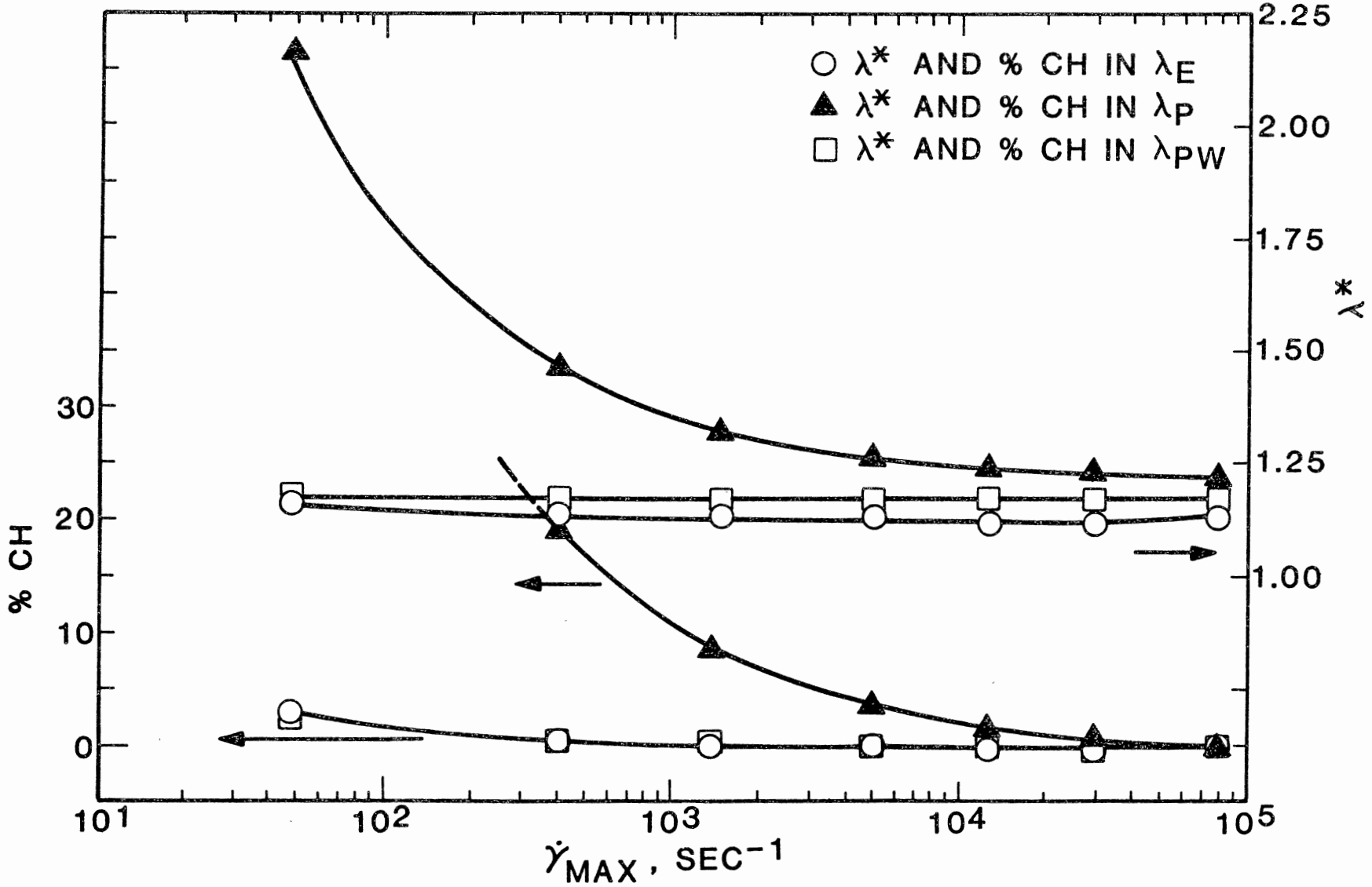

Figure 16. Effect of Shear Rate Range on Different Time Constants From Data Set 5.03

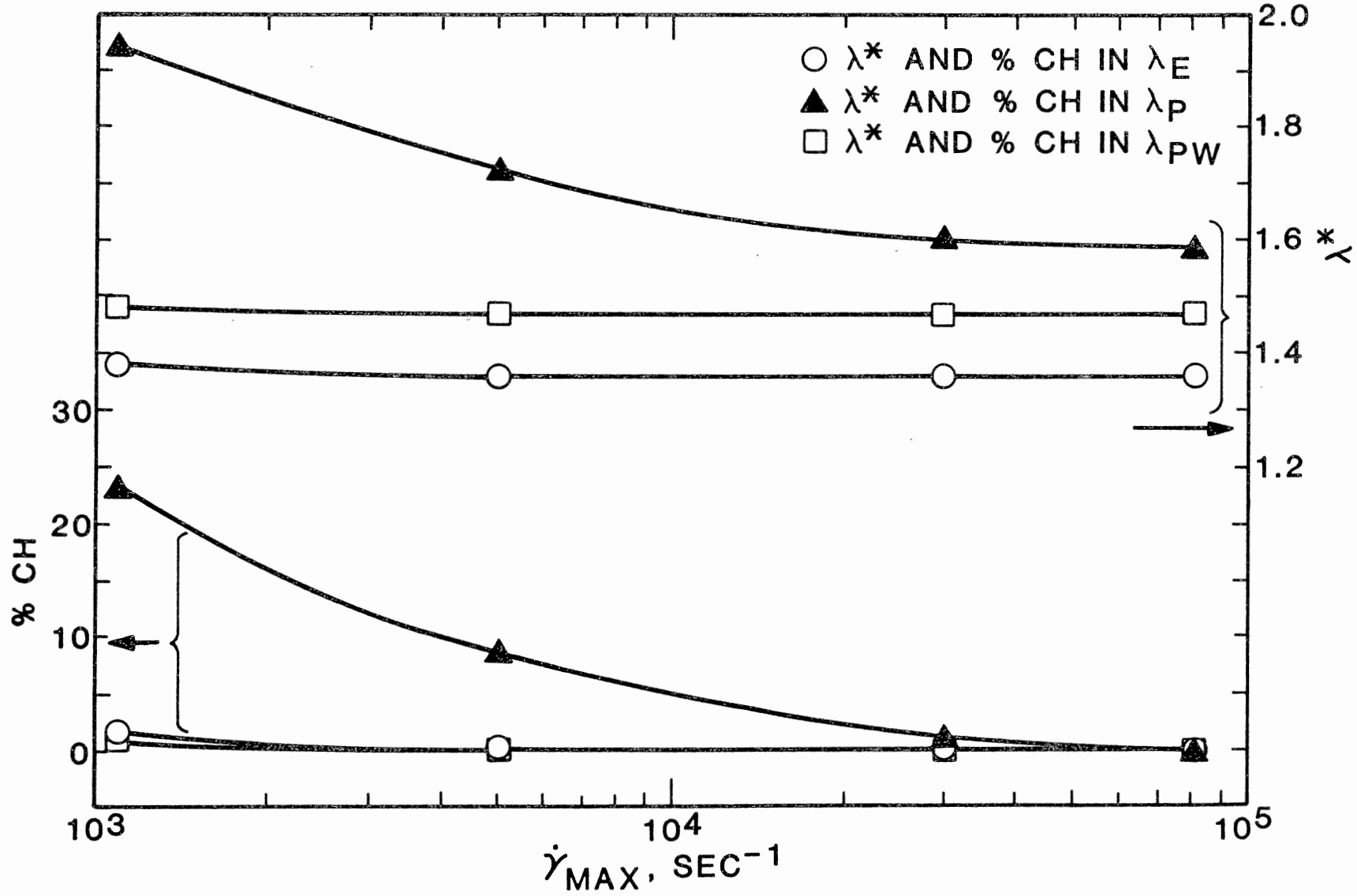

Figure 17. Effect of Shear Rate Range on Different Time Constants From Data Set 5.21

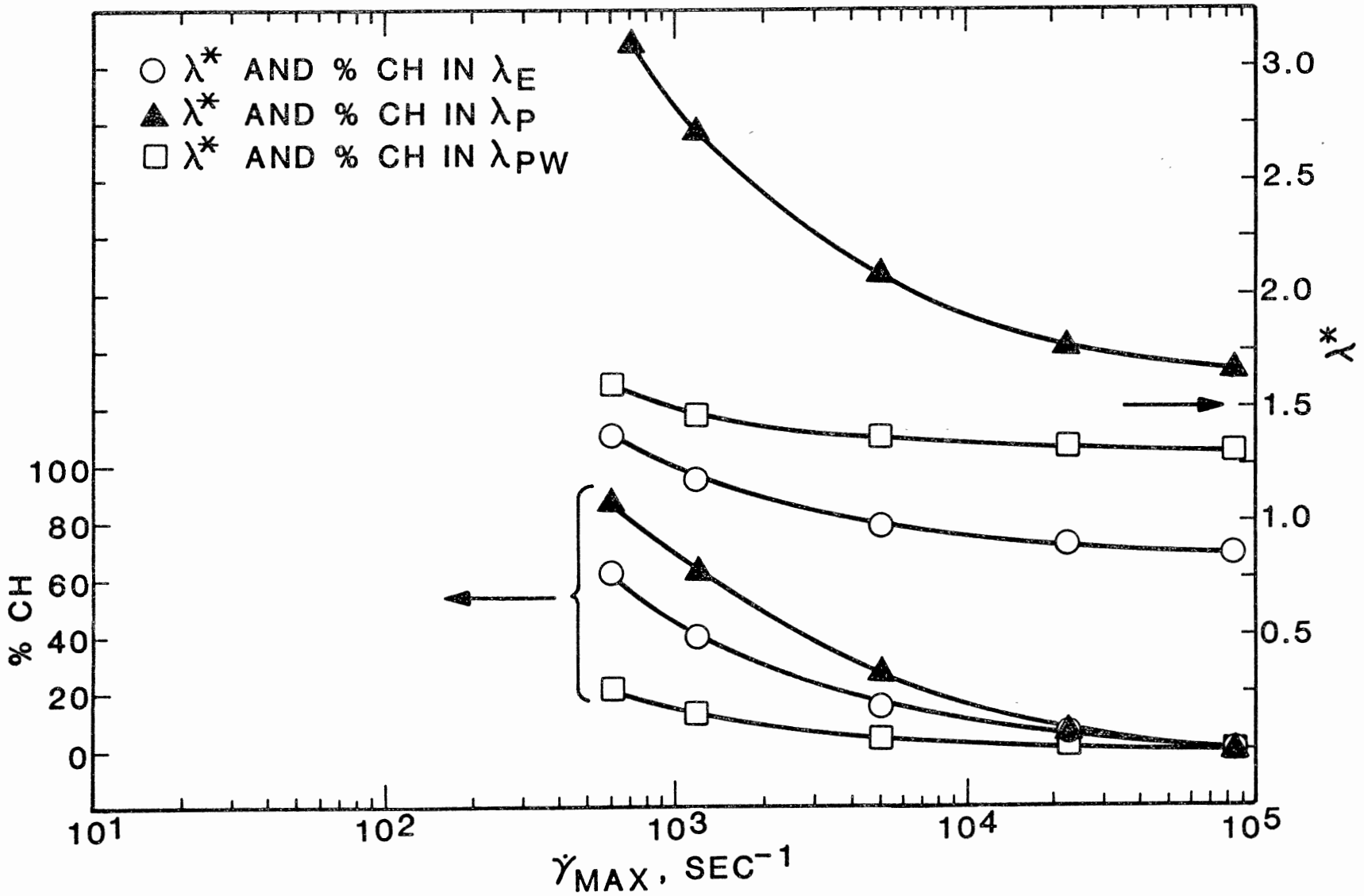

Figure 18. Effect of Shear Rate Range on Different Time Constants From Data Set 5.66

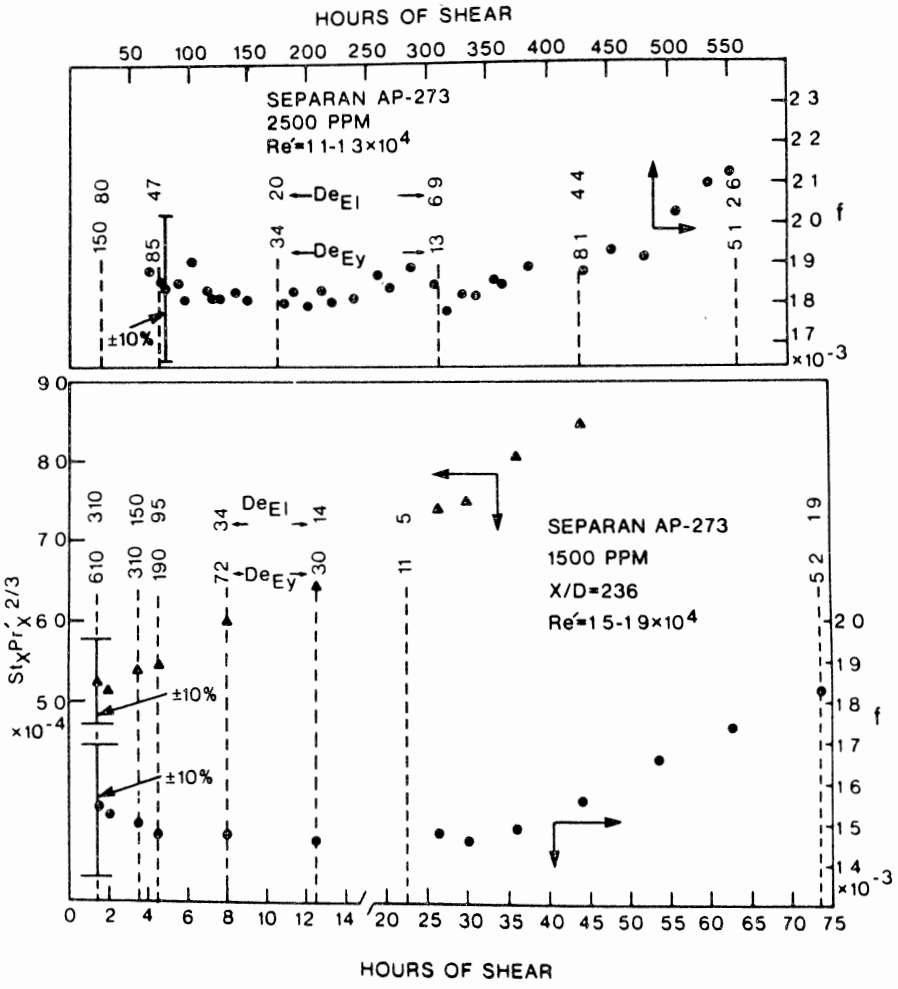

Figure 19. Dimensionless Heat Transfer Coefficient and Fanning Friction Factor Versus Hours of Shear With Deborah Numbers Shown at Different Hours of Shear, Taken From [2]

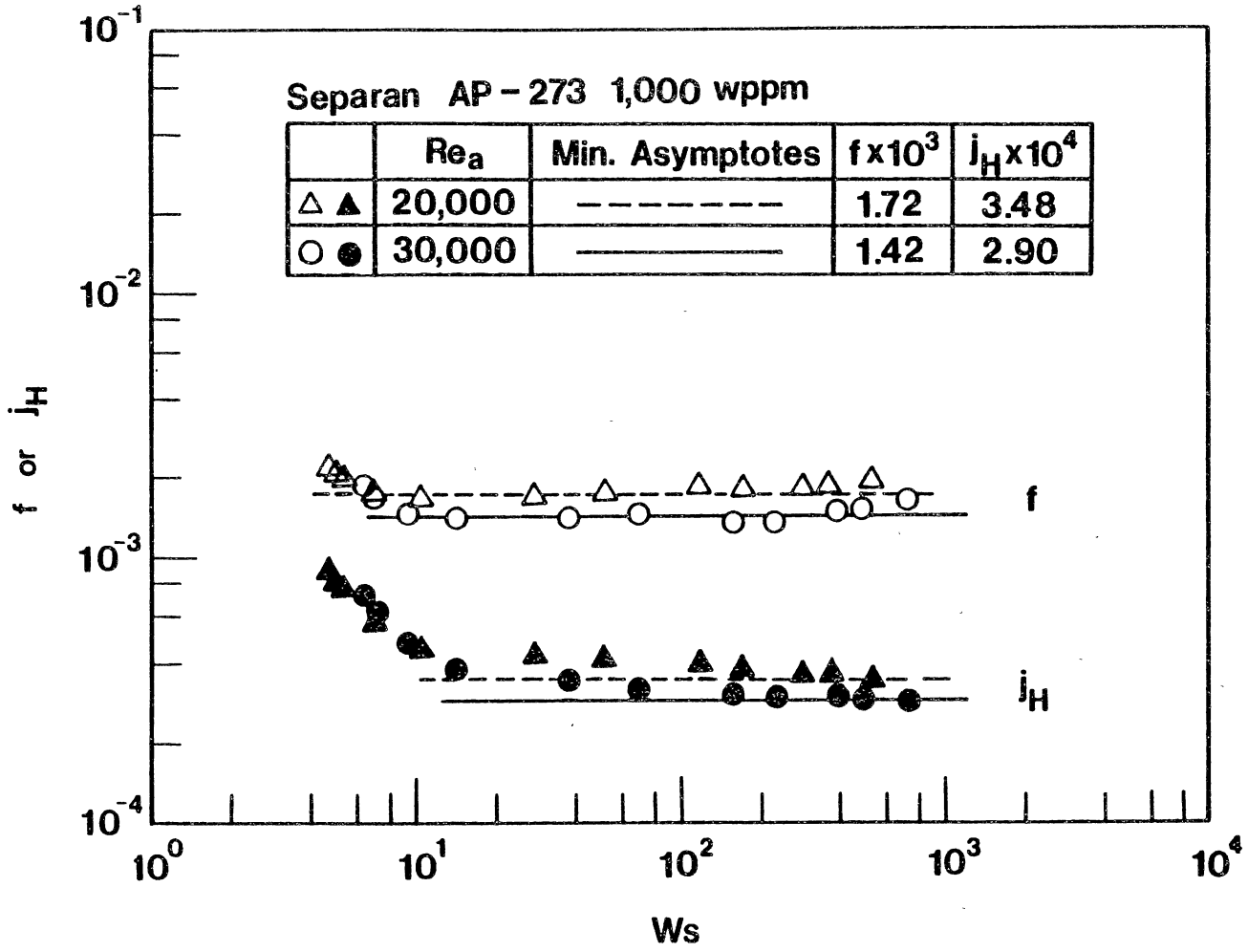

(a) 1000 wppm Separan Solution

Figure 20. Fanning Friction Factor and Dimensionless Heat Transfer Factor Versus Ws

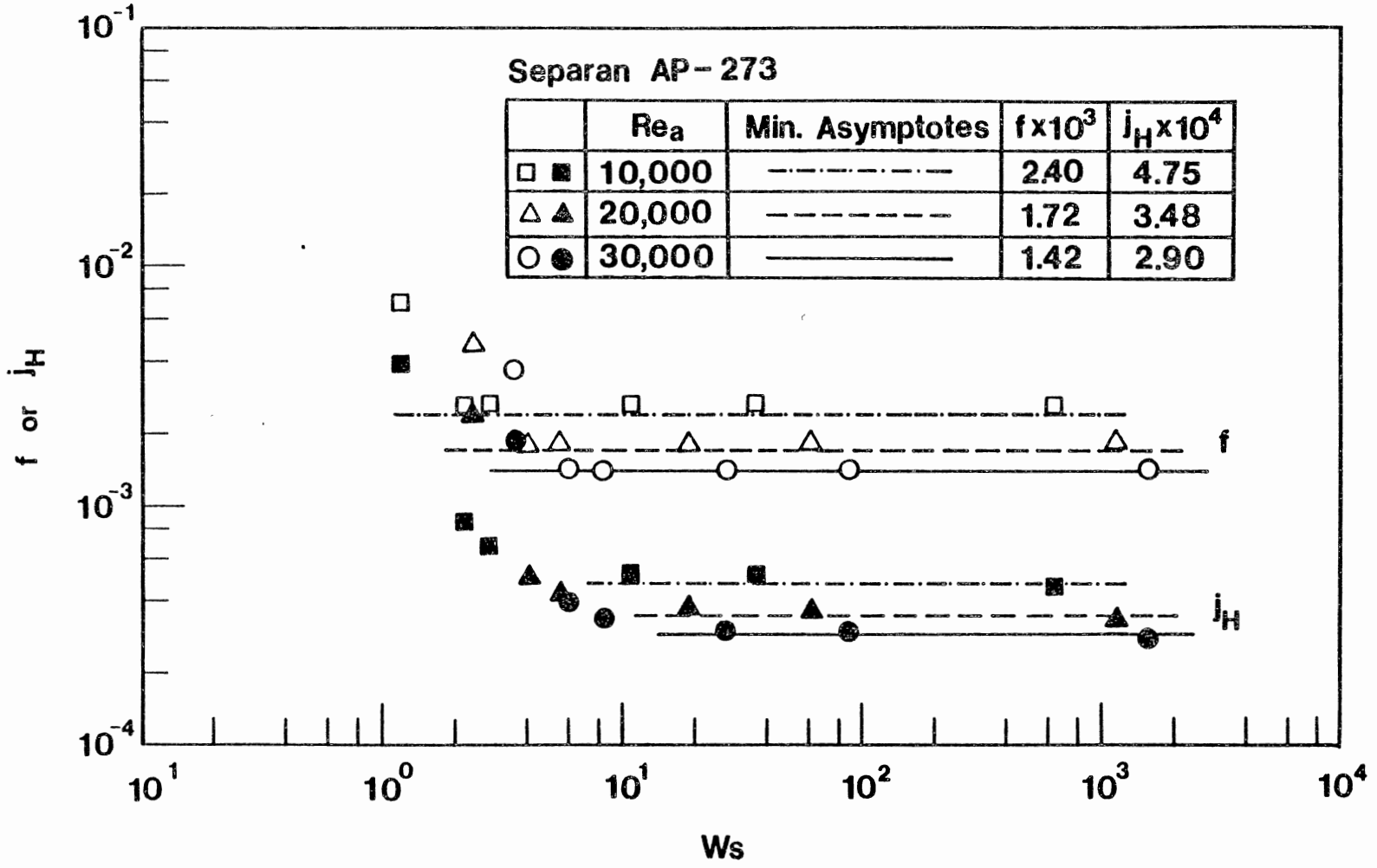

(b) Various Concentrations of Separan Solution

Figure 20. (Continued)

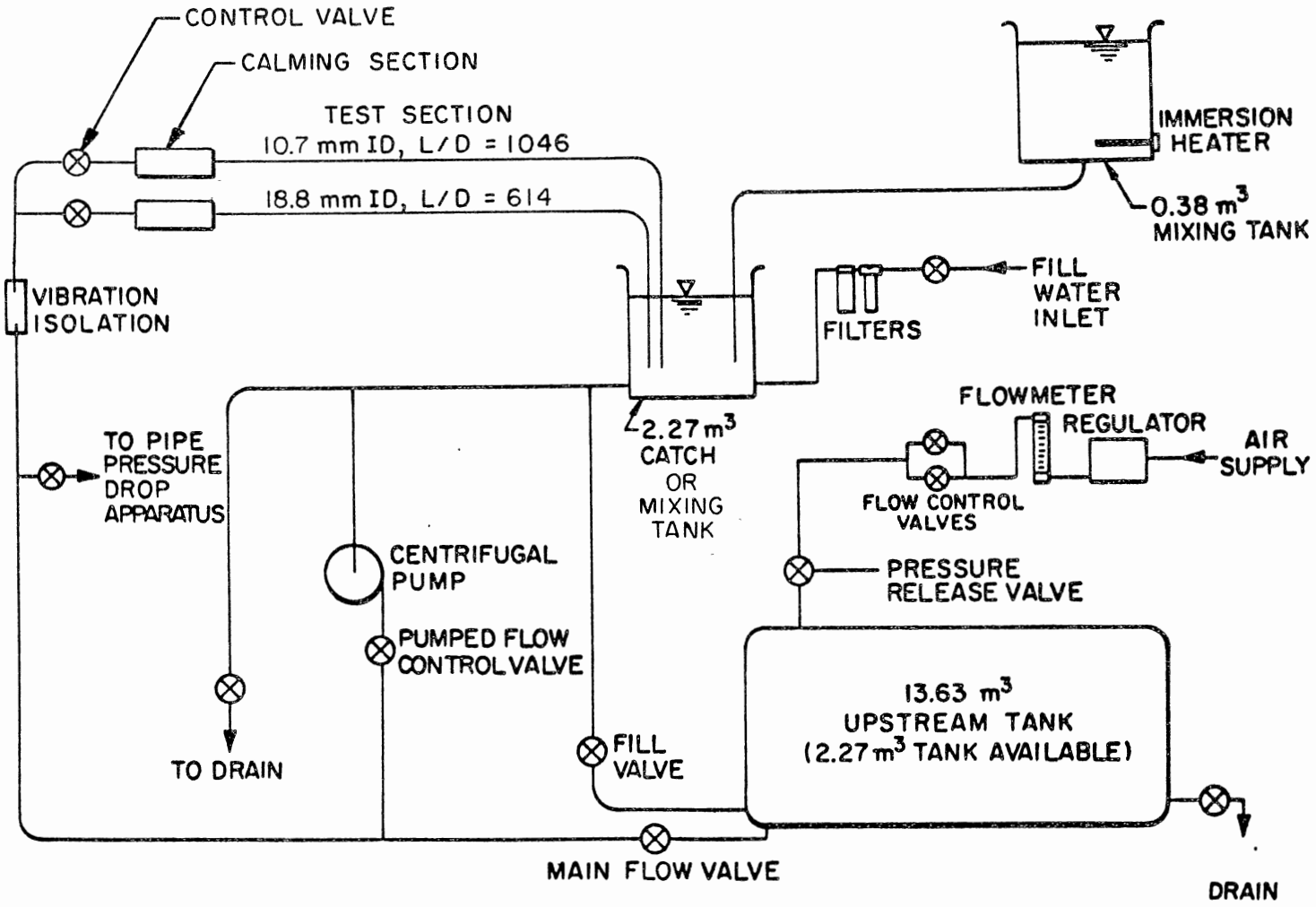

Figure 21. Schematic of the Flow Circulation System

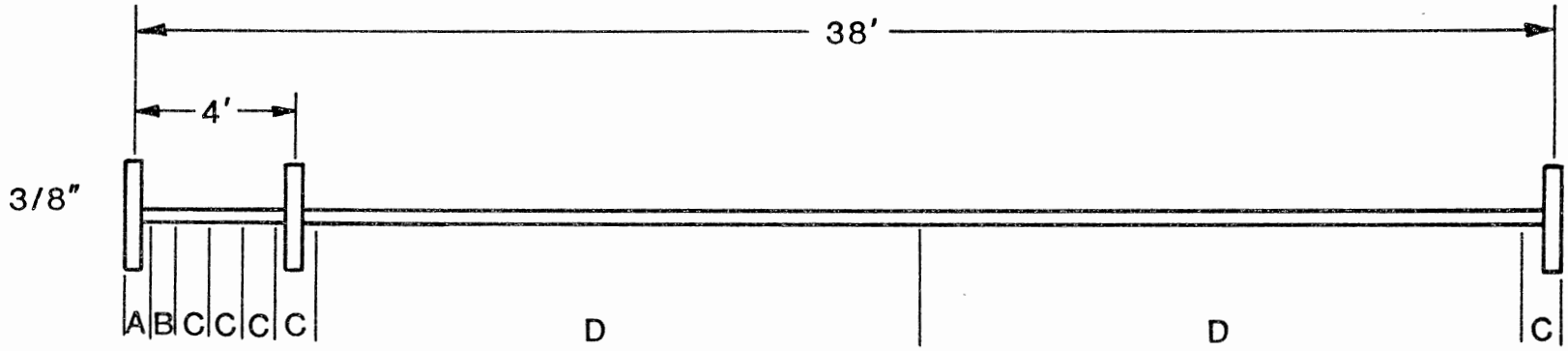

A = 4" B = 6" C = 12" D = 16'

Figure 22. Pressure Tap Locations

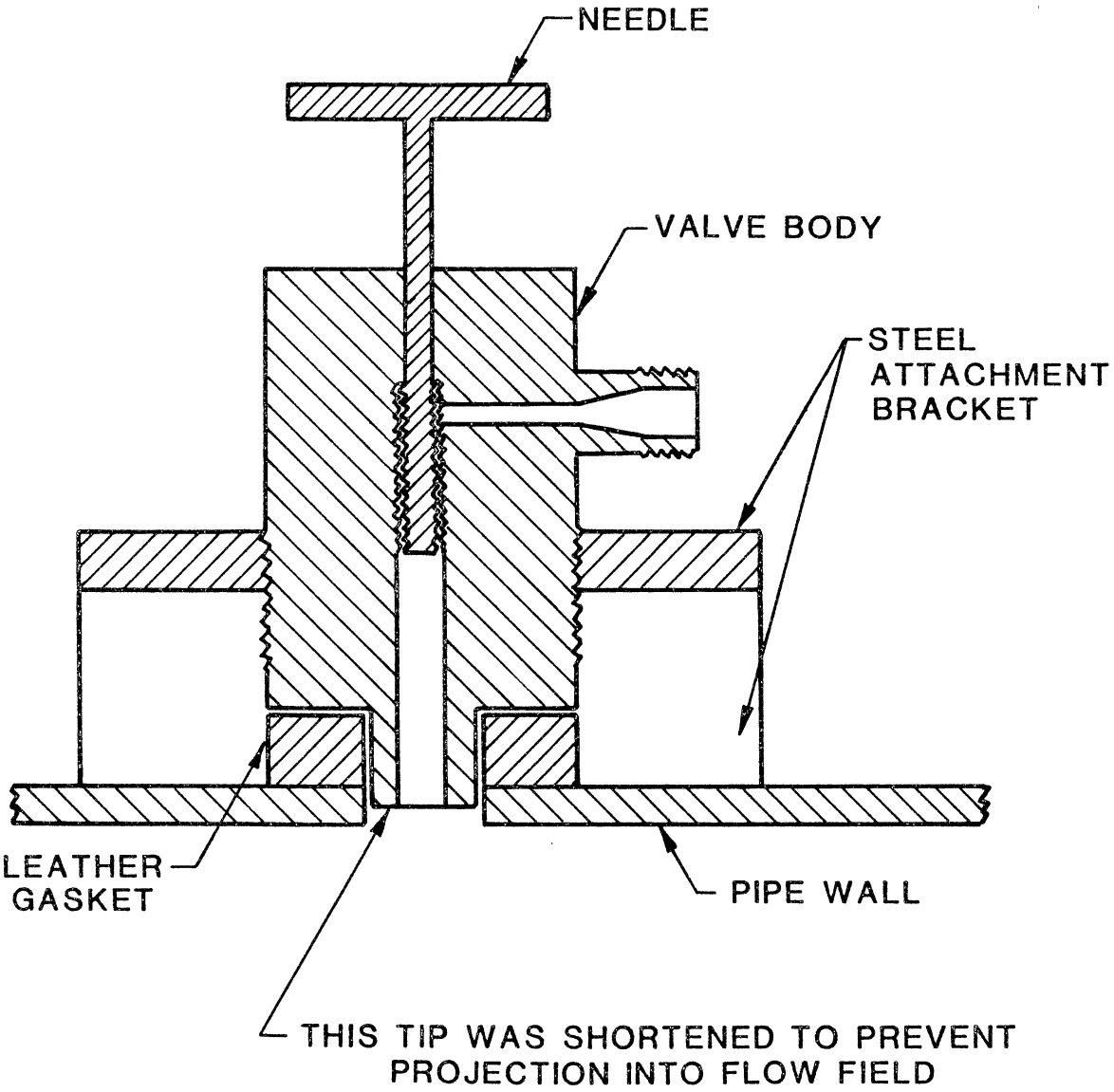

Figure 23. Schematic of a Closed Needle Valve; No Scale

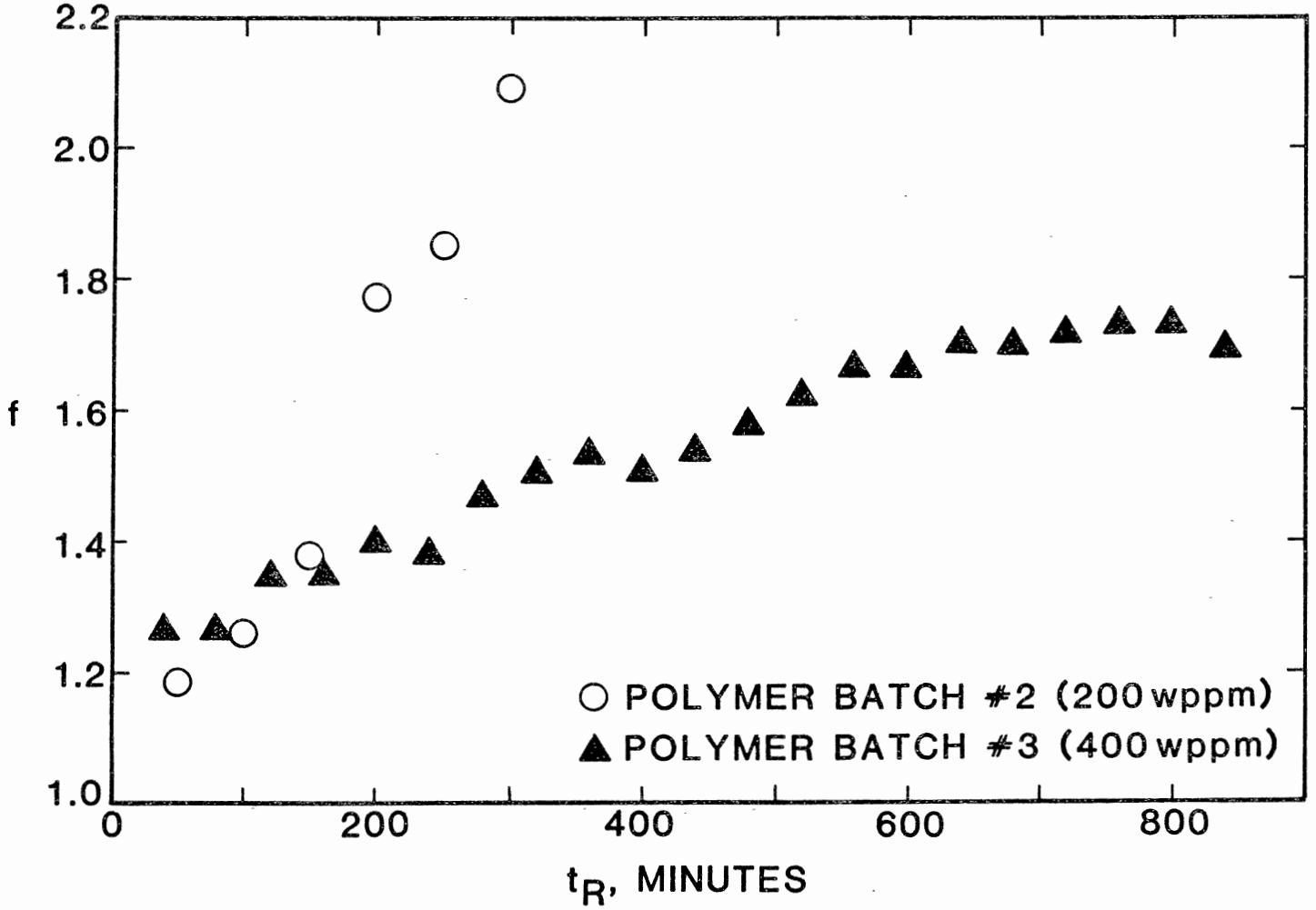

Figure 24. Effect of Fluid Residence Time on Friction Factor

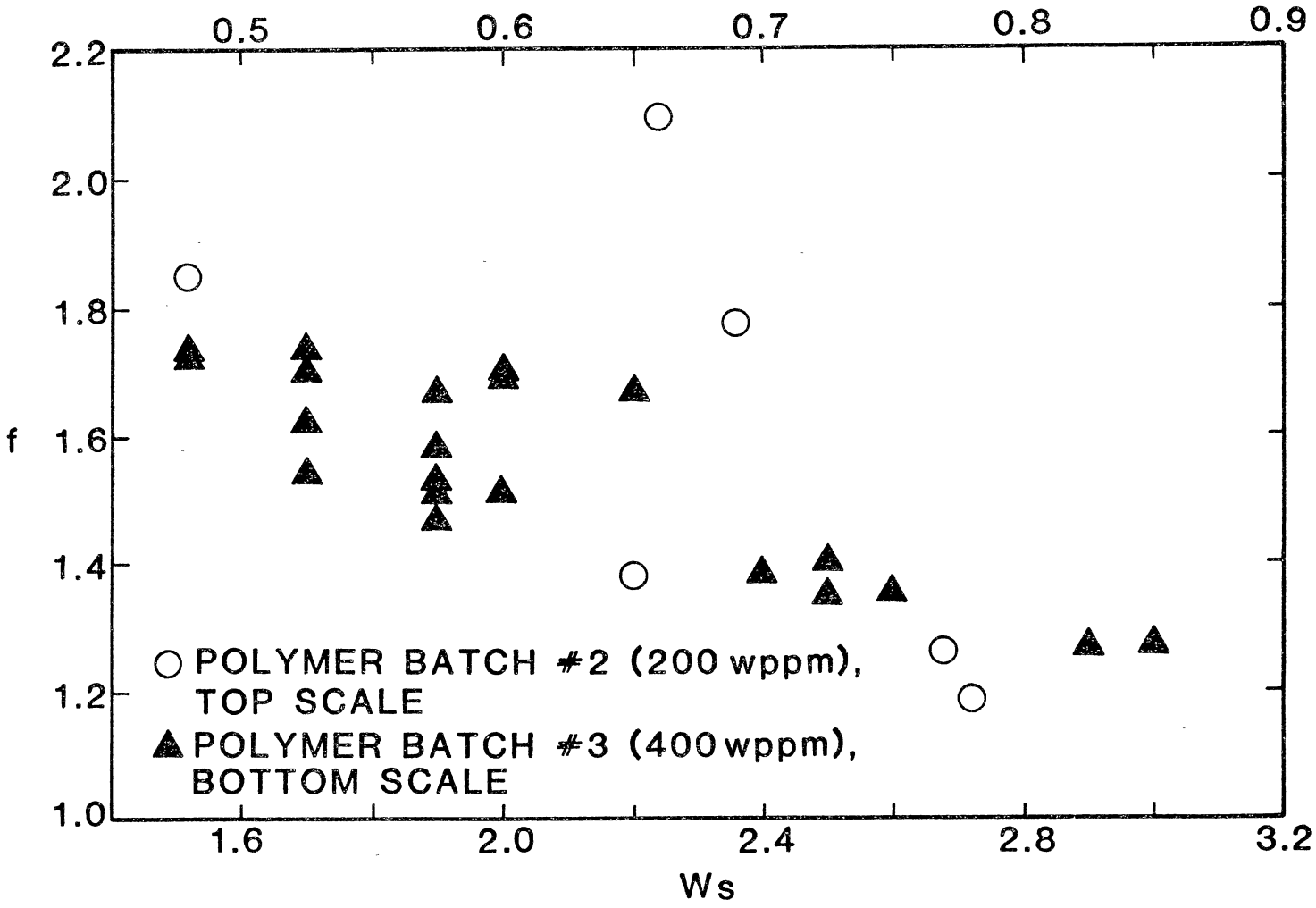

Figure 25. Effect of Weissenberg Number on Friction Factor

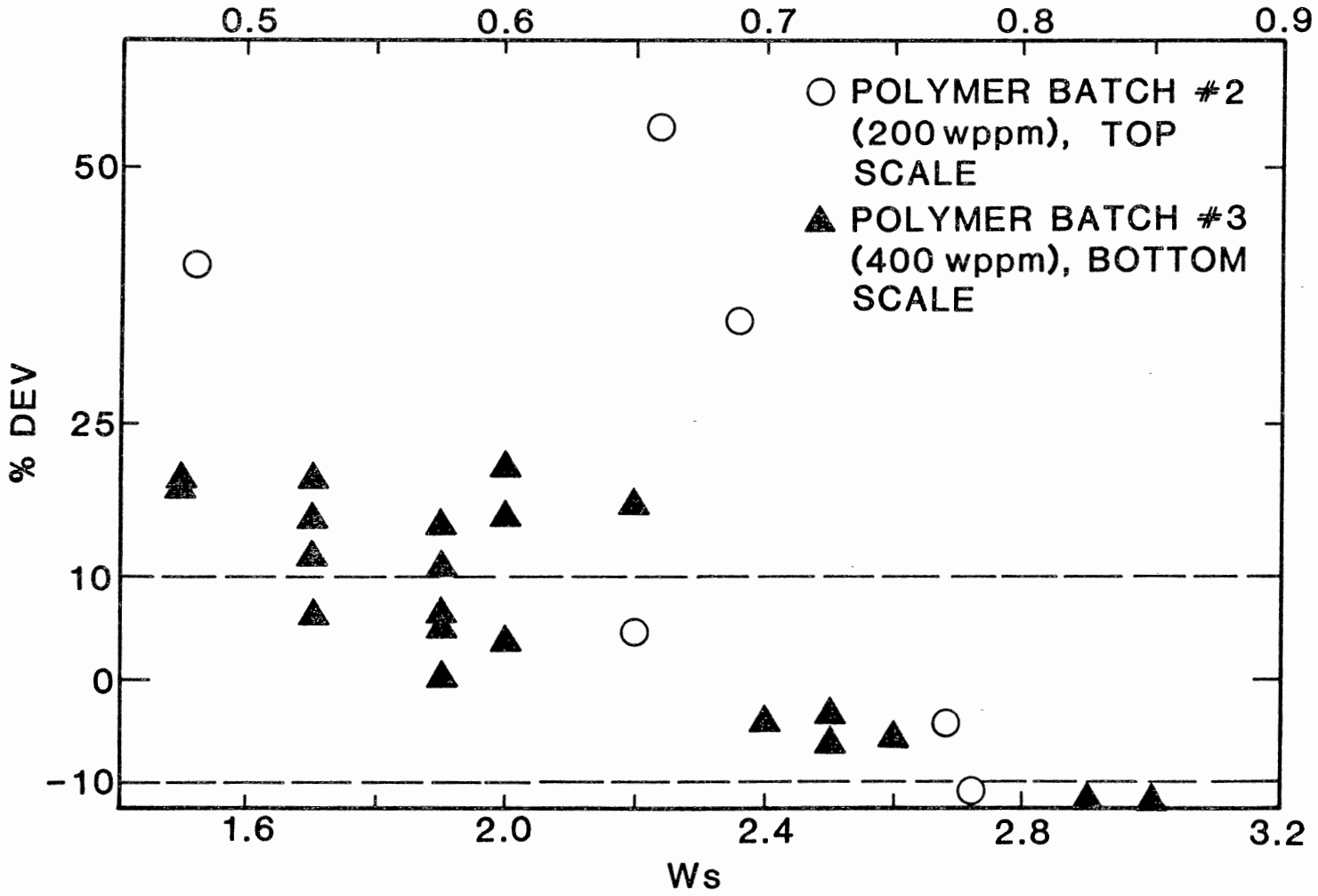

Figure 26. Effect of Weissenberg Number on Deviation of Friction Factor From Asymptotic Conditions

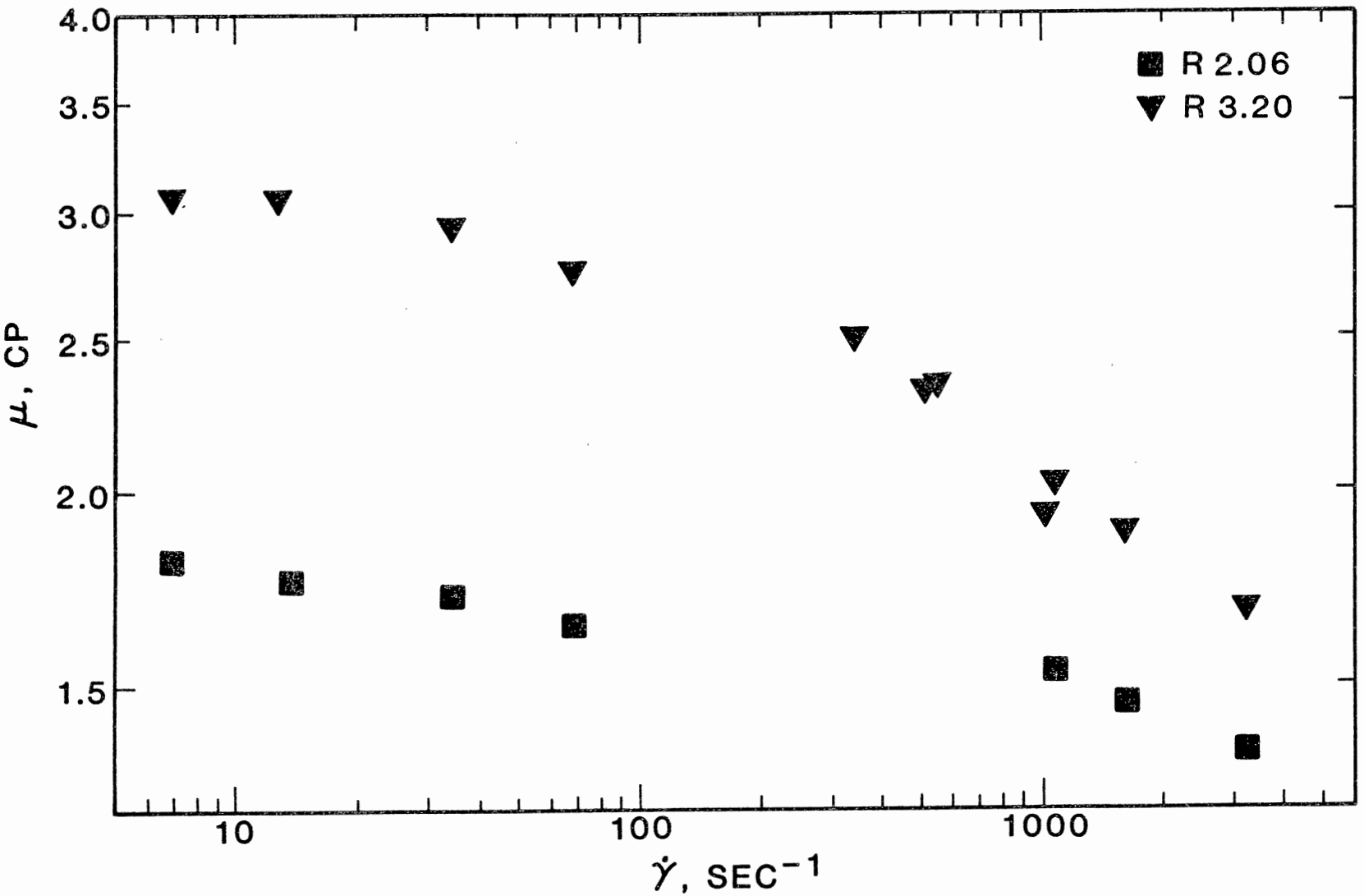

Figure 27. Rheological Data From Runs R2.06 and R3.20

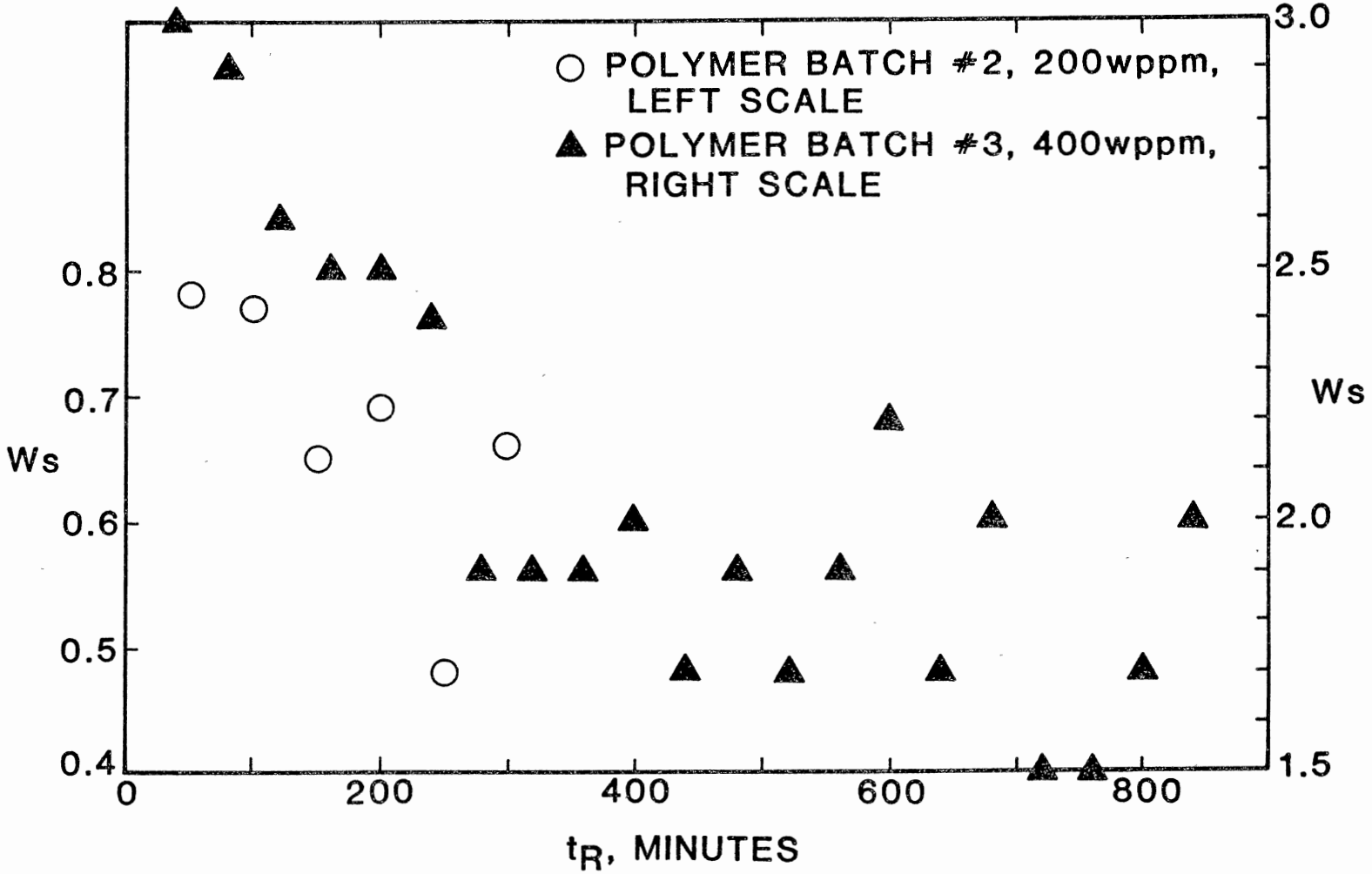

Figure 28. Effect of Residence Time on Weissenberg Number

APPENDIX B

TABLES

TABLE I

CONCENTRATION AND RESIDENCE TIME
DEPENDENCE OF TIME CONSTANT

Data Set	λ_E, Sec	λ_P, Sec	λ_{PW}, Sec
3.0010	101 E-6	195 E-4	879 E-5
3.0050	304 E-6	400 E-4	120 E-4
3.0100	304 E-5	693 E-4	233 E-4
3.0300	469 E-4	0.126	892 E-4
3.0500	0.194	0.236	0.262
3.1000	3.240	3.370	3.280
4.0000	0.527	0.770	0.552
4.0200	0.352	0.591	0.371
4.0400	0.189	0.357	0.202
4.0600	0.102	0.221	0.168
4.1000	807 E-4	0.254	897 E-4
4.1600	256 E-4	394 E-4	325 E-4
4.2900	141 E-4	862 E-4	158 E-4
4.5600	126 E-4	769 E-4	142 E-4
5.0000	1.920	2.970	1.960
5.0100	0.957	1.410	0.966
5.0300	0.552	0.598	0.572
5.0900	0.374	0.708	0.389
5.1300	0.146	0.448	0.236
5.2100	980 E-4	0.106	985 E-4
5.6600	995 E-5	194 E-4	152 E-4

TABLE II

$\dot{\gamma}_{MAX}$ DEPENDENCE OF λ^* AND % CH

	$\dot{\gamma}_{max}$, Sec^{-1}	Eyring Model			Powell-Eyring, $\mu_\infty = \mu(\dot{\gamma}_{max})$			Powell-Eyring, $\mu_\infty = \mu(H_2O)$		
		λ, Sec	% CH	λ^*	λ, Sec	% CH	λ^*	λ, Sec	% CH	λ^*
Data Set: 3.0010	11700	101 E-6	---	---	195 E-4	---	---	879 E-5	---	---
	4520	272 E-6	170	---	195 E-4	0	---	906 E-5	3.1	---
λ_R = 212 E-4 (from [13])	2520	489 E-6	380	---	194 E-4	-0.51	---	948 E-5	7.8	---
	1080	109 E-5	980	---	205 E-4	5.10	---	996 E-5	13	---
λ_L = Unde-fined	682	152 E-5	1400	---	223 E-4	14	---	103 E-4	17	---
Data Set: 3.0050	8460	304 E-6	---	---	400 E-4	---	---	120 E-4	---	---
	5880	387 E-6	27	---	435 E-4	8.80	---	125 E-4	4.2	---
λ_R = 309 E-4 (from [13])	4380	478 E-6	57	---	442 E-4	11	---	133 E-4	11	---
	3310	607 E-6	100	---	481 E-4	20	---	142 E-4	18	---
λ_L = Unde-fined	682	300 E-5	890	---	649 E-4	62	---	167 E-4	39	---
Data Set: 3.0100	4720	304 E-5	---	---	693 E-4	---	---	233 E-4	---	---
	1080	589 E-5	94	---	101 E-3	46	---	250 E-4	7.3	---
λ_R = 371 E-4 (from [13])	432	999 E-5	230	---	177 E-3	160	---	294 E-4	26	---
	271	127 E-4	320	---	289 E-3	320	---	322 E-4	38	---
λ_L = Unde-fined	172	166 E-4	450	---	334 E-3	380	---	370 E-4	59	---

TABLE II (Continued)

	$\dot{\gamma}_{max}$, Sec^{-1}	Eyring Model			Powell-Eyring, $\mu_\infty = \mu(\dot{\gamma}_{max})$			Powell-Eyring, $\mu_\infty = \mu(H_2O)$		
		λ, Sec	% CH	λ^*	λ, Sec	% CH	λ^*	λ, Sec	% CH	λ^*
Data Set: 3.0300	20200	469 E-4	---	0.87	0.126	---	2.34	892 E-4	---	1.66
	9110	471 E-4	0.43	0.88	0.134	6.30	2.49	893 E-4	0.11	1.66
λ_R = 961 E-4 (from [13])	3950	486 E-4	3.60	0.90	0.144	14	2.68	899 E-4	0.78	1.67
λ_L = 269 E-4	2110	514 E-4	9.60	0.96	0.155	23	2.88	911 E-4	2.10	1.69
	1080	555 E-4	18	1.03	0.176	40	3.27	933 E-4	4.60	1.73
	432	624 E-4	33	1.16	0.204	62	3.79	975 E-4	9.30	1.81
Data Set: 3.0500	98800	0.194	---	1.15	0.236	---	1.40	0.262	---	1.55
	43100	0.194	0	1.15	0.238	0.85	1.41	0.262	0	1.55
λ_R = 0.249 (from [13])	26500	0.194	0	1.15	0.239	1.30	1.42	0.262	0	1.55
λ_L = 843 E-4	8410	0.194	0	1.15	0.244	3.40	1.45	0.262	0	1.55
	4460	0.195	0.52	1.16	0.249	5.50	1.48	0.262	0	1.55
	2630	0.195	0.52	1.16	0.255	8.10	1.51	0.263	0.38	1.56
	869	0.197	1.50	1.17	0.276	17	1.64	0.265	1.10	1.57
	28.1	0.212	9.30	1.26	0.578	140	3.43	0.285	8.80	1.69
Data Set: 3.1000	38200	3.240	---	1.06	3.370	---	1.10	3.280	---	1.08
	17100	3.240	0	1.06	3.380	0.30	1.11	3.280	0	1.08
λ_R = 3.02 sec (from [13])	7180	3.240	0	1.06	3.380	0.30	1.11	3.280	0	1.08
λ_L = 1.53	3380	3.240	0	1.06	3.410	1.20	1.12	3.280	0	1.08
	1580	3.240	0	1.06	3.440	2.10	1.13	3.280	0	1.08

TABLE II (Continued)

	$\dot{\gamma}_{max}$, Sec^{-1}	Eyring Model			Powell-Eyring, $\mu_\infty = \mu(\dot{\gamma}_{max})$			Powell-Eyring, $\mu_\infty = \mu(H_2O)$		
		λ, Sec	% CH	λ^*	λ, Sec	% CH	λ^*	λ, Sec	% CH	λ^*
Data Set: 3.1000 Cont'd.	869	3.240	0	1.06	3.490	3.60	1.14	3.280	0	1.08
	297	3.240	0	1.06	3.630	7.70	1.19	3.280	0	1.08
	118	3.240	0	1.06	3.850	14	1.26	3.290	0.30	1.08
	47.30	3.260	0.62	1.07	4.250	26	1.39	3.300	0.61	1.08
	7.47	3.400	4.90	1.11	5.970	77	1.96	3.430	4.60	1.12
	1.88	3.740	15	1.23	9.390	180	3.08	3.770	15	1.24
Data Set: 4.00	303	0.527	---	1.08	0.770	---	1.58	0.552	---	1.14
	75.10	0.546	3.60	1.12	0.955	24	1.97	0.569	3.10	1.17
λ_R = 0.489 (from [14])										
λ_L = 0.243										
Data Set: 4.02	191	0.352	---	1.13	0.591	---	1.89	0.371	---	1.19
λ_R = 0.345 sec (from [14])										
λ_L = 0.156 sec										

TABLE II (Continued)

	$\dot{\gamma}_{max}$, Sec^{-1}	Eyring Model			Powell-Eyring, $\mu_\infty = \mu(\dot{\gamma}_{max})$			Powell-Eyring, $\mu_\infty = \mu(H_2O)$		
		λ, Sec	% CH	λ^*	λ, Sec	% CH	λ^*	λ, Sec	% CH	λ^*
Data Set: 4.04 λ_R = 0.201 sec (from [14]) λ_L = 847 E-4 sec	189	0.119	---	1.12	0.357	---	2.11	0.202	---	1.19
Data Set: 4.06 λ_R = 0.166 sec (from [14]) λ_L = 687 E-4 sec	189	0.102	---	0.74	0.221	---	1.61	0.168	---	1.22
Data Set: 4.10 λ_R = 683 E-4 sec (from [14]) λ_L = 298 E-4 sec	185	807 E-4	---	1.35	0.254	---	4.26	897 E-4	---	1.51

TABLE II (Continued)

	$\dot{\gamma}_{max}$, Sec^{-1}	Eyring Model			Powell-Eyring, $\mu_\infty = \mu(\dot{\gamma}_{max})$			Powell-Eyring, $\mu_\infty = \mu(H_2O)$		
		λ, Sec	% CH	λ^*	λ, Sec	% CH	λ^*	λ, Sec	% CH	λ^*
Data Set: 4.16	49400	256 E-4	---	1.43	394 E-4	---	2.20	325 E-4	---	1.81
	22800	263 E-4	2.70	1.47	406 E-4	3.00	2.27	326 E-4	0.31	1.82
λ_R = 298 E-4 sec (from [14])	9060	266 E-4	3.90	1.48	438 E-4	11	2.44	327 E-4	0.62	1.82
	2520	276 E-4	7.80	1.54	511 E-4	30	2.85	333 E-4	2.50	1.86
λ_L = 896 E-5 sec	766	302 E-4	18	1.69	659 E-4	67	3.68	350 E-4	7.70	1.95
	183	324 E-4	27	1.81	149 E-4	280	8.31	367 E-4	13	2.05
Data Set: 4.29	181	141 E-4	---	---	862 E-4	---	---	158 E-4	---	---
λ_R = 134 E-4 sec (from [14])										
λ_L = Undefined										
Data Set: 4.56	181	126 E-4	---	---	769 E-4	---	---	142 E-4	---	---
λ_R = 104 E-4 sec (from [14])										
λ_L = Undefined										

TABLE II (Continued)

	$\dot{\gamma}_{max}$, Sec^{-1}	Eyring Model			Powell-Eyring, $\mu_\infty = \mu(\dot{\gamma}_{max})$			Powell-Eyring, $\mu_\infty = \mu(H_2O)$		
		λ, Sec	% CH	λ^*	λ, Sec	% CH	λ^*	λ, Sec	% CH	λ^*
Data Set: 5.00 λ_R = 1.69 sec (from [13]) λ_L = 0.891 sec	76.0	1.920	---	1.08	2.970	---	1.67	1.960	---	1.10
Data Set: 5.01 λ_R = 0.906 sec (from [13]) λ_L = 0.431 sec	76.0	0.957	---	1.11	1.410	---	1.64	0.966	---	1.12
Data Set: 5.03 λ_R = 0.524 sec (from [13]) λ_L = 0.245 sec	78800	0.552	---	1.13	0.598	---	1.22	0.572	---	1.17
	29200	0.511	-0.18	1.12	0.601	0.50	1.23	0.572	---	1.17
	12600	0.551	-0.18	1.12	0.607	1.50	1.24	0.572	---	1.17
	4920	0.552	0	1.13	0.619	3.50	1.26	0.572	---	1.17
	1380	0.552	0	1.13	0.649	8.50	1.32	0.573	0.17	1.17
	399	0.554	0.36	1.13	0.713	19	1.46	0.574	0.35	1.17
	47.6	0.568	2.90	1.16	1.060	77	2.16	0.587	2.60	1.20

TABLE II (Continued)

	$\dot{\gamma}_{max}$, Sec^{-1}	Eyring Model			Powell-Eyring, $\mu_\infty = (\dot{\gamma}_{max})$			Powell-Eyring, $\mu_\infty = \mu(H_2O)$		
		λ, Sec	% CH	λ^*	λ, Sec	% CH	λ^*	λ, Sec	% CH	λ^*
Data Set: 5.09	75.1	0.374	---	1.20	0.708	---	2.27	0.389	---	1.25
λ_R = 0.176 sec (from [13]) λ_L = 0.156 sec										
Data Set: 5.13	73.7	0.146	---	0.87	0.448	---	2.66	0.236	---	1.40
λ_R = 961 E-4 sec (from [13]) λ_L = 841 E-4 sec										
Data Set: 5.21	81900	908 E-4	---	1.36	0.106	---	1.58	985 E-4	---	1.47
	29900	909 E-4	0.11	1.36	0.107	0.94	1.60	985 E-4	0	1.47
λ_R = 356 E-4 sec	5020	911 E-4	0.33	1.36	0.115	8.50	1.72	987 E-4	0.20	1.47
(from [13]) λ_L = 335 E-4 sec	1180	922 E-4	1.50	1.38	0.130	23	1.94	993 E-4	0.81	1.48

TABLE II (Continued)

	$\dot{\gamma}_{max}$, Sec^{-1}	Eyring Model			Powell-Eyring, $\mu_\infty = \mu(\dot{\gamma}_{max})$			Powell-Eyring, $\mu_\infty = \mu(H_2O)$		
		λ, Sec	% CH	λ^*	λ, Sec	% CH	λ^*	λ, Sec	% CH	λ^*
Data Set: 5.66	84300	995 E-5	---	0.85	194 E-4	---	1.66	152 E-4	---	1.30
	22800	105 E-4	5.50	0.90	205 E-4	5.70	1.76	154 E-4	1.30	1.32
λ_R = 166 E-4 sec	5070	114 E-4	15	0.98	244 E-4	26	2.09	158 E-4	3.90	1.36
(from [13])	1190	139 E-4	40	1.19	316 E-4	63	2.71	191 E-4	13	1.47
λ_L = 583 E-5 sec	604	161 E-4	62	1.38	361 E-4	86	3.10	186 E-4	22	1.60

TABLE III

EFFECT OF RHEOLOGICAL DATA ACCURACY

Data Set	λ_5, Sec	λ_3, Sec	% Diff.
3.0010	879 E-5	897 E-5	2.00
3.1000	3.280	3.300	0.61
4.0000	0.552	0.553	0.18
4.5600	142 E-4	141 E-4	0.70
5.0000	1.960	1.970	0.51
5.0100	0.966	0.968	0.21
5.6600	152 E-4	151 E-4	-0.66

TABLE IV

EXPERIMENTAL STUDIES OF MECHANICAL DEGRADATION IN VISCOELASTIC FLUIDS

Year	Investigators	Characterization	Solute Concentration	Pipe Dia.	L/D	Re	Solvent Chemistry	Fluid Model	Ws_{cf}	Results and Conclusions
1970	Paterson and Abernathy [7]	Specific Apparatus --molecular weight and residence time	Polyox WSR-301, WSR-205, WSR-35, WSR-N750, WSR-N80	0.024 in. and 0.686 in.	1700 670	3,000 ≤ Re ≤ 80,000	?	---	---	Rate of mechanical degradation is dependent on polymer molecule size, shear stress, and pipe diameter
1970	Ram and Kadim [10]	Specific apparatus --number of passes	PIB[1] Oppanol B-200, Oppanol B-100, Vistanex L-120 0.264-1.05 g/dℓ	0.33 mm	232	?	?	---	---	Mechanical degradation controlled by shear stress
1971	Fisher and Rodriquez [8]	Specific apparatus --number of passes	Polyox FRA, W-301, Coagulant; Polyacrylamide 1-50 g/kℓ	0.346 cm	173	8,600 ≤ Re ≤ 12,000	?	---	---	Friction data collapses to a single curve when plotted against the independent variable P/C^a, where P represents number of passes, C represents concentration, and a is a constant
1971	Kenis [28]	Specific apparatus --number of passes	Polyox WSR-301, Polyhall 295, Guar Gum J2S1, Bacterial Polysaccharide	0.117 cm	350	Re = 13,000	?	---	---	Higher molecular weight polymers are subjected to greater mechanical degradation, and eventually become less effective drag reducers than lower molecular weight polymers
1973	Ting and Little [9]	Based on dissipation energy, $E = \int_o^t \tau_w \dot{\gamma}\, dt$	Polyox WSR-205, WSR-1105, FRA, Coagulant, WSR-301	0.62 cm	?	Re = 9,000	Distilled Water	---	---	Normalized molecular weight and dissipated energy function may be used to correlate mechanical degradation data
1973	Gold et al. [27]	Specific apparatus --shear rate and residence time in disk flows	Polyox WSR-205, WSR-301, Coagulant; 2, 10, 25, 50, 100, 150, and 200 wppm	---	---	?	?	---	---	The friction factor is a function of previous shear history
1978	Tung et al. [6]	Specific apparatus --residence time	Separan AP-273 2500 wppm	2.21 cm	?	Re' = 12,000	?	---	---	Friction factor increases after 500 hours of shear. Suggested future use of Deborah number to correlate mechanical degradation data

TABLE IV (Continued)

Year	Investigators	Characterization	Solute Concentration	Pipe Dia.	L/D	Re	Solvent Chemistry	Fluid Model	Ws_{cf}	Results and Conclusions
1979	Ng and Hartnett [2]	Dimensionless	Separan AP-273 1500 and 2500[2] wppm	2.25 cm	285	$1.5\times10^4 \leq Re' \leq 1.9\times10^4$	?	Ellis Eyring	4	First published report containing estimates of the critical Weissenberg number
1982	Kwack et al. [13]	Dimensionless	Separan AP-273 10, 50, 130, 300, 500, and 1000 wppm	1.30 cm	475	$20,000 \leq Re \leq 30,000$	Chicago tap water	Powell-Eyring		Ws_{cf} is a weak function of Re_a. Ws is a major parameter in viscoelastic flow. $f = f(Re_a)$ if $Ws > Ws_{cf}$ $f = f(Re_a, Ws)$ if $Ws \leq Ws_{cf}$
1982	Kwack and Hartnett [14]	Dimensionless	Separan AP-273 1000 and 1500[3] wppm	0.98 cm 1.30 cm 2.25[4] cm	620 475 285	$20,000 \leq Re_a \leq 30,000$	Chicago tap water	Powell-Eyring	5~10	Ws_{cf} is independent of pipe diameter
1982	Kwack and Hartnett [15]	Dimensionless	Separan AP-273 1000 wppm	1.30 cm	475	$20,000 \leq Re_a \leq 30,000$	Chicago tap water	Powell-Eyring	5~10	Ws_{cf} is independent of solvent chemistry
							Chicago tap water w/100 wppm NaOH, ph = 9.2	Powell-Eyring		
		Dimensionless	Polyox WSR-301 5000 wppm	1.30 cm	475	$Re_a = 10,000$	Chicago tap water	Powell-Eyring	5~10	Ws_{cf} is independent of solute.

[1] Polyisobutylene.

[2] 2500 wppm data were taken from Reference [6] by the authors of Reference [2].

[3] 1500 wppm, 2.25 cm ID data taken from Reference [2] by the authors of Reference [14].

[4] Ibid.

TABLE V

TEST SECTION CALIBRATION RESULTS

		Blasius		Prandtl		Colebrook		Moody	
Re_D	$f \times 10^3$	$\hat{f} \times 10^3$	% Diff.	$\hat{f} \times 10^3$	% Diff.	$\hat{f} \times 10^3$	% Diff.	$\hat{f} \times 10^3$	% Diff.
21,300	6.42	6.55	-2.00	6.37	0.78	6.34	1.30	6.34	1.30
24,800	6.42	6.30	1.90	6.14	4.60	6.10	4.90	6.09	5.10
26,200	6.68	6.22	7.40	6.06	10.20	6.02	11.00	6.00	11.30
27,500	6.74	6.14	9.80	5.99	12.50	5.95	13.30	5.93	13.70
29,800	6.17	6.02	2.50	5.88	4.90	5.84	5.40	5.81	5.80
30,200	6.29	6.00	4.80	5.86	7.30	5.82	7.50	5.79	8.00
31,500	6.07	5.94	2.20	5.81	4.50	5.76	5.10	5.73	5.60
32,000	5.93	5.91	0.34	5.78	2.60	5.74	3.20	5.71	3.70
37,400	6.17	5.69	8.40	5.58	10.60	5.53	11.60	5.49	12.40
38,500	5.62	5.65	-0.53	5.54	1.40	5.50	2.20	5.45	3.00
40,300	5.55	5.58	-0.54	5.48	1.30	5.44	2.00	5.39	2.90
41,700	6.13	5.54	10.60	5.44	12.70	5.40	13.50	5.34	14.80
42,300	5.30	5.52	-4.00	5.42	-2.20	5.38	-1.50	5.32	-0.40
47,500	5.19	5.36	-3.20	5.28	-1.70	5.24	-0.94	5.17	0.40
49,500	5.29	5.30	-0.19	5.24	0.95	5.19	1.90	5.12	3.20
50,200	5.30	5.28	0.38	5.22	1.50	5.17	2.40	5.10	3.80
50,500	5.22	5.28	-1.10	5.21	0.19	5.17	1.00	5.09	2.50
51,500	5.53	5.25	5.30	5.19	6.60	5.14	7.00	5.07	8.30
53,600	5.23	5.20	0.58	5.14	1.20	5.10	2.50	5.02	4.00

TABLE V (Continued)

Re_D	$f \times 10^3$	Blasius		Prandtl		Colebrook		Moody	
		$\hat{f} \times 10^3$	% Diff.	$\hat{f} \times 10^3$	% Diff.	$\hat{f} \times 10^3$	% Diff.	$\hat{f} \times 10^3$	% Diff.
55,400	5.10	5.16	-1.20	5.11	-0.20	5.06	0.77	4.98	2.40
57,100	5.05	5.12	-1.40	5.07	-0.39	5.03	0.45	4.95	2.00
57,800	5.15	5.10	0.98	5.06	1.80	5.01	2.70	4.93	4.30
60,400	5.00	5.05	-1.00	5.01	-0.20	4.97	0.70	4.88	2.40
61,600	4.95	5.02	-1.40	4.99	-0.80	4.94	0.13	4.86	1.80
62,600	4.92	5.00	-1.60	4.97	-1.00	4.93	-0.12	4.84	1.60
63,400	5.03	4.98	1.00	4.96	1.40	4.91	2.30	4.82	4.20
65,000	4.99	4.95	0.81	4.93	1.20	4.89	2.10	4.79	4.00

Blasius: $f = 0.0791\ Re_D^{-1/4}$.

Prandtl: $1/\sqrt{f} = 4.0 \log (Re_D \sqrt{f}) - 0.4$.

Colebrook: $1/\sqrt{f} = 3.6 \log (Re_D/6.9)$.

Moody: $f = 0.0055/4\ [1 + 100\ Re_D^{-1/3}]$.

TABLE VI

SUMMARY OF EXPERIMENTAL RESULTS

Run No.	Re_a	$f \times 10^3$	$f_A \times 10^3$	% Dev.	Ws
R2.01	34,500	1.19	1.33	-11.0	0.78
R2.02	35,100	1.26	1.32	- 4.5	0.77
R2.03	34,900	1.38	1.32	4.5	0.65
R2.04	35,200	1.77	1.31	35.0	0.69
R2.05	35,300	1.85	1.31	41.0	0.48
R2.06	32,900	2.09	1.36	54.0	0.66
R3.01	28,600	1.27	1.45	-12.0	3.00
R3.02	28,700	1.27	1.45	-12.0	2.90
R3.03	29,500	1.35	1.43	- 5.6	2.60
R3.04	29,100	1.35	1.44	- 6.3	2.50
R3.05	28,700	1.40	1.45	- 3.4	2.50
R3.06	29,000	1.38	1.44	- 4.2	2.40
R3.07	28,000	1.47	1.47	0	1.90
R3.08	29,100	1.51	1.44	4.9	1.90
R3.09	28,900	1.53	1.44	6.3	1.90
R3.10	28,600	1.51	1.45	4.1	2.00
R3.11	28,600	1.54	1.45	6.2	1.70
R3.12	29,700	1.58	1.42	11.0	1.90
R3.13	28,600	1.62	1.45	12.0	1.70
R3.14	28,700	1.67	1.45	15.0	1.90
R3.15	29,500	1.67	1.43	17.0	2.20
R3.16	28,500	1.70	1.46	16.0	1.70
R3.17	30,200	1.70	1.41	21.0	2.00
R3.18	28,700	1.72	1.45	19.0	1.50
R3.19	28,200	1.73	1.46	18.0	1.50
R3.20	28,600	1.73	1.45	19.0	1.70
R3.21	28,400	1.69	1.46	16.0	2.00

TABLE VII

RHEOLOGICAL DATA

Run	$\dot{\gamma}$ (Sec^{-1})	μ (cp)	Run	$\dot{\gamma}$ (Sec^{-1})	μ (cp)
Initial Mixture, Batch #2	6.88	1.98	R2.01	6.88	1.78
	13.80	1.85		13.80	1.78
	34.40	1.81		34.40	1.73
	68.80	1.70		68.80	1.66
	1090	1.57		1090	1.48
	1630	1.46		1630	1.40
	3260	1.36		3260	1.31
	λ_{PW} = 2.43 E-3 sec			λ_{PW} = 2.07 E-3 sec	
R2.02	6.88	1.80	R2.03	6.88	1.74
	13.80	1.78		13.80	1.78
	34.40	1.74		34.40	1.69
	68.80	1.66		68.80	1.65
	1090	1.45		1090	1.50
	1630	1.38		1630	1.40
	3260	1.28		3260	1.30
	λ_{PW} = 2.39 E-3 sec			λ_{PW} = 1.73 E-3 sec	
R2.04	6.88	1.72	R2.05	6.88	1.60
	13.80	1.74		13.80	1.68
	34.40	1.68		34.40	1.61
	68.80	1.60		68.80	1.57
	1090	1.46		1090	1.46
	1630	1.38		1630	1.38
	3260	1.28		3260	1.28
	λ_{PW} = 1.86 E-3 sec			λ_{PW} = 1.27 E-3 sec	
R2.06	6.88	1.81	Initial Mixture, Batch #3	6.88	4.00
	13.80	1.75		13.80	3.82
	34.40	1.71		34.40	3.47
	68.80	1.65		68.80	3.15
	1090	1.54		344	2.83
	1630	1.47		516	2.56
	3260	1.37		544	2.49
				1030	2.15
				1090	2.14
				1630	1.99
				3260	1.78
	λ_{PW} = 1.78 E-3 sec			λ_{PW} = 7.12 E-3 sec	

TABLE VII (Continued)

Run	$\dot{\gamma}$ (Sec^{-1})	μ (cp)	Run	$\dot{\gamma}$ (Sec^{-1})	μ (cp)
R3.01	6.88	4.02	R3.02	6.88	3.88
	13.80	3.96		13.80	3.67
	34.40	3.49		34.40	3.33
	68.80	3.14		68.80	3.03
	344	2.90		344	2.79
	516	2.57		516	2.49
	544	2.41		544	2.47
	1030	2.14		1030	2.06
	1090	2.09		1090	2.08
	1630	1.94		1630	1.93
	3260	1.72		3260	1.71
	λ_{PW} = 7.38 E-3 sec			λ_{PW} = 7.11 E-3 sec	
R3.03	6.88	3.57	R3.04	6.88	3.50
	13.80	3.51		13.80	3.40
	34.40	3.23		34.40	3.19
	68.80	2.97		68.80	2.91
	344	2.62		343	2.60
	515	2.40		515	2.35
	544	2.31		544	2.29
	1030	2.02		1030	1.99
	1090	1.99		1090	2.00
	1630	1.86		1630	1.87
	3260	1.66		3262	1.66
	λ_{PW} = 6.47 E-3 sec			λ_{PW} = 6.36 E-3 sec	
R3.05	6.88	3.51	R3.06	6.88	3.47
	13.80	3.46		13.80	3.41
	34.40	3.15		34.40	3.11
	68.80	2.90		68.80	2.91
	344	2.61		343	2.59
	515	2.37		515	2.36
	544	2.29		544	2.31
	1030	1.99		1030	1.99
	1090	2.00		1090	1.99
	1630	1.84		1630	1.85
	3260	1.64		3260	1.65
	λ_{PW} = 6.47 E-3 sec			λ_{PW} = 6.21 E-3 sec	

TABLE VII (Continued)

Run	$\dot{\gamma}$ (Sec^{-1})	μ (cp)	Run	$\dot{\gamma}$ (Sec^{-1})	μ (cp)
R3.07	6.88	3.19	R3.08	6.88	3.16
	13.80	3.21		13.80	3.18
	34.40	3.01		34.40	2.96
	68.80	2.81		68.80	2.76
	343	2.52		343	2.48
	515	2.30		515	2.27
	543	2.35		544	2.34
	1030	1.93		1030	1.91
	1090	2.03		1090	2.05
	1630	1.91		1630	1.84
	3260	1.69		3260	1.63
	λ_{PW} = 4.77 E-3 sec			λ_{PW} = 4.88 E-3 sec	
R3.09	6.88	3.16	R3.10	6.88	3.17
	13.80	3.20		13.80	3.17
	34.40	2.96		34.40	2.96
	68.80	2.76		68.80	2.79
	343	2.54		343	2.45
	515	2.31		515	2.27
	544	2.25		544	2.29
	1030	1.93		1030	1.91
	1090	1.94		1090	2.00
	1630	1.85		1630	1.86
	3260	1.64		3260	1.67
	λ_{PW} = 4.98 E-3 sec			λ_{PW} = 5.15 E-3 sec	
R3.11	6.88	3.03	R3.12	6.88	3.04
	13.80	3.05		13.80	3.05
	34.40	2.94		34.40	2.94
	68.80	2.75		68.80	2.74
	343	2.43		343	2.48
	514	2.25		515	2.29
	543	2.28		544	2.20
	1030	1.91		1030	1.92
	1090	2.05		1090	1.91
	1630	1.88		1630	1.80
	3260	1.67		3260	1.61
	λ_{PW} = 4.40 E-3 sec			λ_{PW} = 4.78 E-3 sec	

TABLE VII (Continued)

Run	$\dot{\gamma}$ (Sec^{-1})	μ (cp)	Run	$\dot{\gamma}$ (Sec^{-1})	μ (cp)
R3.13	6.88	3.04	R3.14	6.88	3.15
	13.80	3.03		13.80	3.08
	34.40	2.94		34.40	2.96
	68.80	2.75		68.80	2.79
	343	2.48		343	2.57
	514	2.28		514	2.34
	543	2.29		543	2.26
	1030	1.90		1030	1.97
	1090	2.00		1090	1.98
	1630	1.86		1630	1.86
	3260	1.66		3260	1.66
	λ_{PW} = 4.45 E-3 sec			λ_{PW} = 4.86 E-3 sec	
R3.15	6.88	3.10	R3.16	6.88	2.99
	13.80	3.05		13.80	3.03
	34.40	2.93		34.40	2.91
	68.80	2.78		68.80	2.78
	343	2.38		343	2.46
	515	2.23		514	2.26
	544	2.15		543	2.28
	1030	1.90		1030	1.90
	1090	1.91		1090	1.99
	1630	1.81		1630	1.86
	3260	1.62		3260	1.68
	λ_{PW} = 5.56 E-3 sec			λ_{PW} = 4.29 E-3 sec	
R3.17	6.88	3.04	R3.18	6.88	3.00
	13.80	3.00		13.80	3.03
	34.40	2.94		34.40	2.92
	68.80	2.76		68.80	2.76
	343	2.45		343	2.57
	515	2.25		514	2.34
	544	2.18		543	2.34
	1030	1.91		1030	1.97
	1090	1.91		1090	2.02
	1630	1.77		1630	1.88
	3260	1.59		3260	1.67
	λ_{PW} = 5.03 E-3 sec			λ_{PW} = 3.89 E-3 sec	

TABLE VII (Continued)

Run	$\dot{\gamma}$ (Sec^{-1})	μ (cp)	Run	$\dot{\gamma}$ (Sec^{-1})	μ (cp)
R3.19	6.88	3.02	R3.20	6.88	3.05
	13.80	3.02		13.80	3.04
	34.40	2.90		34.40	2.92
	68.80	2.76		68.80	2.75
	343	2.63		343	2.49
	514	2.39		514	2.30
	543	2.34		543	2.32
	1030	1.98		1030	1.93
	1090	2.02		1090	2.02
	1630	1.91		1630	1.88
	3260	1.69		3260	1.68
	λ_{PW} = 3.80 E-3 sec			λ_{PW} = 4.34 E-3 sec	
R3.20	6.88	3.18			
	13.80	3.15			
	34.40	3.04			
	68.80	2.88			
	343	2.50			
	514	2.34			
	543	2.30			
	1030	2.00			
	1090	2.03			
	1630	1.91			
	3260	1.71			
	λ_{PW} = 4.94 E-3 sec				

APPENDIX C

UNCERTAINTY ANALYSIS

For a complete discussion of the theory of uncertainty analysis, refer to Kline and McClintock [45]. The "uncertainty" is the possible value an error might have.

The friction factor was found to be

$$f = \frac{\pi^2 (\rho_m - \rho_s) g h D^5}{32 \rho_s L Q^2} \tag{3.2}$$

with g and ρ_m assumed constant. The uncertainty may then be found from

$$w_f = \left[\left(\frac{\partial f}{\partial \rho_s} w_{\rho_s}\right)^2 + \left(\frac{\partial f}{\partial h} w_h\right)^2 + \left(\frac{\partial f}{\partial D} w_D\right)^2 + \left(\frac{\partial f}{\partial L} w_L\right)^2 + \left(\frac{\partial f}{\partial Q} w_Q\right)^2\right]^{\frac{1}{2}} \tag{C.1}$$

The partial derivatives are

$$\frac{\partial f}{\partial \rho_s} = -\frac{\pi^2 g h D^5}{32 L Q^2} \frac{\rho_m}{\rho_s^2} \tag{C.2}$$

$$\frac{\partial f}{\partial h} = \frac{\pi^2 (\rho_m - \rho_s) g D^5}{32 \rho_s L Q^2} \tag{C.3}$$

$$\frac{\partial f}{\partial D} = \frac{5\pi^2 (\rho_m - \rho_s) g h D^4}{32 \rho_s L Q^2} \tag{C.4}$$

$$\frac{\partial f}{\partial L} = \frac{\pi^2 (\rho_m - \rho_s) g D^5}{32 \rho_s L^2 Q^2} \tag{C.5}$$

$$\frac{\partial f}{\partial Q} = \frac{2\pi^2 (\rho_m - \rho_s) g D^2}{32 \rho_s L Q^3} \tag{C.6}$$

Substituting Equations (C.2) through (C.6) into Equation (C.1) and dividing by Equation (3.2), the desired form is

$$\frac{w_f}{f} = \left[\left(\frac{\rho_m}{\rho_m - \rho_s}\ \frac{w_{\rho_s}}{s}\right)^2 + \left(\frac{w_h}{h}\right)^2 + \left(\frac{5w_D}{D}\right)^2 + \left(\frac{-w_L}{L}\right)^2 + \left(\frac{-2w_Q}{Q}\right)^2\right]^{\frac{1}{2}} \tag{C.7}$$

The uncertainty of each variable was estimated as follows at 20 to 1 odds for each variable:

1. Density. ρ_s was assumed constant, so $\rho_m/\rho_m - \rho_s = 1.079$. Also, Yoo [16] determined a probable error of 0.4 percent using the density of water, so $w_{\rho_s}/\rho_s = 0.004$.

2. Height. The average height difference was about eight inches. Reading accuracy was ± 0.1 inch. Adding some error for bubbles or other system problems, $w_h/h = 0.02$.

3. Diameter. The diameter was measured as $0.436'' \pm 0.002''$, so $w_D/D = 0.00459$.

4. Length was measured as $16' \pm 1/4''$, so $w_L/L = 0.0013$.

5. From the turbine meter calibration results, $w_Q/Q = 0.04$.

Substituting and solving,

$$\frac{w_f}{f} = 0.086.$$

The Reynolds number was found to be

$$Re_a = \frac{\rho\ VD}{\mu_a} \tag{2.4}$$

or

$$Re_a = \frac{4 \rho Q}{\pi \mu_a D} \tag{C.8}$$

The uncertainty may be determined from

$$w_{Re} = \left[\left(\frac{\partial Re}{\partial \rho} w_\rho\right)^2 + \left(\frac{\partial Re}{\partial Q} w_Q\right)^2 + \left(\frac{\partial Re}{\partial \mu_a} w_{\mu_a}\right)^2 + \left(\frac{\partial Re}{\partial D} w_D\right)^2\right]^{\frac{1}{2}} \tag{C.9}$$

The partial derivatives are

$$\frac{\partial Re}{\partial \rho} = \frac{4Q}{\pi \mu_a D} \tag{C.10}$$

$$\frac{\partial Re}{\partial Q} = \frac{4\rho}{\pi \mu_a D} \tag{C.11}$$

$$\frac{\partial Re}{\partial \mu_a} = -\frac{4 \rho Q}{\pi \mu_a^2 D} \tag{C.12}$$

$$\frac{\partial Re}{\partial D} = -\frac{4 \rho Q}{\pi \mu_a D^2} \tag{C.13}$$

Substituting as before,

$$\frac{w_{Re}}{Re} = \left[\left(\frac{w_\rho}{\rho}\right)^2 + \left(\frac{w_Q}{Q}\right)^2 + \left(-\frac{w_\mu}{\mu_a}\right)^2 + \left(-\frac{w_D}{D}\right)^2\right]^{\frac{1}{2}} \tag{C.14}$$

In addition to uncertainties already specified, that of μ_a was estimated to be 0.08 from the observed inconsistencies in viscosity data. Substituting into Equation (C.14) and solving,

$$\frac{w_{Re}}{Re_a} = 0.090.$$

The asymptotic friction factor was found to be

$$f_A = 0.20\ Re_a^{-0.48} \tag{4.1}$$

The uncertainty is

$$w_{f_A} = \frac{f_A}{Re_a} w_{Re_a} \tag{C.15}$$

and

$$\frac{f_A}{Re_a} = -0.096\ Re_a^{-1.48} \tag{C.16}$$

therefore,

$$\frac{w_{f_A}}{f_A} = \left[\left(-0.48\ \frac{w_{Re}}{Re_a}\right)^2\right]^{\frac{1}{2}} \tag{C.17}$$

From above,

$$\frac{w_{Re}}{Re_a} = 0.090$$

therefore,

$$\frac{w_{f_A}}{f_A} = 0.043$$

The uncertainty estimate of the asymptotic friction factor does not include the effect of deviations from Equation (4.1).

The Weissenberg number was defined as

$$Ws = \lambda V/D \tag{2.8}$$

Since velocity was measured in terms of volume flowrate, Equation (2.8) becomes

$$Ws = \frac{4\ Q}{D^3} \tag{C.18}$$

The uncertainty may be determined from

$$w_{Ws} = \left[\left(\frac{\partial Ws}{\partial \lambda} w_\lambda\right)^2 + \left(\frac{\partial Ws}{\partial Q} w_Q\right)^2 + \left(\frac{\partial Ws}{\partial D} w_D\right)^2\right]^{\frac{1}{2}} \tag{C.19}$$

The partial derivatives are

$$\frac{\partial Ws}{\partial \lambda} = \frac{4Q}{\pi\ D^3} \tag{C.20}$$

$$\frac{\partial Ws}{\partial Q} = \frac{4\lambda}{\pi\ D^3} \tag{C.21}$$

$$\frac{\partial Ws}{\partial D} = \frac{12\ \lambda Q}{\pi\ D^4} \tag{C.22}$$

Substituting as previously,

$$\frac{w_{Ws}}{Ws} = \left[\left(\frac{w_\lambda}{\lambda}\right)^2 + \left(\frac{w_Q}{Q}\right)^2 + \left(3\ \frac{w_D}{D}\right)^2\right]^{\frac{1}{2}} \tag{C.23}$$

The uncertainty of the critical Weissenberg number was estimated at 10 to 1 odds. The uncertainty for each variable was:

1. Uncertainty in the time constant was estimated by the procedure described in section 4.2 to be $w_\lambda/\lambda = 1.5$ ($Re_a = 34,700$) and 1.0 ($Re_a = 28,900$).

2. At 20 to 1 odds, $w_Q/Q = 0.04$. At 10 to 1 odds, $w_Q/Q = 0.035$.

3. At 20 to 1 odds, $w_Q/Q = 0.00459$. At 10 to 1 odds, $w_Q/Q = 0.0035$.

The resulting uncertainty is 150 percent for $Re_a = 34,700$ and 100 percent for $Re_a = 28,900$.

In summary, the uncertainties at 20 to 1 odds are 8.6 percent for the friction factor, 9.0 percent for the Reynolds number, and 4.3 percent for the asymptotic friction factor. The uncertainty in the critical Weissenberg number at 10 to 1 odds is 150 percent for Re_a = 34,700 and 100 percent for Re_a = 28,900.

APPENDIX D

DATA NUMBER CODE

Rheological data tabulated by Kwack [35] are shown in Figures 3 through 5. All data sets in these figures are numbered n.xxxx, where n represents the figure in which the data are plotted, and xxxx represents the concentration in wppm or residence time in hours--whichever is applicable.

The author's experimental data are represented by Rn.xx, where n represents batch number, and xx represents the individual data run in that batch.

APPENDIX E

COMPUTER PROGRAM

E.1 User's Manual

This computer program may be used to determine the Powell-Eyring time constant for polymer solutions in pipe flow. It was written specifically for use at Oklahoma State University and may require adaptation for use on other computer systems.

There are two distinct sections:

1. Calculates and plots the sum squared error of the mathematical model versus the Powell-Eyring time constant. Insures that the time band used in the numerical scheme of section 2 contains the absolute minimum sum squared error value, and only the absolute minimum is contained in the time band. If the time band contains any other local minima or does not contain the absolute minimum, the time constant calculated may not be the best value according to the least squares method.

2. A numerical procedure to calculate the Powell-Eyring time constant which gives the best fit of the mathematical model to the experimental data. Details of the numerical search technique are discussed later in Appendix E.

Program input variables are:

GAM - Experimental shear rate, sec^{-1}.

H - Step value of the time constant, in seconds. The time constant is incremented this much each time a new data point is generated for plotting.

NP - The number of data points on the shear rate-shear viscosity curve.

TC - Initial estimate of the time constant, in seconds.

TOL - Accuracy desired for the final estimate of the time constant. For

example, if the user desires to know the time constant to within ±0.01 seconds, TC = 0.01.

VINF - The viscosity of water. It should be evaluated at the same temperature and in the same units as those of the visco-elastic fluid's rheological data.

VIS - Experimentally determined visocosity, in any consistent units.

The program calls a plotting subroutine available to Oklahoma State University Mechanical Engineering faculty and students. Thus the plotting section will have to be revised if the program is used at other institutions.

Instructions for User's Manual

Logging onto the computer will require different procedures at most installations. Running the program should be very similar, however. In the following instructions, TX represents a terminal message, UX represents a user instruction. This program was written for interactive use on a terminal with plotting capability.

T1: Message indicating READY or MONITOR mode.

U1: Command to execute program.

T2: ENTER THE VISCOSITY OF WATER AT EXPERIMENTAL TEMPERATURE. UNITS MUST BE CONSISTENT WITH THOSE REPORTED FROM SHEAR RATE-VISCOSITY CURVE.

U2: VINF <CR>* NOTE: Be certain units are the same as those used later in the program.

T3: ENTER THE # OF DATA POINTS.

---

*<CR> = CARRIAGE RETURN.

U3: NP <CR> NOTE: NP is the number of experimental data points on the shear rate-shear viscosity curve.

T4: ENTER THE VISCOSITY AND CORRESPONDING SHEAR RATE FOR EACH DATA POINT. THE FIRST DATA POINT ENTERED MUST CONTAIN THE MINIMUM SHEAR RATE VALUE.

U4:
```
VIS(1), GAM(1)    <CR>
VIS(2), GAM(2)    <CR>
VIS(3), GAM(3)    <CR>
      :
      :
VIS(NP), GAM(NP)  <CR>
```

NOTE: Viscosity can be entered in any consistent units, although they must be the same as those used for the viscosity of water. Shear rate must be in sec^{-1}. The zero shear rate is GAM(1), and must be in the first data pair entered.

T5: PLEASE CHECK YOUR DATA FOR TYPO ERRORS

DATA #	VISCOSITY	SHEAR RATE
1	VIS(1)	GAM(1)
2	VIS(2)	GAM(2)
3	VIS(3)	GAM(3)
:	:	:
NP	VIS(NP)	GAM(NP)

PAUSE

NOTE: T5 allows the user to scan the rheological data for errors made entering the data. If errors were made, note the data numbers and they can be corrected in the next step. Continue after scanning the data.

U5: <CR>

T6: DO YOU NEED TO CORRECT ANY OF THE RHEOLOGICAL DATA?

1. YES
2. NO

U6: ICHECK <CR>

NOTE: If ICHECK = 1, continue.

If ICHECK = 2, go to T9.

T7: ENTER THE DATA #

U7: ICOR <CR> NOTE: ICOR is the data # of the data point which needs corrected.

T8: ENTER THE VISCOSITY AND SHEAR RATE

U8: VIS(ICOR), GAM(ICOR) <CR> NOTE: T6 appears on the screen next. There is no limit to how many data points may be corrected or how many times one point may be corrected.

T9: ENTER THE INITIAL ESTIMATE OF TIME CONSTANT, IN SECONDS

U9: TC <CR> NOTE: A good initial estimate is $2\lambda_L$ (λ_L = Ellis time constant).

T10: ENTER TIME CONSTANT INCREMENT FOR PLOTTING PURPOSES

U10: H <CR> NOTE: H is recommended to lie in the interval $TC/20 \leq H \leq TC/50$. If replotting, substitute (LAMMAX - LAMMIN) for TC in the above formula. LAMMAX and LAMMIN are entered in instruction U13.

T11: The terminal displays a plot of sum squared error versus Powell-Eyring time constant. The plot is used to determine if the time band contains the absolute minimum sum squared error, and no local minima.

U11: <CR>

T12: ENTER THE NUMBER CORRESPONDING TO WHAT YOU WISH TO DO.

1. CONTINUE EXECUTION
2. RESPECIFY ENDPOINTS AND PLOT AGAIN

U12: ITEST1 <CR> NOTE: If the plot showed the time band was satisfactory, ITEST1 = 1 and the next message is T14. If the time band was unsatisfactory, ITEST1 = 2 and the next message is T13.

T13: ENTER NEW ENDPOINTS FOR THE TIME CONSTANT. ENTER THE MINIMUM VALUE FIRST.

U13: LAMMIN, LAMMAX <CR> NOTE: LAMMIN $\neq$ 0, or a divide-by-zero error will occur. The new endpoints are used to change the time band and generate a new plot. The next message is T10.

T14: ENTER THE ACCURACY DESIRED FOR THE ESTIMATE OF THE TIME CONSTANT.

U14: TOL <CR>

T15: LAMBDA = X

PAUSE

NOTE: X $\equiv$ the calculated value of the time constant, in seconds. This is the value used to find the Weissenberg number.

U15: <CR>

T16: 1. RETURN TO TOP OF PROGRAM

2. EXIT THE PROGRAM

ENTER THE INTEGER CORRESPONDING TO YOUR CHOICE.

U16: ITEST3 NOTE: If the user wishes to analyze other data sets, ITEST3 = 1 and the next message is T2. If the user is through, ITEST3 = 2.

T17: READY or MONITOR mode.

E.2 Program Listing

```
C
C     DEFINE AND DIMENSION THE VARIABLES.
C
      REAL,LAM,LAMBDA,LAMI,LAMJ,LAMK, LAML,LAMMIN,LAMMAX
      DIMENSION GAM(100),LAMBDA(1000),SSE(1000),VIS(100)
C
C     INPUT DATA
C
 1010 WRITE(6,1902)
      READ(5,*)VINF
      WRITE(6,1903)
      READ(5,*)NP
      WRITE(6,1904)
      DO 1020 IA=1,NP
      READ(5,*)VIS(IA),GAM(IA)
 1020 CONTINUE
      PAUSE
      WRITE(6,1920)
      WRITE(6,1921)
      DO 25 ISCAN=1,NP
      WRITE(6,1922)ISCAN,VIS(ISCAN),GAM(ISCAN)
   25 CONTINUE
      PAUSE
   27 WRITE(6,1925)
      READ(5,*)ICHECK
      IF(ICHECK.EQ.2) GO TO 28
      WRITE(6,1926)
      READ(5,*)ICOR
      WRITE(6,1927)
      READ(5,*)VIS(ICOR),GAM(ICOR)
      GO TO 27
   28 WRITE(6,1905)
      READ(5,*)TC
C
      LAMMIN=.5*TC
      LAMMAX=1.5*TC
      VZERO=VIS(1)
C
C     TOP OF REPLOTTING ROUTINE.
C
 1030 LAMBDA(1)=LAMMIN
      WRITE(6,1906)
      READ(5,*)H
      PTSMAX=(LAMMAX-LAMMIN)/H
      IF(PTSMAX.GE.1000.) H=(LAMMAX-LAMMIN)/998.
      VZERO=VIS(1)
C
C     TOP OF REPLOTTING ROUTINE.
C
```

```
      I=0
 1040 I=I+1
      IF (I.GT.1) LAMBDA(I)=LAMBDA(I-1)+H
C
C     LOOP TO SUM THE ERROR AND SQUARE IT.
C
      ERRSUM=0.
      DO 1050 K=1,NP
      X=LAMBDA(I)*GAM(K)
      Z=X+(X**2+1.)**0.5
      ERR=VIS(K)-(VINF+(VZERO-VINF)*ALOG(Z)/X)
 1050 ERRSUM=ERRSUM+ERR**2
C
C     SAVE THE SUM SQUARED ERROR FOR PLOTTING.  TEST TO SEE IF SSE HAS
C     BEEN FOUND FOR ALL VALUES OF LAMBDA.
C
      SSE(I)=ERRSUM
      IF(LAMBDA(I).LT.LAMMAX) GO TO 1040
C
C     PLOT THE DATA USING THE QUICKPLOT SUBROUTINE.
C
      CALL QCKPLT(LAMBDA, SSE, I, 'TIME CONSTANTS',
     1 'SUM SQUARED ERRORS', 'PLOT TO EXAMINE LOCAL MINIMAS',
     2 4, 5, 0)
      PAUSE
C
C     CHOOSE THE NEXT STEP.
C
      WRITE(6,1907)
      READ(5,*)ITEST1
      IF(ITEST1.EQ.1) GO TO 1060
      WRITE(6,1908)
      READ(5,*)LAMMIN,LAMMAX
      GO TO 1030
C
C     SECTION 2
C
C     NEW INPUT DATA
C
 1060 WRITE(6,1909)
      READ(5,*)TOL
      J=1
C
C     DEFINE THE FIRST FOUR VALUES OF LAMBDA
C
      LAMI=LAMMIN
      LAML=LAMMAX
      LAMJ=LAMI+0.3819660115*(LAML-LAMI)
      LAMK=LAMI+0.6180339885*(LAML-LAMI)
C
```

```
 1070 IF (J.EQ.1) LAM=LAMI
      IF (J.EQ.2) LAM=LAMJ
      IF (J.EQ.3) LAM=LAMK
      IF (J.EQ.4) LAM=LAML
      GO TO 1100
C
C     RECALCULATE LAMJ FOR THE CASE WHERE REGION K-L
C     IS DISCARDED.
C
 1080 LAMJ=LAMI+0.3819660115*(LAML-LAMI)
      LAM=LAMJ
      GO TO 1100
C
C     RECALCULATE LAMK FOR I-J BEING DISCARDED.
C
 1090 LAMK=LAMI+0.6180339885*(LAML-LAMI)
      LAM=LAMK
C
C     LOOP TO FIND SUM SQUARED ERROR.
C
 1100 ERRSUM=0.
      DO 1110 L=1,NP
      X=LAM*GAM(L)
      Z=X+(X**2+1.)**0.5
      ERR=VIS(L)-(VINF+(VZERO-VINF)*ALOG(Z)/X)
 1110 ERRSUM=ERRSUM+ERR**2
      J=J+1
C
C     DETERMINE FUNCTION VALUES
C
      IF (LAM.EQ.LAMI) FI=ERRSUM
      IF (LAM.EQ.LAMJ) FJ=ERRSUM
      IF (LAM.EQ.LAMK) FK=ERRSUM
      IF (LAM.EQ.LAML) FL=ERRSUM
C
      IF (J.LE.4) GO TO 1070
C
C     REDEFINE POINTS AS NEEDED.
C
      IF (FJ.LE.FK) N=1
      IF (FJ.LE.FK) LAML=LAMK
      IF (FJ.LE.FK) LAMK=LAMJ
      IF (FJ.LE.FK) FL=FK
      IF (FJ.LE.FK) FK=FJ
C
      IF (FJ.GT.FK) N=2
      IF (FJ.GT.FK) LAMI=LAMJ
      IF (FJ.GT.FK) LAMJ=LAMK
      IF (FJ.GT.FK) FI=FJ
      IF (FJ.GT.FK) FJ=FK
C
C     TEST TO SEE IF LAMBDA VALUES HAVE CONVERGED TO A SMALL
C     ENOUGH VALUE.
```

```
C
      DEL=LAML-LAMI
      IF (DEL.LT.TOL) GO TO 1120
      IF (N.EQ.1) GO TO 1080
      IF (N.EQ.2) GO TO 1090
C
C     PRINT FINAL ESTIMATE OF THE EYRING TIME CONSTANT.
C
 1120 LAM=0.5*(LAMI+LAML)
      WRITE(6,1900)LAM
      PAUSE
C
C
C     CHOOSE WHETHER TO EXIT PROGRAM OR TO EXECUTE AGAIN.
C
      WRITE(6,1911)
      READ(5,*)ITEST3
      IF(ITEST3.EQ.1) GO TO 1010
C
 1900 FORMAT(//10X,'LAMBDA = ',E11.4)
 1901 FORMAT(10X,I2,2(15X,E11.4))
 1902 FORMAT(//5X,'ENTER THE VISCOSITY OF WATER AT',
     1/5X,'EXPERIMENTAL TEMPERATURE.  UNITS MUST BE',
     2/5X,'CONSISTENT WITH THOSE REPORTED FROM THE',
     3/5X,'SHEAR RATE-VISCOSITY CURVE.')
 1903 FORMAT(/5X,'ENTER THE # OF DATA POINTS')
 1904 FORMAT(/5X,'ENTER VISCOSITY AND THE CORRESPONDING',/
     15X,'SHEAR RATE FOR EACH DATA POINT.  THE FIRST',
     2/5X,'DATA POINT ENTERED MUST CONTAIN THE MINIMUM',
     3/5X,'SHEAR RATE VALUE, AND THE LAST MUST CONTAIN',
     4/5X,'THE MAXIMUM SHEAR RATE VALUE.')
 1905 FORMAT(/5X,'ENTER THE INITIAL ESTIMATE OF THE',
     1/5X,'POWELL-EYRING TIME CONSTANT, IN SECONDS.')
 1906 FORMAT(/5X,'ENTER TIME CONSTANT INCREMENT FOR',/
     15X,'PLOTTING PURPOSES.')
 1907 FORMAT(/5X,'ENTER THE NUMBER CORRESPONDING TO',/
     15X,'WHAT YOU WISH TO DO.',/
     210X,'1.  CONTINUE EXECUTION',/
     310X,'2.  RESPECIFY PLOT ENDPOINTS AND PLOT AGAIN.')
 1908 FORMAT(/5X,'ENTER NEW ENDPOINTS FOR TIME CONSTANT.',
     1/5X,'ENTER THE MINIMUM VALUE FIRST.')
 1909 FORMAT(/5X,'ENTER THE ACCURACY DESIRED FOR THE',
     1/5X,'ESTIMATE OF THE EYRING TIME CONSTANT.')
 1911 FORMAT(/5X,'1.  RETURN TO TOP OF PROGRAM',
     1/5X,'2.  EXIT THE PROGRAM',
     2/5X,'ENTER THE INTEGER CORRESPONDING TO YOUR CHOICE.')
 1920 FORMAT(//5X,'PLEASE CHECK YOUR DATA FOR TYPO ERRORS')
 1921 FORMAT(//5X,'DATA #',10X,'VISCOSITY',10X,'SHEAR RATE'//)
 1922 FORMAT(7X,I2,9X,E11.4,10X,E11.4)
 1925 FORMAT(//5X,'DO YOU NEED TO CORRECT ANY OF THE
     1/5X,'VISCOSITY-SHEAR RATE DATA?',//10X,
     2'1.  YES',/10X,'2.  NO')
 1926 FORMAT(//5X,'ENTER THE DATA #')
```

```
1927 FORMAT(//5X,'ENTER VISCOSITY & SHEAR RATE')
 1150 STOP
      END
```

E.3 Numerical Search Technique

The numerical search technique used in the computer program is best explained with reference to Figures 29 and 30.

Four initial points are chosen, X_i, X_j, X_k, and X_ℓ, respectively. The values of X_i and X_ℓ are chosen so that $X_i \leq X_c \leq X_\ell$, where $F(X_c)$ is the minimum value of $F(X)$. The plot is used to aid in the selection of X_i and X_ℓ. The values of X_j and X_k are chosen relative to X_i and X_ℓ by a method discussed later.

The value of $F(x)$ corresponding to each value of X is calculated and named F_i, F_j, F_k, or F_ℓ. Next, the values of F_j and F_k are compared.

If $F_j > F_k$, $F(X_c)$ cannot be in the region i-j (see Figure 29). The region i-j is discarded, X_j becomes X_i, and F_j becomes F_i. New values are assigned to X_j and X_k, with F_j and F_k being recalculated. Refer to Figure 30 for clarification.

If $F_k > F_j$, $F(X_c)$ cannot be in the region k-ℓ (see Figure 29). Region k-ℓ is discarded, X_k becomes X_ℓ, and F_k becomes F_ℓ. New values are assigned to X_j and X_k, with F_j and F_k being recalculated. Again, refer to Figure 30 for clarification.

After a region has been discarded, the remaining bandwidth is compared with the accuracy desired in the final estimate of X_c. If the bandwidth is greater than the allowable error, the process returns to the beginning and iterates. If the bandwidth is less than the tolerance, $X_c = 1/2\ (X_i + X_\ell)$.

If the values of X_i and X_j are chosen judiciously, only one new function value need be calculated during each iteration. From Figure 29, note that

$$X_j = X_i + a\,(X_\ell - X_i) = X_\ell - b\,(X_\ell - X_i) \tag{E.1}$$

and

$$X_k = X_i + b\,(X_\ell - X_i) = X_\ell - a\,(X_\ell - X_i) \tag{E.2}$$

By choosing a and b such that

$$a + b = 1 \tag{E.3}$$

and

$$\frac{a}{b} = \frac{b}{1} \tag{E.4}$$

the work involved can be decreased. Solving Equations (E.3) and (E.4) yields

$$a = 0.381966012$$

and

$$b = 0.618033989.$$

Then, as illustrated in Figure 31,

1. If region i-j is discarded, j becomes i, k becomes j, and new values are determined for X_k and F_k.

2. If region k-ℓ is discarded, k becomes ℓ, j becomes k, and new values are determined for X_j and F_j.

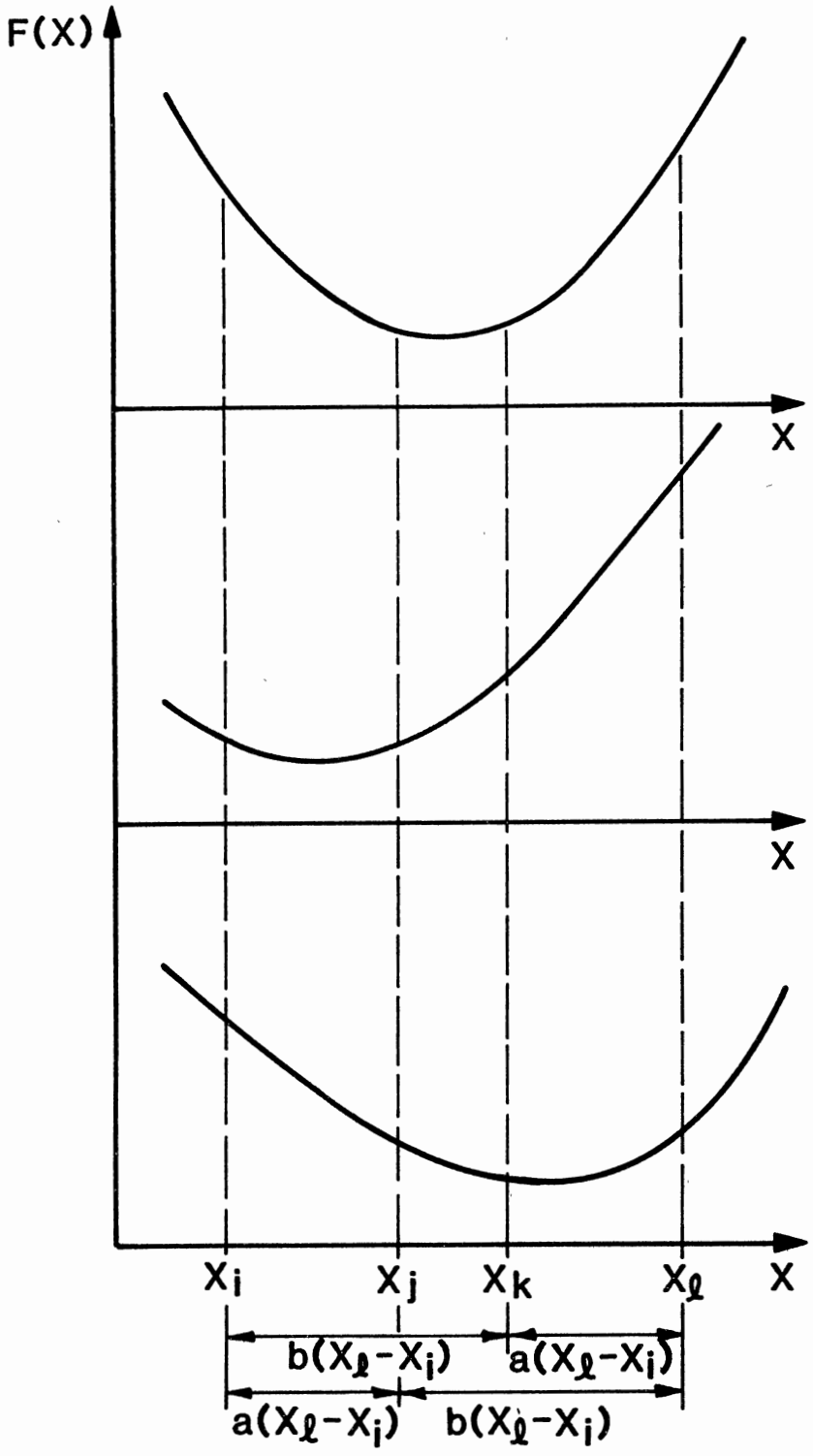

Figure 29. Possible Situations if $X_i \leq X_c \leq X_j$

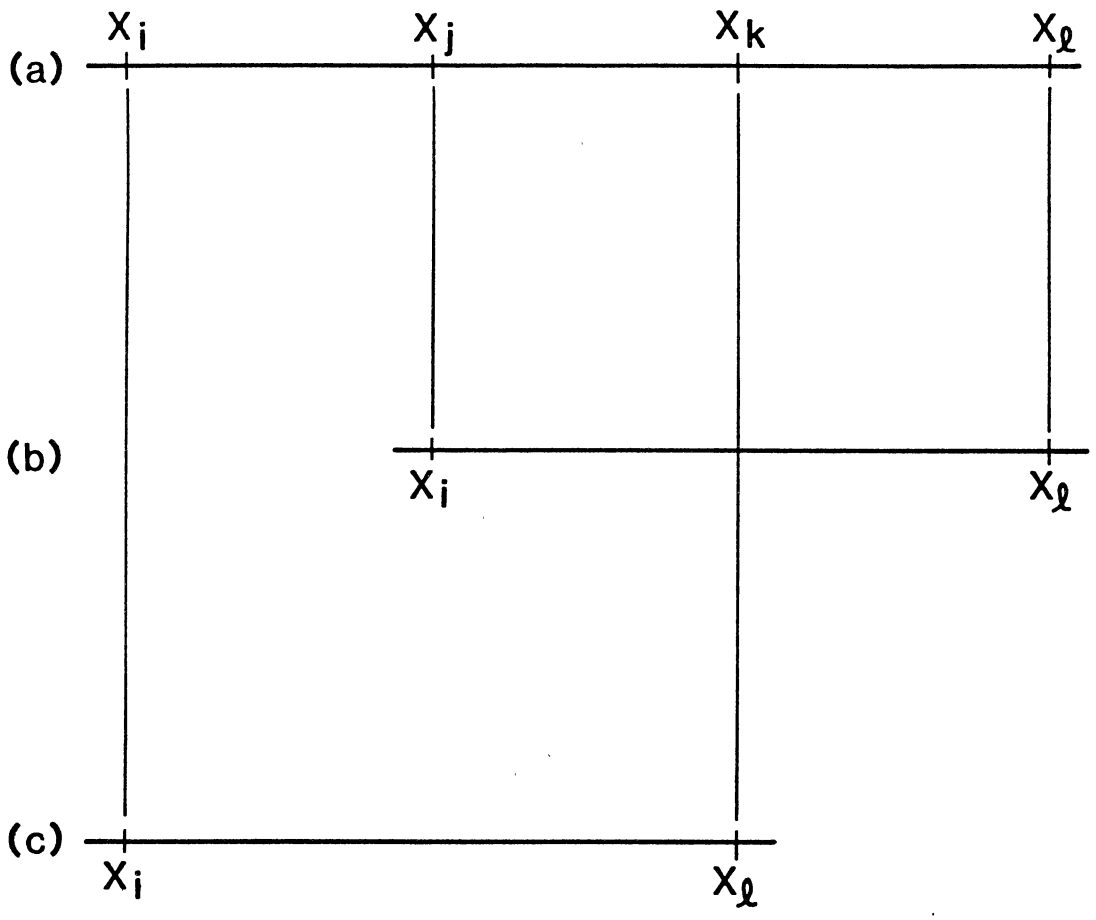

Figure 30. (a) Initial Situation; (b) i-j Discarded, X_j and X_k Not Yet Reassigned; (c) k-ℓ Discarded, X_j and X_k Not Yet Reassigned

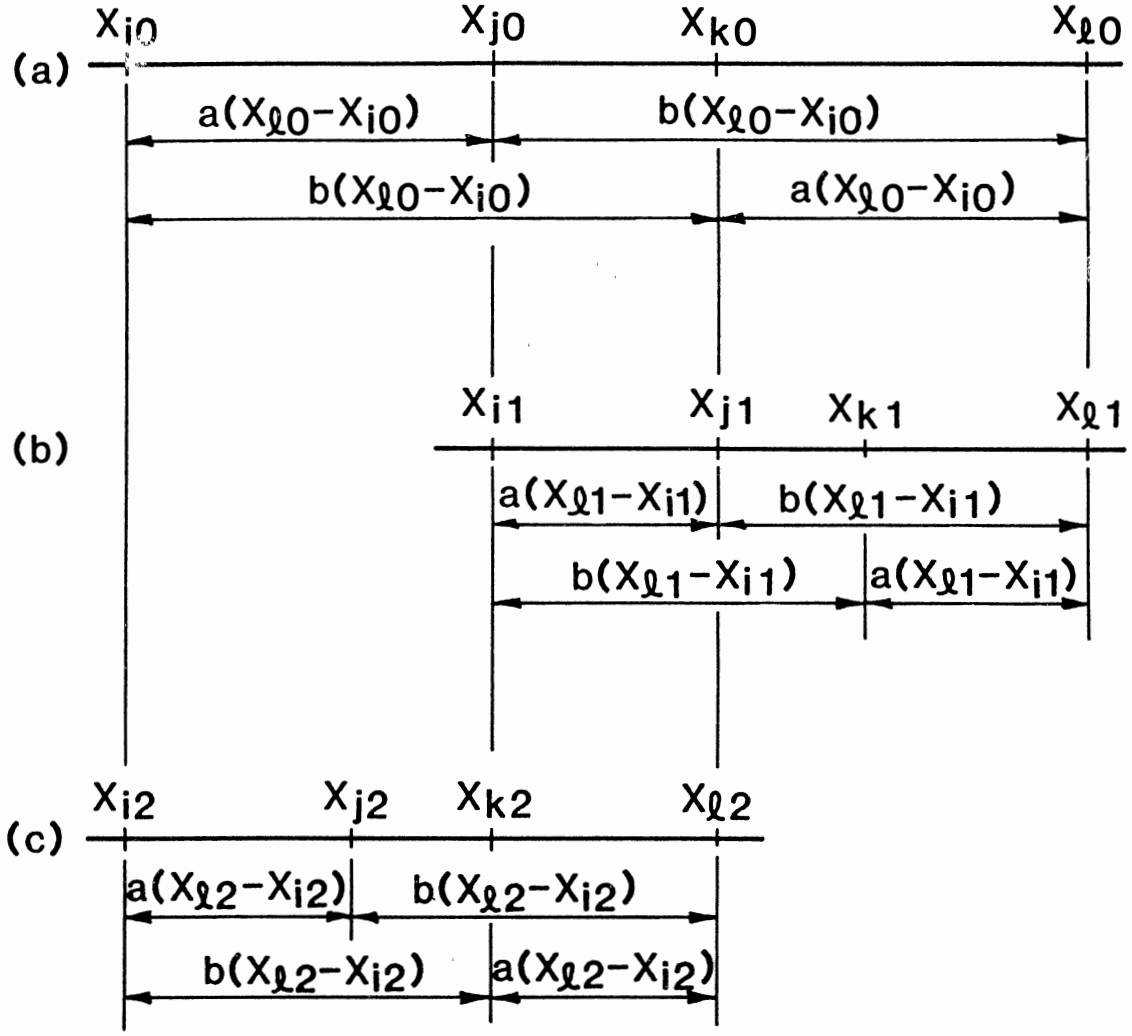

Note that

$$b(X_{\ell 1} - X_{i 1}) = a(X_{\ell 0} - X_{i 0})$$

and

$$a(X_{\ell 1} - X_{i 1}) = a[b(X_{\ell 0} - X_{i 0})]$$

Similar relations exist for (a) and (c).

Figure 31. (a) Initial Situation; (b) i_0-j_0 Discarded; (c) k_0-ℓ_0 Discarded

VITA 2

Claude Clifford Eberle

Candidate for the Degree of

Master of Science

Thesis: A STUDY OF THE CRITICAL WEISSENBERG NUMBER IN MECHANICALLY DEGRADING POLYMER SOLUTIONS

Major Field: Mechanical Engineering

Biographical:

Personal Data: Born in Oakland, Nebraska, December 7, 1959, the son of Mr. and Mrs. Claude H. Eberle.

Education: Graduated from Sasakwa High School, Sasakwa, Oklahoma, in May, 1978; received the Bachelor of Science degree in Mechanical Engineering from Oklahoma State University in May, 1983; completed requirements for the Master of Science degree at Oklahoma State University in December, 1984.

Professional Experience: Mechanical Engineer, Dow Chemical U.S.A., Texas Division, summer, 1982; graduate teaching and research assistant, School of Mechanical and Aerospace Engineering, Oklahoma State University, 1983-1984; Mechanical Engineer II, Martin Marietta Energy Systems, Inc., beginning September 10, 1984.